Exosome-Mediated Remodeling of Hematopoietic and Mesenchymal Stem Cell Niches in the Leukemic Bone Marrow

By

Ben Doron

A DISSERTATION

Presented to the Department of Cell, Developmental, and Cancer Biology
and the Oregon Health & Science University
School of Medicine
in partial fulfillment of
the requirements for the degree of
Doctor of Philosophy
January 2018

School of Medicine

Oregon Health & Science University

CERTIFICATE OF APPROVAL

This is to certify that the PhD dissertation of

Ben Doron

has been approved

_____
Peter Kurre, MD; Mentor/Advisor

_____
Philip J. Stork, MD, MS; Chair

_____
Andrew Adey, PhD; Member

_____
Hiroyuki Nakai, MD; Member

_____
Jeffrey W. Tyner, PhD; Member

_____

Melissa Wong, PhD; Member

Table of Contents

List of Figures	1
List of Abbreviations	2
Acknowledgments	3
Abstract	7
Chapter 1: Introduction	11
1.1 Cancer Biology	12
1.2 Hematopoiesis and Acute Myeloid Leukemia	15
1.3 Bone Marrow Microenvironment	25
1.4 Cell Signaling and Exosomes	32
1.5 MicroRNA	35
1.6 The Unfolded Protein Response	38
1.7 Conclusion	41
1.8 General Hypothesis and Specific Aims	42
Chapter 2: AML-Exosome Cargo and Trafficking	45
2.1 Abstract	46
2.2 Introduction	47
2.3 Results	50
2.4 Discussion	56
2.5 Materials and Methods	62
Chapter 3: AML-Exosome Impact on the Hematopoietic Stem Cell Niche	67
3.1 Abstract	68
3.2Introduction	69
3.3 Results	70
3.4 Discussion	76
3.5 Materials and Methods	78
Chapter 4: Transmissible ER Stress via Extracellular Vesicles Reconfigures the AML Bone Marrow Microenvironment	83
4.1 Abstract	84
4.2 Introduction	85
4.3 Results	87
4.4 Discussion	101
4.5 Materials and Methods	106
Chapter 5: Conclusions	117
5.1 Future Directions	118
5.2 Disease Modeling	122
5.3 Bone Marrow Population Isolation	123
5.4 Exosome Isolation	125
5.5 Conclusions	126
5.6 Curriculum Vitae	131
References	136

List of Figures

1-1 The Hallmarks of Cancer
1-2 The Hematopoietic Hierarchy
1-3 The endosteal and perivascular bone marrow niches
1-4 Mesenchymal Stem Cell Hierarchy
1-5 Intrinsic and Extrinsic Mechanisms of Leukemogenesis
1-6 MicroRNA are Negative Regulator of Gene Expression
1-7 The Unfolded Protein Response

2-1 Leukemia Exosomes Suppress HSPC Function and are Enriched with Specific miRNA Transcripts
2-2 Exosome miRNA Target Networks Overlap at Key Hematopoietic Regulators
2-3 Exosome miRNA Target Networks Overlap at Key Hematopoietic Regulators

3-1 Leukemia Systemically Impairs HSPC Function
3-2 Exosome-delivered miR-155 downregulates recipient c-Myb
3-3 c-Myb suppression by exosomal miR-155 compromises HSPC clonogenicity

4-1 AML negatively impacts the endosteal niche
4-2 MSCs and OPCs exhibit differential fates in the leukemic bone marrow
4-3 MSCs and OPCs exhibit increased ER stress
4-4 AML EVs traffic to the ER of MSCs and OPCs
4-5 AML cells exhibit an UPR *in vivo*
4-6 AML cells alter their EV cargo upon UPR induction

List of Abbreviations

3’UTR, 3’ untranslated region
AML, acute myeloid leukemia
BMP, bone morphogenic protein
CAR, CXCL12-abundant reticular cell
CFU-C, colony-forming unit in culture
CFU-F fibroblastic colony forming unit
cMYB, v-myb avian myeloblastosis viral oncogene homolog
EC, endothelial cell
ESCT, endosomal sorting complex required for transport
ER, endoplasmic reticulum
EV, extracellular vesicle
FBS, fetal bovine serum
FDR, false discovery rate
FLT3, FMS-like tyrosine kinase 3
GFP, green fluorescent protein
Hsa, Homo sapiens
HSC, hematopoietic stem cell
HSPC, hematopoietic stem and progenitor cell
ILV, intralumenal vesicle
KITLG, Kit ligand
LC, leukemic cell
Lin-, lineage depleted
Luc, Luciferase
miRNA, microRNA
MSC, mesenchymal stem cell
MVB, multivesicular body
Mmu, Mus musculus
NOD, non-obese diabetic
NSG, NOD/SCID/IL-2rγ^{null}
NTA, nanoparticle tracking analysis
OB, osteoblast
OPC, osteoblastic Progenitor Cell
OPN, Osteopontin
PBS, phosphate buffered saline
PCR, polymerase chain reaction
qRT-PCR, quantitative reverse transcriptase - polymerase chain reaction
RISC, RNA-induced silencing complex
RNA, ribonucleic acid
SCF, stem cell factor
SCID, severe combined immunodeficiency
TIE2, TEK tyrosine kinase
UPR, unfolded protein response
VF-FBS, vesicle-free fetal bovine serum

ACKNOWLEDGEMENTS

It takes a village to raise an idiot…or something like that. Self-deprecating humor aside, I guess what I'm trying to say is that this document represents the culmination of four years of work that could not have materialized without the tireless support of the people around me, both inside and outside the OHSU community. When I applied for this program I had rough idea of what I was getting into but of course being the naïve optimist that I am, I did not really grasp the amount of effort that was required to get to these final stages. The stark and sometimes brutal realizations of what it takes to be a true scientist were at times very difficult for me acknowledge. Despite the setbacks, endless troubleshooting, and despair I often felt (completely offset of course when things actually worked), I had an amazing support system, and for that I am incredibly thankful. I would like to highlight some of the people that were paramount in both helping me arrive at this document, and shaping the scientist I have become.

First and foremost I have to thank Dr. Peter Kurre for agreeing to be the primary mentor for my doctoral training, despite breaking a centrifuge during my first-year rotation. The work we accomplished together both enlivened my views on science and will shape the way I conduct research in the great beyond (I think that's what they call post-doc positions). Peter taught me how to be self-reliant, how to work hard, and how to write good (I promise the rest of the document is serious). A boss tells you what to do, a leader sets an example by doing. Peter is the latter. Days when I would come in early, Peter would already be there, probably a few cups of coffee deep. I would anticipate a few days respite from a grant or manuscript we were writing together after sending him a draft…but there it was waiting for me, usually the next day, inevitably saturated with red corrections and sassy comments. Somehow Peter is able to do this with *everyone* in the lab, which ranged from four to twelve people during my tenure. On top of this he manages to maintain a medical practice and a family of four. It remains a mystery to me how this is accomplished and sustained, but suffice it to say I aspire to be at least half as driven and compassionate as Peter in regards to my career as a scientist. Another trait I respect in Peter is his willingness to take risks (taking me on as his student should be evidence enough of this), but mostly in his pursuit of exosomes in the context of AML biology. When I joined the lab "exosomes" were invisible little things that people scoffed at the mention of. I think it took a lot of trust in his lab to explore the role of these vesicles. We have discovered some really exciting biology regarding exosomes. Finally, what I admire most in Peter is his determination to blaze his own trail and not to rely on the success of others to propel himself forward. While this makes him somewhat of a lone wolf, I think at the end of the day that this route provides deeper satisfaction.

Noah Hornick was the graduate student in the Kurre lab when I joined, and he immediately took me under his wing. He was a much needed "big brother" and helped get me on the right track both in my science and navigating

other aspects of the lab. I was constantly inspired by Noah's work ethic, kindness, and ability to write beautifully crafted sentences with what seemed like very little effort (a skill I remain quite envious of). Noah set the bar for what it takes to be a good graduate student, something I am still trying to reach.

The rest of the Kurre lab, both past and present members were outstanding in their efforts to help move my projects along, whether by intellectually contributing to ideas, or by sharing their skills at the bench. Santhosh exhibits incredible patience and endless optimism in the face of dire cloning projects…an aspect of bench work that to do this day I believe requires divine intervention. Jianya, Natalya, Ashley, and Young helped me get over some of my anxiety regarding mouse work, and they each taught me different aspects of bone marrow harvests and subsequent flow cytometry, two skills that I heavily relied on in my dissertation work. Sherif not only cares about his project, but my projects as well…perhaps even more than me! I would not be writing this dissertation right now if it was not for his Herculean efforts during our incredibly stressful 12-hour "harvest days". John, the newest grad student has recently entered the lab with an incredibly useful skillset surrounding microscopy…a technique I don't nearly have enough patience for. Aside from producing beautiful images for my project, the recent team meetings with John, Sherif, and Peter have been incredibly productive and exciting. The last nine months or so have been an exhilarating mix of fast-moving projects, and it has been great being a part of such a strong team of scientists.

It seems like every other student dreads their DAC meetings. I've always felt the opposite. Maybe it's because I was able to assemble a committee I've felt comfortable around, but I think our five meetings were always incredibly productive and insightful. Each of you provided a unique perspective on my projects, as well as sound career advice (and apparently some strong references, thanks for that!). Additionally a few of you were incredibly helpful and supportive when I was struggling with some personal issues. You know who you are and thank you for being open and honest with me, you really helped me get through some dark times.

OHSU is a fantastic community of faculty, students, technicians, and administration. To name everyone who helped me through the last few years would add way too many pages to this document, which already might be bursting at the seams (it feels that way, at least). I hope those of you reading this are aware that your actions provided me with the community aspect of science that I greatly appreciated, and hopefully contributed to as well.

I have been blessed with an incredible family that supported me more than I can even comprehend. My parents instilled in me a wonder for the world around me and galvanized the attitude that I could do anything I put my mind to (and followed through with…always the hard part). My brother Lee, even being my younger brother, is my hero. I aspire to be as good a brother to you as you have

been to me. I am incredibly proud of you and you inspire me to be a better person.

My friends, both old and new, hold me down. You guys balanced me out for the last four and a half years (and longer) by both listening to me ramble on about science and by telling me to shut up about science. Somehow you guys always know when to employ each strategy. I feel like my ability to talk in "layman speak" about my work greatly improved by sharing my ideas and projects with you over beers etc. Thank you guys so much.

Finally, Anna. We met at the first PMCB retreat and the rest is history, as they say. Those early days were a tumultuous time in both our lives, but it was easier to get through together. If anyone was there to support me, constantly, it was you. You're my partner, my roommate, my adventure-buddy, my secret collaborator, and my best friend. Thank you for everything, you made this journey wonderful. I'm excited for the next adventure with you, and all of the excitement we have waiting for us.

I love you.

To anyone reading this document: enjoy.

“But cancer is not simply a clonal disease; it is a clonally *evolving* disease. This mirthless, relentless cycle of mutation, selection, and overgrowth generates cells that are more and more adapted to survival and growth. In some cases, mutations speed up the acquisition of other mutations. The genetic instability, like a perfect madness, only provides more impetus to generate mutant clones.

Cancer thus exploits the fundamental logic of evolution unlike any other illness. If we, as a species, are the ultimate product of Darwinian selection, then so, too, is this incredible disease that lurks inside us.”

-Siddhartha Mukherjee
The Emperor of All Maladies

ABSTRACT

Hematopoiesis is the process by which the body constantly replenishes the supply of blood cells into circulation, and is maintained by a hierarchy of stem and progenitor cells that ensure lifelong function. This system is primarily sustained by supportive stromal cells in the bone marrow. Together, these stromal cell populations form discrete niches that maintain homeostasis. Despite the checks and balances that multicellular organisms have developed over time, neoplastic events in the hematopoietic lineage can result in a form of cancer known as leukemia.

Acute myeloid leukemia, the cancer studied in this dissertation, is a malignancy that occurs within the myeloid branch of hematopoiesis. The progression of this disease results in the manipulation of resident bone marrow cells, ultimately the remodeling hematopoietic and mesenchymal stem cell niches. These interactions contribute to both the comorbidities associated with this disease, and the reduction in the efficacy of chemotherapy. While these clinical outcomes of the disease have been identified, the underlying mechanisms driving them remain poorly described. Furthermore, the interactions between the growing malignancy and the resident hematopoietic and stromal cells is the driving force behind the reduction in hematopoietic output and functional remodeling of stromal niches that prevents successful chemotherapeutic outcomes. The overarching hypothesis underlying this work is as follows: *extrinsic forces imparted by leukemia drastically alter the resident,*

nonmalignant cells in the bone marrow, resulting in compositional and functional changes and a leukemic-supportive microenvironment, by which the fitness of the cancer increases at the expense of homeostatic function. In the work that follows explores the molecular mechanisms that contribute to both of these phenomena. By understanding the extrinsic forces that shape the leukemic microenvironment, we can identify promising routes for therapeutic intervention.

In the experiments describe herein, the role of exosomes in shaping the leukemic microenvironment is dissected. Exosomes are small secreted vesicles containing biological information that is trafficked to recipient cells. While a normal form of cellular signaling within tissues, this mechanism is hijacked by leukemia and is utilized to alter the function of discrete nonmalignant populations.

In a series of experiments focused on the content of AML-derived exosomes, we demonstrate that the process of leukemogenesis alters the exosomal cargo of the neoplastic cell, specifically in the context of their microRNA profile. The trafficking of these AML-specific microRNA has severe consequences in recipient cells as demonstrated by the RISC-trap experiment, which biochemically isolates the mRNA targets of microRNA-155, an abundant transcript found in AML exosomes. The identification of the unique microRNA profile of AML exosomes also provides an opportunity to use these vesicles as biomarkers for monitoring residual disease and early stages of relapse. Because AML exosomes can be isolated in the peripheral blood while the blasts that

secrete them can hide in the bone marrow, they can be harnessed as a diagnostic tool that can signify the reemergence of the cancer long before the leukemic cells can be detected.

Following the characterization of the cargo of exosomes, we explore the mechanism by which the transfer of specific microRNA can contribute to the cytopenias common in patients with this disease. Cytopenias are the result of inefficient or hampered hematopoiesis, and cause a reduction in blood production that can leave the patient tired, unable to clot wounds, or fight infections. We show that the trafficking of microRNA-155, and microRNA-150 by leukemic exosomes to hematopoietic stem and progenitor cells is sufficient to disrupt hematopoietic potential. This finding was important, as the mechanistic detail describing direct hematopoietic suppression by AML has been missing.

The focus is then shifted to the stromal contributions to AML progression, specifically the mesenchymal stem cells and their osteoblastic progeny residing in the endosteal niche of the bone marrow. After developing a protocol for the isolation of these two populations, we delve into the functional consequences of leukemia's influence on them. Importantly, we demonstrate that both populations exhibit differential responses to AML, and this leads to an aberrant microenvironment containing an altered stromal composition. We identify the exosomal contributions to driving these changes, and intriguingly discover that

the unfolded protein response, and ancient and conserved stress response pathway, is a critical regulator of the fates of both stromal populations.

In sum, the work contained in this document explores the role of exosome signaling in shaping a tumor microenvironment. This is an important contribution to the leukemia field, as it demonstrates the dynamic regulatory range of exosomal communication and the specific cell-type responses in the leukemic microenvironment. We demonstrate that AML exosomes are sufficient to promote cytopenias, a common comorbidity of leukemia that has lacked a causative molecular mechanism. Our experiments dissecting the promotion of ER stress in stromal cells as a result of exosome signaling may be the missing link between the niche remodeling phenotypes that we and others have shown, and the subsequent chemoprotective niches that result from leukemic influence. While the research utilizes AML as a model for unveiling the nuances of this phenomenon, readers are urged to consider how this paradigm may shape the microenvironments of other cancer-types, as well as consider the role of exosome trafficking within homeostatic niches.

CHAPTER 1: Introduction

Compiled in part from:

Doron, B., et al. (2017). "Concise Review: Adaptation of the Bone Marrow Stroma in Hematopoietic Malignancies: Current Concepts and Models." Stem Cells. PMID: 29235199*

*The use of figures from this manuscript is acceptable under the Wiley Online Library Article Sharing Policy.

1.1 CANCER BIOLOGY

In 1859 Charles Darwin published *On the Origin of Species*, which described the mechanisms by which species change over generational time and thus initiated the field of evolutionary biology. His theory provided the common thread by which all life on Earth is connected. Later, his theory was combined with the principles of heredity initially conceived by Gregor Mendel, and has since undergone successive adaptations by the contributions of countless scientists to generate The Extended Evolutionary Synthesis. This is the current theory that propels the life sciences forward, and can be applied to every tier of biology from molecular interactions within single proteins to the population dynamics of complex ecosystems. The essay "*Nothing in Biology Makes Sense Except in the Light of Evolution*"[1] written in 1973 by the evolutionary biologist Theodosius Dobzhansky emphasizes the idea that evolution connects the interrelatedness of all the various facets of biology, and thus makes biology make sense. Indeed, this concept has shaped this author's approach to science and influenced his personal philosophy on the mechanisms of cancer biology.

The quintessential example of this theory in action is the development of antibiotic resistance by bacteria. A beautiful study conducted in the Kishony lab utilizing a large petri dish with zones of increasing antibiotic resistance captures the evolutionary trajectories of *E. coli* as it successively adapts to extrinsic changes in its environment[2]. Eventually the dish is overwhelmed by multiple

distinct progeny of the parental population as these organisms successfully evolve to inhabit the space provided them. This same force drives the evolution of every species on Earth and, to date, has produced every living thing, including us: *Homo sapiens*[*].

Humans are organisms composed of trillions of cells, the basic unit of life, and within each of our cells lies the potential to evolve, much like the bacteria described in Kishony's experiment. Our evolution as multicellular organisms has generated a host of defense mechanisms to prevent this from occurring in somatic cells; however, in extremely rare cases a cell can evade these security measures and escape the confines of its role within the organism. The successive evolutionary adaptations that propel this malignant transformation, granting a cellular population independence to repopulate the organism unchecked, is defined as cancer. An incredible irony that the very mechanisms that have allowed the emergence of organisms capable of understanding the natural world are the same mechanisms that kills millions of these same organisms annually. Cancer, in a sense, is the price paid to be multicellular organisms[3].

For a mutant clone to successfully become a cancer, it must evolve the ability to elude the intrinsic and extrinsic mechanisms set in place to prevent tumorigenesis. This is a multistep process that involves discrete mutational

[*] To be clear, the quote from Siddhartha Mukherjee suggesting humans to be the ultimate product of evolution is simply not true. We are just the *current* product of this ongoing process.

changes to the genome, and broad changes to the phenotypic behavior of the tumor. Ultimately the malignant population achieves independence and exhibits collective traits described in the seminal paper by Hanahan and Weinberg as the "The Hallmarks of Cancer"[4]. These traits were then expanded a decade later[5] and are summarized in Figure 1-1:

FIGURE 1-1

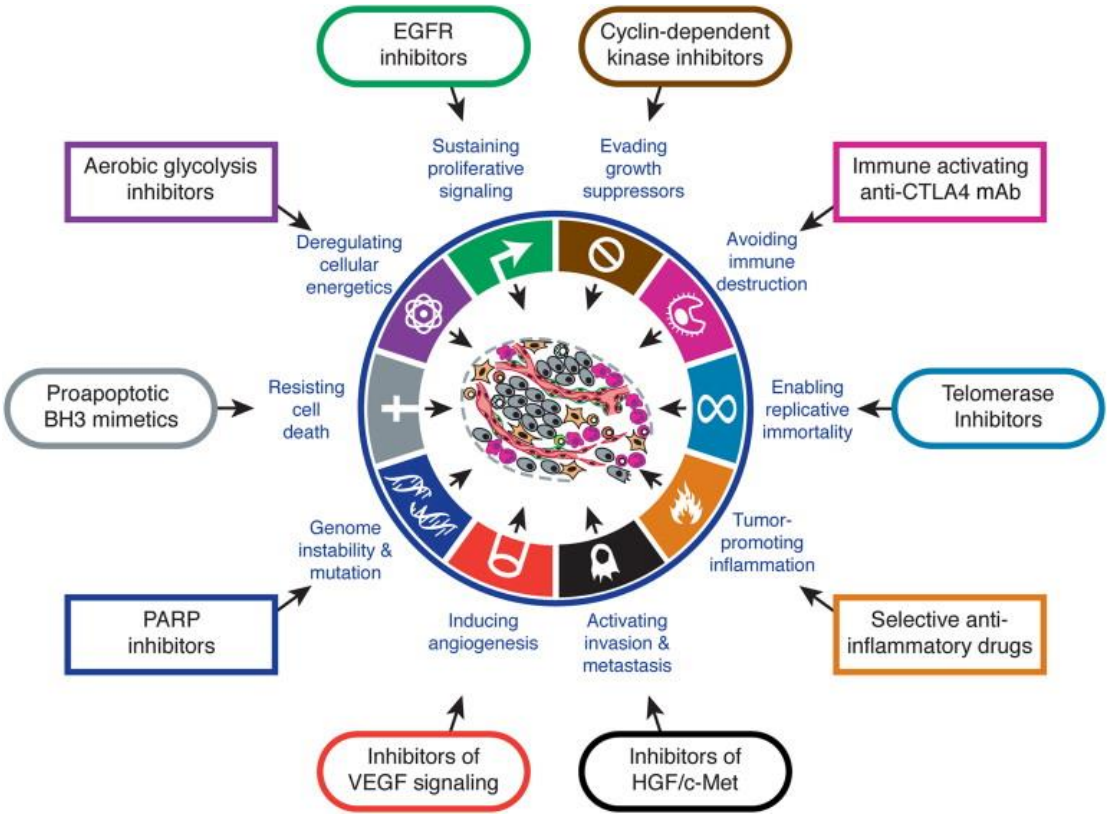

The Hallmarks of Cancer. The collective traits that provide the ability for tumors to grow unchecked and independently of the host. Potential therapeutic avenues targeting each Hallmark are also described. Reprinted from Cell, 144(5), Hanahan, D. and R. A. Weinberg, "Hallmarks of Cancer: The Next Generation", 646-674, Copyright 2011, with permission from Elsevier (license number: 4300871207032).

Each item in this list promises worthwhile endeavors to understand and ultimately cure cancer. While the "cure" for cancer is something this author would

consider an asymptotic goal, understanding how cancer utilizes these traits will allow for the development therapies aimed at exploiting the disparities between tumor and healthy tissue, and thus increase the means by which this disease is treated. Being a liquid tumor, leukemias do not fit the definitions of each Hallmark perfectly. However, with this caveat in mind, the work presented in this dissertation explores Hallmark 6: *They invade local tissue and spread to distant sites*. Which may be translated to leukemia as: *They corrupt local tissue to promote disease pathophysiology*.

The dissertation work presented henceforth will be a summation of the author's acquired knowledge in the field of cancer biology, which has been strongly shaped by the paradigms outlined here.

1.2 HEMATOPOIESIS AND ACUTE MYELOID LEUKEMIA

In order to understand cancer, we must understand the tissue from which it is derived. Leukemia originates from neoplastic events that occur within hematopoietic tissue: the cells that comprise the entire blood system. Hematopoiesis is the process by which the body constantly replenishes its supply of mature blood cells, accomplishing this through the organization of a stem cell hierarchy within the bone marrow[6] (Figure 1-2). At the apex of this hierarchy reside a population of rare hematopoietic stems cells (HSC), which are

maintained by self-renewal of daughter cells following division. Some daughter cells are influenced to become mature blood cells and therefore, through a series of expansions and differentiation decisions, all hematopoietic lineages can be represented in abundance by the progeny of a single HSC[7,8].

FIGURE 1-2

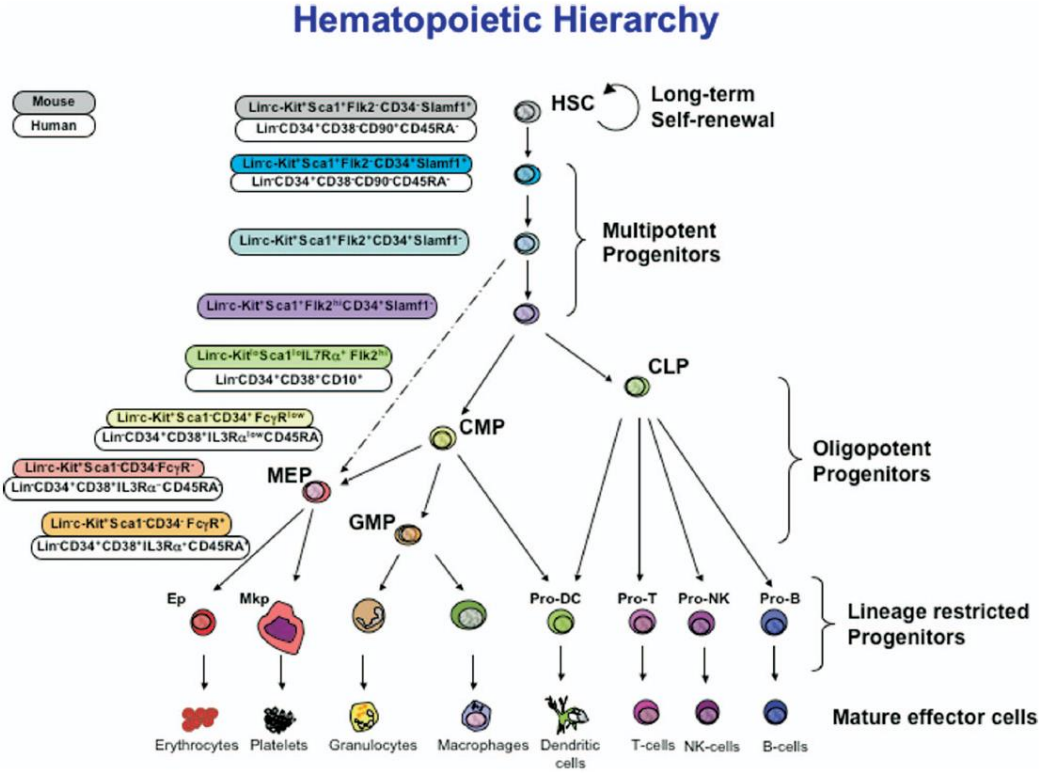

The Hematopoietic Hierarchy. The stem cell hierarchy that is the source of blood production throughout the lifetime of the organism. The HSC at the apex can self-renew or commit to become a mature blood cell through a series of expansions and differentiation decisions. Common surface markers found on different populations are also labeled. Reprinted from Blood, 112(9), Weissman I. L. and J. A. Shizuru, "The origins of the identification and isolation of hematopoietic stem cells, and their capability to induce donor-specific transplantation tolerance and treat autoimmune diseases", 3543-3553, Copyright 2008, with permission from Blood : journal of the American Society of Hematology (license number: 4304880003574).

Hematopoiesis has become a paradigm for stem cell biology, owing much of its renown to the ability to resolve discrete populations from the entirety of the tissue. In addition to morphological features distinct to each differentiated blood cell[9], the differential expression of surface proteins has provided researchers with the ability to use combinations of antibodies to define, measure, and isolate distinct hematopoietic populations throughout the stem cell hierarchy[10].

The constant cell division occurring within hematopoietic tissue increases the chances of mutations accumulating within pools of differentiating cells. We define a leukemia as an Acute Myeloid Leukemia (AML) when the neoplasm emerges within the myeloid lineage of hematopoiesis and results in a rapidly expanding clone or clones[11]. Even within the “AML” nomenclature, the combination of mutations sufficient to drive the disease, and the stage of hematopoiesis where this occurs contribute to the broad heterogeneity and further subtypes of this disease[12]. This is one aspect of AML that makes treatment difficult, as a universal exploitable target for AML has not yet been found.

AML is the most common acute leukemia that occurs in adults, representing 80% of total leukemias. This equates to over 20,000 new cases and 10,000 deaths per year in the United States alone[13,14]. With a median age at diagnosis of 72 years, AML is primarily a disease of the elderly. The incidence of

disease also strongly correlates with age, rising from 1.3 to 12.2 cases per 100,000 people upon crossing the 65 year old threshold[15]. AML also occurs in a substantial number (20%) of pediatric cases as well[13]. Among these pediatric patients, AML is responsible for the majority of all leukemia deaths[16]. Advances in treatment have increased the five year survival rate of adults with AML from 5% in the 1970s to 25% in the 2000s, however these rates remain unacceptably low, especially considering elderly patients in which 70% of patients over the age of 65 succumb to the disease within one year of diagnosis[15]. These numbers speak to the need for continued basic and clinical research in this field.

AML can arise from an underlying hematological disorder such as myelodysplastic syndrome (MDS), or as a consequence of prior chemotherapy (exposure to DNA damaging agents such as topoisomerases II, alkylating agents or radiation, for example)[17]. However in the majority of cases, it appears *de novo* in previously healthy individuals. The mutations driving the disease range from large chromosomal translocations such as t(8:21) or t(15:17) which generate chimeric protein products, to discrete genetic mutations in key genes, such as a Dnmt3a and Npm1[18]. The Knudsen hypothesis, better known as the two-hit hypothesis, as model of tumorigenesis has offered a framework by which leukemias may be classified[19,20]. Mutations found in leukemic cells can thus be binned into two classes: class I mutations which stimulate pro-proliferative pathways, and class II mutations which block normal hematopoietic differentiation[21]. Together, these two mutational classes synergize to drive the rapid expansion of immature hematopoietic clones.

With the classification of the mutational landscape of AML comes prognosis and treatment options. For example, patients bearing the t(8;21), t(15;17) or inv(16) chromosomal rearrangements confer a favorable prognosis[22], although this can change through compounding with distinct genetic mutations, as is the case when mutations in c-KIT coincide with t(8;21) rearrangements[18,23]. Of note, one genetic abnormality that nearly always confers a poor prognosis is internal tandem duplications within FMS-Like Tyrosine Kinase 3 (FLT3-ITD), or point mutations found in the activation loop of FLT3[24,25]. Furthermore, the FLT3 mutations are the most commonly found mutation in AML, represented in 30% of cases[25]. The extensive classification of the mutational spectrum of AML (only touched upon here) and the subsequent molecular characterization has driven the development of specific targeted therapies. This has been shown with tyrosine kinase inhibitors in chronic myeloid leukemia[26] and FLT3 inhibitors in AML[27]. These therapies act in addition to standard-of care therapeutics such as cytosine arabinoside[28] and the use of hematopoietic stem cell transplant[29,30]. The functional analysis of the roles of common oncogenes found in leukemia, combined with the ongoing efforts in personalizing medicine promise to improve outcomes for people afflicted with this disease.

Relapse is the primary cause of patient mortality in AML[31]. While, treatment of AML achieves remission in up to 80% of patients, the majority of both adult and pediatric cases will experience relapse. Successful treatment of relapsed AML is rare, due to the aggressive kinetics of relapsing AML[32]. This

underscores the need for improved early detection of residual disease after therapy. The current methodologies for detection rely on identifying leukemia at the cellular level[33] either from peripheral blood assays which require the presence of leukemic blasts in the circulation, or invasive bone marrow aspirates that only sample from a single physical location. Additionally, both flow cytometry and PCR require the presence of a known leukemia-specific marker, which is lacking in AML due to the inherent heterogeneity of the disease. The need for biomarkers that can detect residual disease at earlier stages of relapse promise to greatly improve treatment outcomes for relapsed AML. A novel platform utilizing an AML-specific miRNA signature in exosomes found in the peripheral blood is the focus on of Chapter 2 of this dissertation. Furthermore there are several hypotheses aimed at describing the events that contribute to the high rate of relapse in AML. These include clonogenic evolution of the tumor following treatment[34], and the conversion of bone marrow niches into leukemic sanctuary sites[35]. The latter being the focus of Chapter 4 of this dissertation.

A common morbidity that develops with leukemia is the suppression of normal hematopoiesis, leading to anemia, neutropenia, and thrombocytopenia[36]. Despite the clinical impact of hematopoietic insufficiency in AML, the molecular mechanisms causing the phenomenon are poorly understood. Microenvironmental contributions have recently been reported in that AML manipulates and impairs the function of bone marrow stromal cells, which is a significant contributor to the reduction of physiologic hematopoiesis[37]. A

mechanism of hematopoietic suppression caused via direct signaling between AML blasts and HSPCs is explored in Chapter 3 of this dissertation.

There are multiple approaches to studying AML, each with its own advantages and drawbacks. The disease can be studied in patients, and years of observation in this regard have provided the clinical symptoms and consequences of AML progression. This approach precludes thorough experimentation however, and in order to dissect nuanced mechanisms we must turn to models of disease. A model is a simplified version of a real life system, and therefore lacks some of the complexities that exist within patients.

Current techniques in genetic engineering have generated a number of murine leukemia models using transgenic mice with global or tissue specific loss- or gain-of-function phenotypes intended to mimic common genetic lesions encountered in patients. Genetically Engineered Mouse Models (GEMM) provide faithful alterations to genes of interest with a high degree of disease penetrance, as well as an intact immune system. Recently developed GEMMs utilize tissue specific approaches to dysregulate gene expression in specific cell types or tissues, and provide temporal control of Cre-recombinase mediated excision and disease onset[38]. These allow for the study of tumor initiation and provide an intact microenvironment that contains stromal and immune populations more representative of disease propagation in patients[39,40]. These models allow for the study of potential modifier effects resulting from multiple genetic lesions frequently encountered in patients. As an example, one GEMM of Acute

Myelogenous Leukemia (AML) is the *PU.1/p53* double-mutant mouse, with homozygous loss of the upstream element of the hematopoietic proto-oncogene *PU.1* and deletion of *p53: PU.1(ure/ure)p53(-/-)*[41]. Individually, these mutations are insufficient to induce disease, but together result in a highly aggressive model of AML. Other GEMMs of human leukemias include *Nras:Bcl-2* and *AML-ETO* for AML[42]; *BCR-ABL1* fusion for Chronic Myelogenous Leukemia (CML)[43]; and *E2A–PBX1* fusions and *PRDM14* mutations for Acute Lymphoblastic Leukemia[44,45]. These models have been instrumental in the identification of the mechanisms of leukemogenesis, providing advances in understanding leukemic progression, the role of the niche, and aiding in the identification of novel therapeutic targets. Many of the referenced models have also contributed key insights into stromal remodeling, detailed below[39,40,46-48].

In contrast to GEMMs, immune-deficient mouse strains have allowed researchers to study the biology of human leukemias *in vivo* across xenogeneic immunologic barriers that would otherwise lead to rejection between species. Xenograft models, in which leukemic cell lines or primary patient-derived tissues (discussed below) are engrafted into mice, provide invaluable insight in translating *in vitro* observations to an *in vivo* context. Several immunocompromised strains have been derived, but most investigators rely on the NOD-*scid* IL2R γ^{null} (NSG) strain. These mice are deficient in both B- and T-lymphocytes and Natural Killer cells, providing high levels of bone marrow engraftment for human hematopoietic and patient leukemic cells, albeit without

the ability to evaluate systemic immune responses to the tumor or the composition of the tumor immune microenvironment. In addition to the *in vivo* biology of the AML cells themselves, xenograft models also allow the role of stroma in disease propagation to be addressed[49,50]. A powerful example for the faithful stroma interactions between human leukemia and murine bone marrow stroma is provided by the study of a peptide inhibitor of CXCR4/CXCL12-mediated adhesion, named E5[51]. This peptide prevented stromal cell-mediated chemoprotection, and increased the sensitivity of AML cells to a standard chemotherapeutic regimen, demonstrating both the role of stroma-derived CXCL12 in AML progression and the potential to target this molecule to increase chemotherapeutic efficacy[51].

Historically, many leukemia xenograft models utilized immortalized tumor cells but more recently patient-derived xenograft (PDX) models have been used to study of primary cancer tissue, especially in understanding disease progression and evaluating drug responses[52,53]. Generally, leukemia cells isolated from patients are injected into sublethally irradiated NSG mice with subsequent orthotopic establishment and expansion of leukemic cells in the bone marrow. This has provided a solid platform for observing disease biology and for measuring the response to chemotherapy, including combinatorial drug approaches[52]. More recent studies illustrate how NSG mice grafted with HLA mismatched patient AML cells and healthy human control hematopoietic cells can further refine the study of BM interactions. Moreover, the PDX model allows

for the development of translational biomarker platforms where peripheral blood can be analyzed to track cancer-specific signatures such as cell-free DNA[54], or miRNA contained in exosomes[55]. While PDX models provide useful *in vivo* context, insufficient or heterotopic engraftment has proven to be a significant barrier. The variability among PDX models also reflects the heterogeneous leukemic subtypes, genetic variation, and patient-to-patient variability. To alleviate these shortcomings, new strategies of grafting include the use of humanized mice, which provide an immune system and express specific human hematopoietic supportive factors to enhance engraftment success[56].

The work in this dissertation has primarily relied on studying the human AML cell lines Molm-14, HL60, and U937. Each of these cell lines contain a different set of mutations, chromosomal aberrations, and behaviors. Molm-14 are driven by the notorious FLT3-ITD lesion, providing a model of lethal and relapse prone AML. HL-60, while resembling a promyelocytic leukemia, are driven by mutations in c-Myc[57], instead of the t(15;17)(q22;q12) translocation (generating a *PML–RAR*α fusion gene), which is exclusively associated with acute promyelocytic leukemia[58]. Finally U937 cells contain t(10;11)(p13;q14) in the U937 cell line resulting in the fusion of the AF10 gene and CALM which contribute to malignant growth[59]. The use of these cell lines allows for highly reproducible experiments, especially when used to generate xenografts in the NSG mouse, to provide a window into tumor biology with which we can detect extremely nuanced phenomena. The observations we make using this model can

then be translated to models that more accurately represent disease progression, or can be explored in AML patients.

1.3 BONE MARROW MICROENVIRONMENT

The collective term *stroma* is used to describe the diverse population of nonparenchymal cells within a tissue. They provide the architecture of the organ and maintain tissue homeostasis through reciprocal signaling with their parenchymal counterparts. Within the bone marrow, stroma refers to the bone, cartilage, fat, vasculature, innervation, and the stem and progenitor cells that give rise to these populations. Together, these diverse populations coordinately regulate lifelong function and hematopoietic support[60-62]. The contributions of discrete bone marrow stromal populations have been thoroughly investigated in murine models, whereby the benefit of experimental intervention and genetic labeling provide a wellspring of information in an *in vivo* context[63]. Under these stringent experimental conditions, hematopoietic stem cells (HSC) appear to localize in discrete anatomic, functionally well-defined locations within the marrow cavity[64,65]: the *endosteal niche* lining the bone surface and the *perivascular niche* in the central marrow cavity, each harboring a unique HSC subset[63], (Figure. 1-3).

The endosteal niche

The cells that comprise the endosteal niche in mice primarily fall within the osteoblastic lineage, lining the interior wall of the bone and providing both function and structure to the niche[61]. Principally, osteoblastic cells are derived from resident mesenchymal stem cells (MSC), that in both human and mouse exhibit trilineage differentiation potential *in vitro* (Figure 1-4). Endosteal MSCs maintain long-term, quiescent HSCs through the presentation of surface signals and the secretion of supportive cytokines[66,67]. Osteolineage differentiation of these MSCs occurs in observable stages, where discrete osteoblastic progenitor cells (OPCs) can be identified immunophenotypically[68], or by using *Osterix* driven reporter mice[69] (Figure 1-3). OPCs are intermediate cells that mature into osteoblasts (OBs) and incorporate into calcified bone to become osteocytes. Homeostasis in calcified bone is maintained through functional feedback between bone forming OBs and bone resorbing osteoclasts[70]. The endosteum is organized in layers, where osteocytes and mature OBs provide a rigid matrix for OPCs, which form a distinct layer with interface to the marrow cavity. Within the OPC layer, endosteal MSCs and other reticular cells form a niche for HSCs. In mice, bone morphogenic protein (BMP) signaling from HSCs induces osteoblastic differentiation of MSCs providing evidence of the crosstalk between hematopoietic and stromal tissues that shape this niche[62]. In turn, OPCs produce Osteopontin (OPN) and C-X-C Motif Chemokine Ligand 12 (CXCL12), providing HSCs with signals that maintain self-renewal, differentiation, and niche retention[68,71-73].

FIGURE 1-3

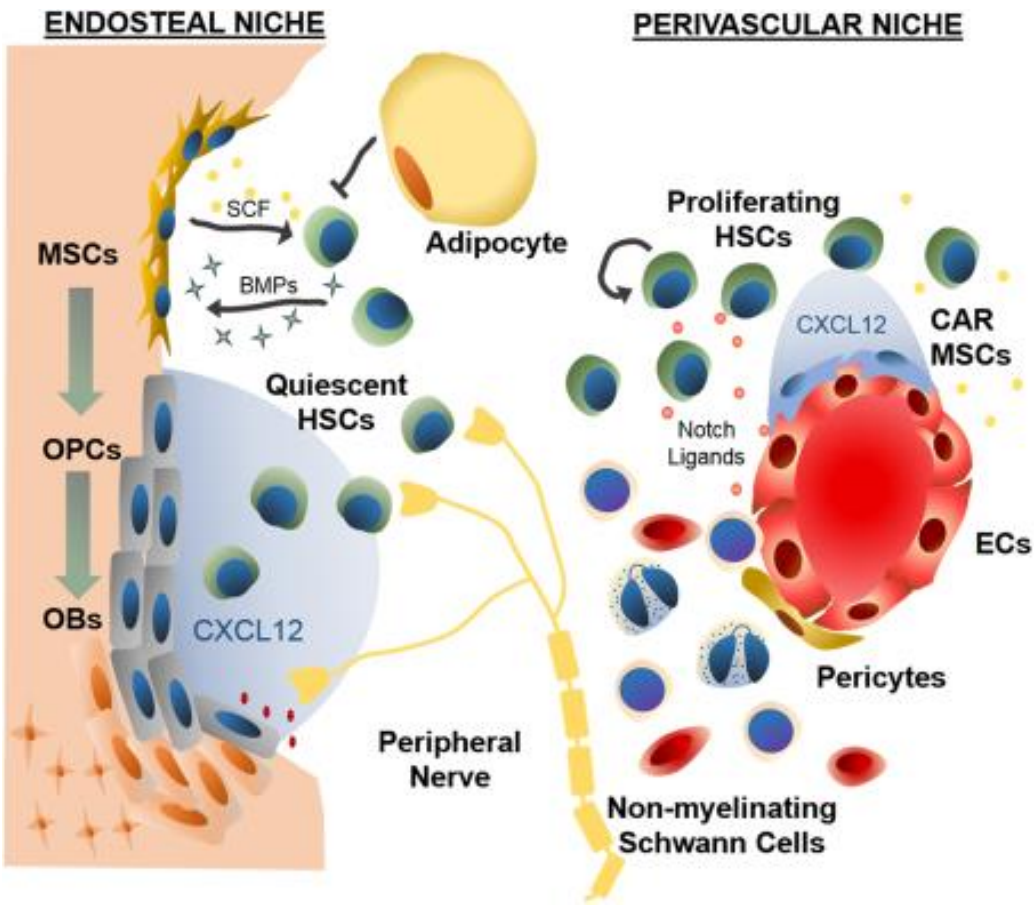

The endosteal and perivascular bone marrow niches. The two main niches of the murine bone marrow and the stromal cells that reside therein. Multiple signaling factors maintain niche homeostasis for both hematopoietic and stromal populations. HSC: hematopoietic stem cell, MSC: mesenchymal stem cell, OPC: osteoblastic progenitor cell, OB: osteoblast, EC: endothelial cell, CAR: CXCL12 abundant reticular cell, SCF: stem cell factor, BMP: bone morphogenic protein.

Unlike MSC and OPC contributions to HSC maintenance, the mature OBs do not appear to strongly influence HSC maintenance, but instead provide the scaffolding for the calcified bone enclosing the marrow. The work in Chapter 4 focuses on the discrepancies between MSCs and OPCs, and their independent responses to AML in the endosteal niche.

FIGURE 1-4

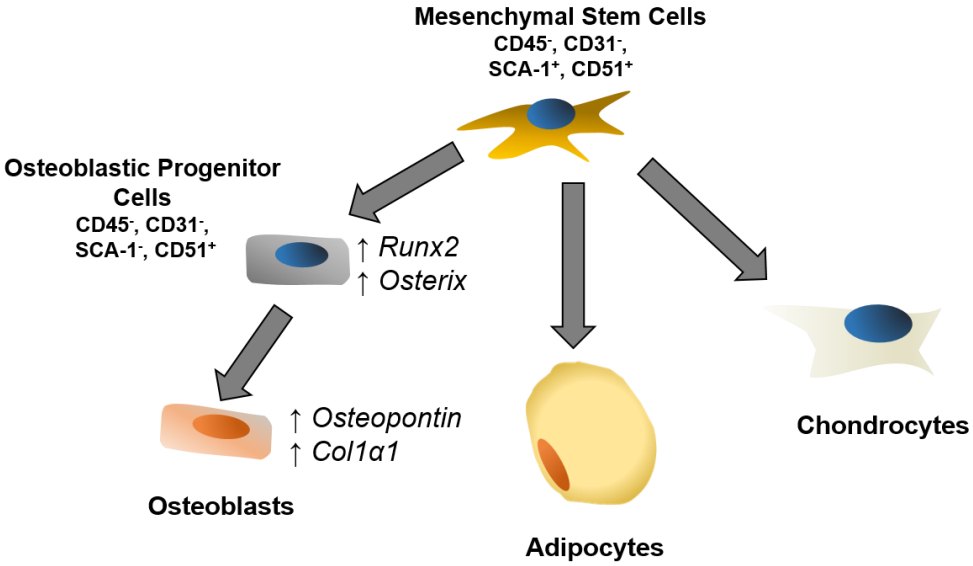

Mesenchymal Stem Cell Hierarchy. Bone marrow MSCs maintain trilineage differentiation potential, and can generate bone (osteoblasts), fat (adipocytes), and cartilage (chondrocytes). This is accomplished through a differentiation cascade in which MSCs either self-renew or commit to differentiation. Differentiation down the osteoblast lineage is accompanied by the upregulation of discrete genes at the progenitor and osteoblast stage. The immunophenotype of MSCs and osteoblastic progenitor cells used throughout this dissertation are labeled.

The perivascular niche

The cells of the perivascular niche include MSCs, and the endothelial cells (ECs) that line the vasculature in the bone marrow. In mice, perivascular MSCs also demonstrate self-renewal and tri-lineage differentiation potential. These MSCs exhibit both distinct and overlapping surface markers with endosteal MSC, including CXCL12, Stem Cell Antigen 1 (SCA-1), and Platelet Derived Growth Factor Receptor (PDGFR). A subset of perivascular MSCs expressing higher levels of CXCL12 have been named CXCL12 Abundant Reticular (CAR) MSCs, and are considered the principal source of this cytokine in the marrow[74]. ECs can

be genetically labeled utilizing the *Tie2* promoter in transgenic mice, or immunophenotypically identified via expression of CD31 and Vascular Endothelial Growth Factor Receptor 2 (VEGFR2)[75,76]. ECs and perivascular stromal cells secrete Notch ligands capable of HSC activation[77]. Unlike MSCs and OPCs, ECs are indispensable for the production of SCF, indicating a necessary and unique function of these cells[78]. Beyond structural differences, the signaling from perivascular and endosteal niches in turn confers distinct functional properties on HSC [63]. For example, the murine endosteal niche contains HSCs that exhibit relatively reduced self-renewal and regenerative capacity compared to perivascular localized HSCs[79], but can rapidly divide and differentiate following bone marrow injury[80]. The endosteal niche also experiences enhanced HSC homing following irradiation, demonstrating the dynamic crosstalk between niches and the subsequent extrinsic cues to HSCs during different physiological states.

It is important to acknowledge that the marrow contains other critical stromal populations that contribute to homeostasis. Peripheral innervation and signaling from non-myelinating Schwann cells, for example, controls HSC cycling and circadian hematopoietic activity[81]. Similarly, adipo-lineage cells contribute to HSC proliferation through secretion of cytokines, and may enhance myelo-erythropoiesis via iron sequestration and trafficking[82,83].

The bone marrow can be thought of as a complex ecosystem, whereby discrete populations of cells each provide critical contributions to the continuity of

the organ, including long-term homeostatic function and response to injury. Importantly, while this ecosystem is remarkably resilient, it remains vulnerable. For example, abnormalities within discrete stromal populations are sufficient to dysregulate entire niches, resulting in an aberrant microenvironment that promotes the development of neoplastic hematopoiesis.

These observations have illuminated a fascinating mechanism of tumorigenesis by which *extrinsic* cues initiate and promote neoplastic growth. This can be contrasted to *intrinsic* tumorigenesis where the serial accumulation of mutations drives cancer evolution (Figure 1-5). Recently, transgenic murine models with mutations in select stromal populations have provided direct evidence that an abnormal microenvironment can directly drive the evolution of abnormal clones. As a powerful illustration, myelodysplasia and leukemia are induced in transgenic mice with disabled *Dicer*$^{-/-}$ function specifically in osteolineage cells[84]. Further, conditional genetic knockouts of critical hematopoietic maintenance factors such as *Cxcl12 and Scf* can be generated using cell-specific promoters driving *Cre* expression crossed with mice containing *floxed* genes of interest. For example, *Tie2*-driven *Cre* excision can generate *Cxcl12*$^{-/-}$, *Scf*$^{-/-}$, and *Rbpj*$^{-/-}$, (a gene knockout that ablates the expression of Notch proteins) specifically in ECs to study the contribution of these genes within the perivascular niche[85]. Mice containing any of these loss-of-function mutations in ECs exhibit myelodysplasia and subsequently develop leukemia[72,78] indicating critical functional roles of marrow endothelium, other than as a vascular scaffold.

FIGURE 1-5

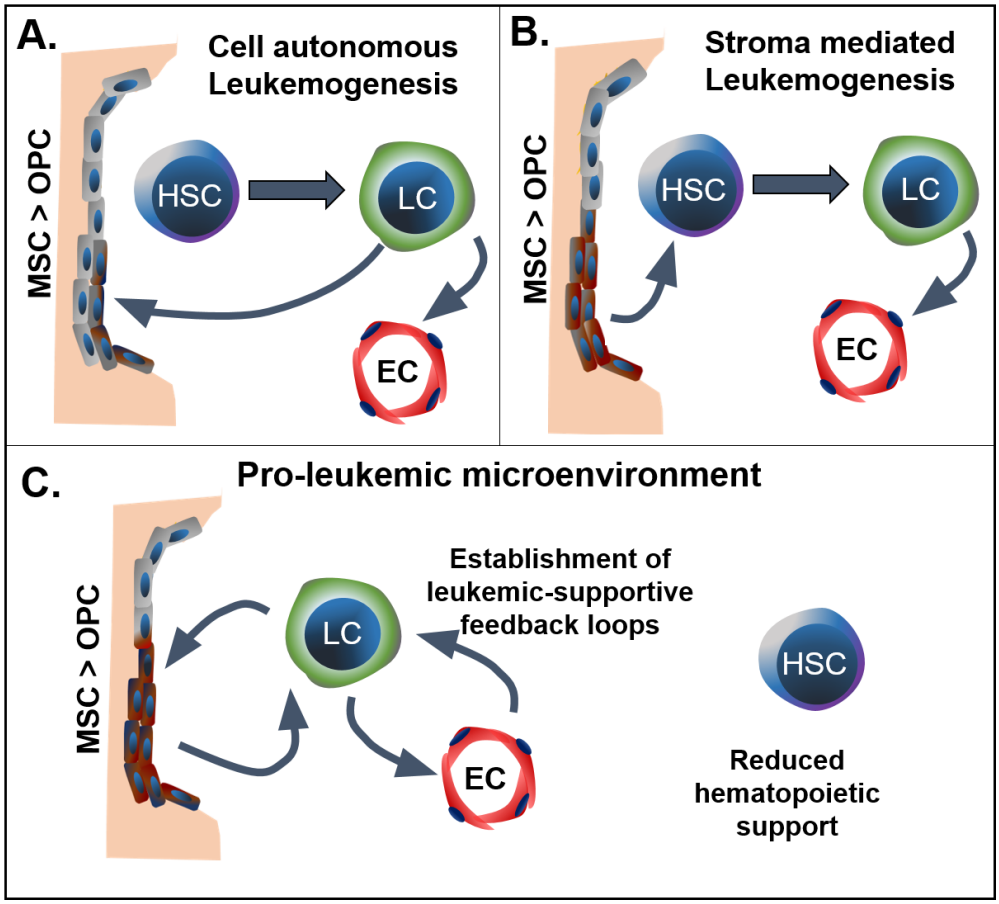

Leukemogenesis can arise from cell intrinsic and extrinsic forces. A. Intrinsic forces, such as the accumulation of mutations and epigenetic aberrations results in a neoplastic event that ultimately results in leukemia. **B.** Aberrant stromal function can synthesize a microenvironment that promotes abnormal growth, creating extrinsic pressures that select for pre-leukemic clones. **C.** Regardless of how the leukemia develops, reciprocal signaling between the cancer and the stroma generates a pro-leukemic microenvironment containing reciprocal feedback loops that continue to remodel the bone marrow into a supportive niche for the cancer at the expense of normal hematopoietic support.

Similarly, the use of animals with other cell-specific Cre-drivers, *Osterix* (OPCs), *Osteocalcin* (OBs), and *Nestin* (MSCs) have demonstrated a critical role for CXCL12 expression in these populations as a factor that promotes hematopoietic niche adhesion[72]. Importantly, these models provide novel experimental

paradigms of leukemogenesis, and identify the specific stromal cell populations whose functional features contribute to neoplastic growth.

1.4 CELL SIGNALING AND EXOSOMES

Communication within complex tissues like the bone marrow is critical for maintaining homeostasis and in response to stimuli such as injury, differentiation cues, and malignancy[6,63,86]. Cells have evolved diverse ways to signal to each other, allowing tissues and organs to remain in concert with one another. These various mechanisms provide cells with the ability to control what information is transferred, what cells will receive the signal, and the intensity of the response. Well defined signaling molecules that mediate hematopoiesis are Wnt, Notch, and *Transforming Growth Factor beta* (TGF-β)[87-89], which trigger signal transduction cascades that ultimately lead to changes in gene expression in recipient cells. In addition to these forms of communication, the secretion of exosomes has recently become appreciated as a dynamic mechanism by which cells transfer biological information[90].

Exosomes are membrane-enclosed vesicles derived from the endocytic compartment and released at the plasma membrane into the extracellular space[91]. These vesicles range from 30-150 nm in diameter and can act as a signaling mechanism in an autocrine, paracrine, and endocrine fashion. In

contrast to the shedding of microvesicles which bud at the plasma membrane, exosomes are contained as vesicles within endosomal compartments, termed multivesicular bodies (MVB)[92]. Exosomes originate as inward buddings of the endosomal membrane to create intraluminal vesicles (ILV), creating multivesicular bodies (MVB) that accrue during the transition of early to late endosomes[93]. Their biogenesis is also reflected in their lipid composition resembling that of early endosomes[94]. Movement towards the plasma membrane is controlled by the cytoskeleton and small GTPases[95]. Secretion occurs when endosomes fuse with the plasma membrane and release their exosomes. This allows the cell to manage exosomal output in a temporally and spatially controlled fashion by using multiple cytoskeletal and membrane proteins to mediate fusion and secretion[92,96].

Exosomes contain a subset of biologically active macromolecules present in the cell including protein, lipids, and nucleic acids[93,97]. The trafficking of these molecules into neighboring cells alters their behavior, a process involved in neuronal signaling, fetal development, tissue homeostasis and repair, adaptive immunity, and cancer progression[91,93,98]. Cells change both the output of exosomes and the cargo within them under stress-inducing conditions, including irradiation, hypoxia, nutrient deprivation, differentiation, cytokine stimulation, and, importantly, following malignant transformation[96,99].

Exosomes contain internal maturation proteins, and the proteins bound for recipient cells within the luminal compartment. To date, close to 5000 different proteins have been shown to associate with exosomes[100]. The cellular origin of exosomes accounts for the fact that many exosomal proteins are involved in endosomal pathways. The most common proteins include tetraspanins CD9, CD63, and CD81, which act as protein scaffolds; Flotillin, which aids in vesicle formation; Alix, an adaptor protein required for endosomal trafficking; and TSG101, a regulator of vesicular trafficking[90]. These proteins are frequently used as markers for the classification of exosomes[97,101]. Exosomes also contain cytoplasmic proteins that have functional roles in recipient cells. One mechanism by which proteins are sorted into exosomes relies upon ESCRT (Endosomal Sorting Complexes Required for Transport), a complex of proteins that coordinates both budding and sorting of proteins into ILVs[102]. This complex was initially described as being required for the sorting of ubiquitinated proteins destined for the lysosomal degradation, but it has also recently been shown to sort proteins into exosomes[103]. The post-translational modifications that ESCRT recognizes for sorting are still unclear, but seem to be primarily orchestrated by a combination of the ubiquitin profile and association of other “guide” proteins[103].

Exosomes are enriched in cholesterol, ceramides, sphingomyelin, and saturated species of phosphatidylcholine and phosphatidylethanolamine[104]. The lipid composition of exosomes contributes to both ILV formation and trafficking within the cell of origin[94]. In studies where components of the ESCRT complex

are knocked out, ILVs are still generated in a mechanism that seems to be aided by the increased incorporation of ceramides, which increase membrane curvature[105]. Sphyngosine-1-phophate was also shown to contribute to ILV formation, as a reduction in flotillin^{+} exosomes was observed in Sphingosine Kinase knockout cell lines[97]. In contrast to microvesicles whose bilayer reflects that of the plasma membrane, exosomes contain additional lipid moieties of endosomal origin[94].

Exosomes mediate the functional transfer of mRNA and microRNA (miRNA) between cells[106,107]. Work in our lab and others has demonstrated that AML cells secrete vesicles that conform to the definition of exosomes and carry transcripts to multiple cell types within the bone marrow microenvironment[108,109]. The unique miRNA profile of leukemic exosomes is the focus of Chapter 2, and the functional consequences of exosomal transfer of these miRNA to healthy HSPCs is the focus of Chapter 3. Perhaps the most fascinating property of exosomes is their ability to be loaded with specific transcripts, imbuing them with an incredibly dynamic ability to transfer biological information.

1.5 MICRO RNA

MicroRNA (miRNA) are small (22 to 24 nucleotides in length) RNA transcripts that act as negative regulators of gene expression. They accomplish this by preventing the translation of specific mRNA transcripts by recognizing and

binding to semi-complementary motifs. The bound transcripts are either degraded immediately, or held in a state that prevents their association with ribosomal machinery. miRNA have been rapidly recognized as a powerful factor by which cells control gene expression[110]. Only a small degree of complementarity is required for miRNA to bind with a target mRNA, allowing a single miRNA transcript to regulate many different targets. This ability grants cells the ability to broadly control gene expression by utilizing miRNA that can dampen multiple transcriptional programs. miRNA targeting also provides indirect effects on gene expression, as miRNA-mediated inhibition of a transcriptional repressor would increase the expression of those otherwise suppressed transcripts. An example of these indirect effects is illustrated in Chapter 2. With more than 60% of all human protein-coding transcripts being regulated by miRNA[111], one can appreciate the powerful role these small molecules play in maintaining cellular homeostasis, and the potential havoc of exosome mediated transfer of these transcripts within tumor microenvironments (the focus of Chapter 3).

MiRNA are transcribed by RNA polymerase II as a long primary miRNA transcript, or 'pri-miRNA', containing a hairpin structure of approximately 70 nucleotides. Processing of this transcript by the enzymes Drosha and Dicer removes the hairpin, generating the mature miRNA 20-24 nucleotides in length[112]. The miRNA is loaded into one of several Argonaute (AGO) proteins to become a component of the mature RNA-induced silencing complex (RISC). This complex, containing the mature miRNA, AGO protein, and GW182, is the

machine that binds to target mRNA (Figure 1-6). Discretion of mRNA targets achieved by semi-complementarity to the miRNA's seed sequence with the miRNA Response Element (MRE) on the mRNA transcript, primarily found within the 3'UTR[113]. After binding of miRNA:mRNA, GW182 then activates cytoplasmic poly-A binding protein (PABPC), which binds the polyadenylated tail of the mRNA recruits several deadenylase complexes and exonucleases, which degrade the transcript[114,115].

FIGURE 1-6

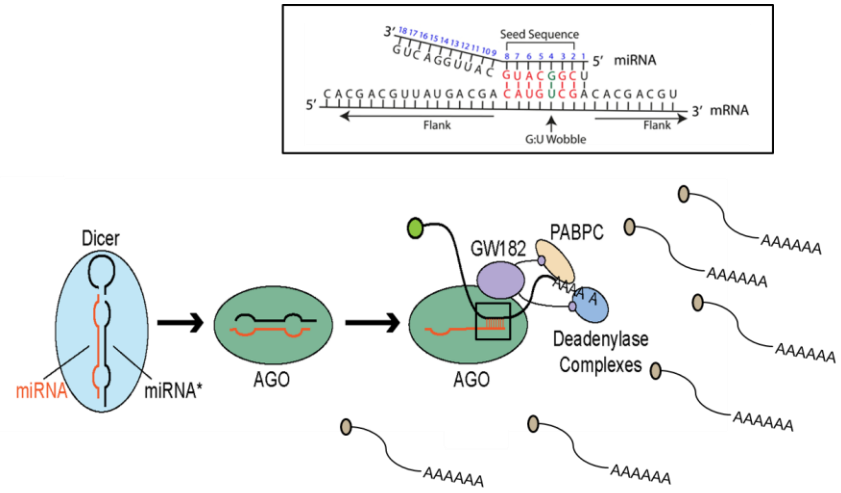

MiRNA are negative regulators of gene expression. Following transcription and initial processing in the nucleus, miRNA are further processed by Dicer and then loaded into the RNA-induced silencing complex (RISC) composed of multiple protein components. Binding of RISC to target mRNA is accomplished by miRNA:mRNA binding of semi-complementary motifs. mRNA transcripts are then subsequently destroyed or bound in a state that prevents their translation into functional protein. Figure generated with the help of Noah Hornick.

The role of miRNA in cancer has expanded dramatically over the last two decades due to their ability to impact the transcriptome of cells within the tumor and the surrounding microenvironment. MiRNA dysregulation plays pivotal roles

in altering the transcriptome of the malignant cells, by acting as oncogenes and tumor suppressors. Because miRNA are negative regulators of gene expression, oncogenic miRNAs target and reduce the expression of tumor suppressing mRNAs. Increased levels of oncogenic miRNAs therefore eliminate the expression of tumor suppressing proteins and in doing so increase cell proliferation and/or inhibit cell death.

Conversely, tumor suppressing microRNAs, target mRNAs encoding oncogenes, and reduced levels of these microRNAs cause an increase in the levels of oncogenic proteins which further malignant cell survival and proliferation[116]. Beyond their cell-intrinsic, tumorigenic role, miRNA are also involved in shaping tumor microenvironments. With respect to hematological malignancies, miRNA trafficking from AML blasts to nonmalignant hematopoietic cells via exosomes has been shown to dramatically alter function in recipient cells[109,117], a phenomenon further explored in Chapters 2 and 3.

1.6 THE UNFOLDED PROTEIN RESPONSE

The Unfolded Protein Response (UPR) is an ancient eukaryotic pathway that allows cells to respond to the accumulation of misfolded proteins in the endoplasmic reticulum (ER) lumen, or to environmental changes such as hypoxia, nutrient deprivation, and calcium fluctuation[118]. In cases where ER stress cannot be ameliorated, the cell will shift from a homeostatic response to

engage in apoptosis. The master regulator of the UPR is GRP78 (also known as BIP and HSPA5), an ER protein that binds the UPR effectors ATF4, IRE-1, and PERK in a non-functional state. The accumulation of unfolded proteins in the ER recruits GRP78 to the ER lumen, and in doing so releases the effectors to activate the pathway. A feedback loop is initiated in which downstream transcription factors increase the expression of GRP78/BIP, XBP1, and other UPR genes. Ongoing UPR stress results in an accumulation of CHOP, a pro-apoptotic protein that facilitates apoptosis through translocation of BAX to the mitochondria, which subsequently amplifies the apoptotic signal[119] (Figure 1-7).

FIGURE 1-7

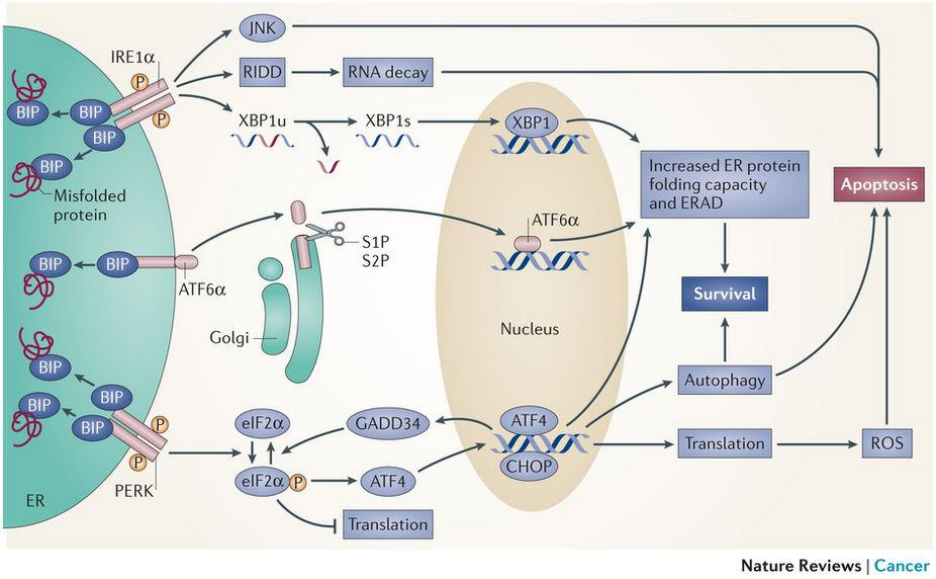

The Unfolded Protein Response. Stress occurring in the ER can arise from misfolded proteins or environmental stressors trigger the unfolded protein response. This pathway is initiated when GRP78/BIP moves to the ER lumen, subsequently activating three distinct branches of the pathway. UPR activation results in global changes to cellular behavior in an attempt to ameliorate the ER stress, or engage in apoptosis. Reprinted from Nature Reviews Cancer, 14(9), Wang M, Kaufman RJ, "The impact of the endoplasmic reticulum protein-folding environment on cancer development", 581–597, Copyright Aug 22, 2014, with permission from Springer Nature (license number: 4304930364341).

Intriguingly, the UPR is induced during and required for osteoblastic differentiation[120], and in the differentiation of other cells with high secretory function such as B-lymphocytes[121]. During homeostasis, hematopoietic stem cells (HSCs) provide extrinsic cues to endosteal MSCs that maintain the stem cell niche in which they both reside[63,122]. Bone morphogenic protein (BMP) -2 and -6 secreted by HSCs prompt osteogenesis in MSCs, and contribute to the balance of bone tissue accomplished by osteoblasts and the bone resorbing osteoclasts[62]. The transitions that occur during osteoblastic differentiation include preparation for increased secretory function, which is achieved by engaging in the UPR. Extrinsic UPR stimulation is also sufficient to promote osteogenesis in MSCs[118]. Cells with high secretory function such as beta cells, B-lymphocytes, and osteoblasts have inherently higher baseline UPR stress due to the increase of protein translation in the ER. BMP signaling promotes osteogenesis in mesenchymal stem cells by stimulating Runx2 expression. This initiation of osteolineage differentiation is accompanied by an increase in the UPR, as the splicing of the Xbp1 transcript by the UPR pathway results in an isoform that is a potent transcription factor that enhances Osterix expression, a critical regulator osteogenesis[120]. Disruption of key facilitators of the UPR, such as the knockout of *Xbp1*, prevents osteogenesis and, conversely, osteogenesis can be induced by exogenous UPR stresses such as low doses of thapsigargin which promotes ER stress via electrolyte disruption[118]. The resultant gene expression changes that result from UPR induction trigger cell fate decisions in cells with multipotent

potential. This is an interesting example of how stress pathways and differentiation cascades are intertwined.

1.7 CONCLUSION

Cancer is the result of the inherit ability within all cells to undergo Darwinian evolution to adapt and proliferate. This aberrant phenomenon within multicellular organisms requires multiple steps of transformation, overcoming intrinsic and extrinsic selection pressures that would otherwise prevent this process from occurring. Leukemias are generated when this occurs within hematopoietic tissue, with AML being a subset of blood cancers that occurs within myeloid cells. Normal and malignant hematopoiesis exists in the bone marrow, a complex tissue containing stromal cells that engage in reciprocal communication with hematopoietic cells, providing extrinsic cues that guide hematopoiesis as well as contribute to leukemic progression, and in some cases, induction.

Cellular signaling is a requirement for maintaining tissue homeostasis. While cells have evolved multiple ways to communicate, the focus of this work is on exosome signaling. This signaling paradigm allows biological information to be packaged within lipid-bound vesicles and transferred to recipient cells in a highly dynamic fashion. miRNA are molecules found to be highly enriched in exosomes, and their transfer to recipient cells can induce broad changes in gene expression due to their ability to directly suppress mRNA targets. My studies also

suggest that the UPR is induced in stromal cells as a result of exosomal signaling. This stress pathway allows cells to ameliorate unfolded and misfolded proteins within the ER, however chronic UPR can also promote apoptosis. The UPR is also a strong contributor to cellular differentiation, with detrimental implications within the tumor microenvironment.

The Chapters herein explore these biological phenomena in the context of AML. Importantly, the mechanisms described above exist in healthy cells and tissues. The successive adaptations occurring during leukemogenesis have altered or exaggerated these processes in a way that increases the fitness of the leukemia, either by direct suppression of competing hematopoietic cells, or through the exploitation of stromal components that reinforce disease progression. In sum, this work explores two various ways that leukemia *corrupts local tissue to promote disease pathophysiology*. These studies open avenues for pharmacological remediation of the alterations occurring within both hematopoietic and mesenchymal stem cell niches in the bone marrow.

1.8 GENERAL HYPOTHESIS AND SPECIFIC AIMS

Currently, AML remains a deadly disease. Despite the success of treatments achieving initial remission, the high rate of relapse keeps the five-year survival rate dismally low. One aspect of AML biology is the tumor's ability to manipulate the resident, nonmalignant hematopoietic and stromal cells within the

bone marrow. These interactions directly and indirectly contribute to suppression of hematopoiesis, a significant comorbidity of AML, and the synthesis of leukemia-supportive niches which reduce the efficacy of therapeutic intervention and complete eradication of disease. The work described in this dissertation attempts to address these issues by investigating the contributions of AML-derived exosomes in the pathophysiology of this disease. The overall hypothesis of this research is that AML-derived exosomes strongly influence the function of recipient cells via trafficking to hematopoietic and stromal tissues; this results in hematopoietic failure and promotes the remodeling of bone marrow niches that support leukemic progression while providing an implicit opportunity to develop a biomarker platform.

SPECIFIC AIMS:

1. *Characterize AML exosome cargo and trafficking*.

The dynamic nature of exosome signaling, particularly in their selective cargo which contains cell-type specific signature of nucleic acids, justifies their exploration in AML. Evaluation of the miRNA profiles of AML-derived exosomes will elucidate both the exploitation of these vesicles as biomarkers, and the regulatory effects in recipient cells.

2. *Identify direct contributory mechanisms that promote cytopenias in resident HSPCs.*

The regulatory potential of miRNA trafficking from AML blasts to HSPC provides a plausible mechanism for the hematopoietic suppression associated with this disease. Understanding how AML produces cytopenias will provide valuable insight into how cancer can directly inhibit parenchymal function. Exploring the broad regulatory potential of trafficked miRNA will shed light on the severity of exosome trafficking within the leukemic microenvironment.

3. *Explore the mechanisms of AML-mediated remodeling of the endosteal niche.*

The stromal components of the bone marrow have been strongly implicated as mediators of disease progression of resistance to therapies. The exploitation of endosteal stromal cells resulting from AML influence contributes to the remodeling of leukemic-supportive niches. The identification of the compositional and functional changes that occurs within discrete stromal populations will provide insight into the synthesis of microenvironments that promote cancer proliferation.

CHAPTER 2: AML-Exosome Cargo and Trafficking

Compiled from:

Hornick, N. I., & Doron, B., et al. (2016). "AML suppresses hematopoiesis by releasing exosomes that contain microRNAs targeting c-MYB." Sci Signal 9(444): ra88. PMID: 27601730

Hornick, N. I., et al. (2015). "Serum Exosome MicroRNA as a Minimally-Invasive Early Biomarker of AML." Sci Rep 5: 11295. PMID: 26067326*

Contributions:

The work contained in this chapter was published in two separate yet related manuscripts. I contributed significantly to both projects and worked primarily under the guidance of Noah Hornick. For the biomarker work published in *Scientific Reports*, I performed the majority of the miRNA qRT-PCR work and analyzed the data. Noah then used these data to construct the ROC curves that identified the efficacy of serum exosome miRNA as a biomarker. The RISCtrap data from our publication in *Science Signaling* was generated through a joint effort between Noah and me to generate the mRNA for sequencing. He analyzed the data to generate the interaction map, and I performed the molecular experiments that validated his *in silico* work.

2.1 ABSTRACT

Signaling via exosomes has increasingly become appreciated as a major mode of cellular communication as these vesicles can equilibrate in and between tissue compartments, and can be isolated from many body fluids. In normal tissue, exosomal crosstalk contributes to homeostasis maintenance, but cancer cells can use exosomal signaling to increase their fitness within the niche. Here, we examined the exosomal cargo of healthy hematopoietic cells and AML cells in the context of their miRNA profile, and show that leukemogenesis produces an altered exosomal miRNA composition. Importantly, these differences can be exploited for use as a noninvasive biomarker of residual disease in AML patients, with the goal of earlier identification of relapse. We identified a set of miRNA

enriched in AML exosomes and track levels of circulating exosome miRNA that distinguish leukemic xenografts from controls. With their robust capacity to actively modulate transcriptional landscapes, miRNA trafficking via exosomes has major implications within bone marrow niches and in the successive microenvironment adaptations that occur during leukemogenesis. To model the consequences of exosomal miRNA trafficking, we conducted the RISCtrap experiment with miR-155, a miRNA highly enriched within AML exosomes. Not only did the RISCtrap identify novel mRNA targets of miR-155, but further analyses show that exogenous delivery of this miRNA has broad consequences in recipient cells. Together, this work demonstrates that cancer cells adopt differential exosomal cargo, these differences can be utilized as a diagnostic tool, and miRNA trafficking via exosomes can exert expansive effects within recipient cells.

2.2 INTRODUCTION

AML causes more than 10,000 deaths annually in the United States, with a 5-year overall survival rate of approximately 25%[123]. Induction treatment of AML achieves disease remission in up to 80% of patients, yet a majority experience relapse. This, along with the aggressive kinetics of relapsing AML[32], underscores the need for improved early detection of residual disease after chemotherapy, as relapse remains the major cause of mortality for these patients. Improved tracking of minimal residual disease (MRD) holds the promise

of timely treatment adjustments to preempt relapse. Unfortunately, current surveillance techniques used to detect circulating blasts poorly reflect MRD during the early stages of relapse.

Deep sequencing of exosomes has revealed the existence of a vast array of RNA species within them[124]. As discussed in Chapter 1, the RNA content of exosomes is not a proportional reflection of the transcriptome of the cell, but exhibits enrichment and exclusion of specific transcripts[109,125]. During leukemogenesis, the global changes to the transcriptome and endosomal machinery are reflected in both exosomal output and cargo composition[109]. As such, the unique content of AML-derived exosomes provides the opportunity for the use of these vesicles as biomarkers for the detection cancer relapse[126]. As they equilibrate with the bloodstream, circulating exosomes provide a minimally invasive source of substrate for relapse detection[127].

Here, we investigate exosomes as a minimally invasive platform for a miRNA biomarker. Following the identification of a set of miRNA enriched in AML exosomes, I track levels of circulating exosome miRNA from peripheral blood draws that distinguish leukemic xenografts from both non-engrafted and human $CD34^+$ controls. Biostatistical models reveal circulating exosomal miRNA can be detected at low marrow tumor burden and before returning AML blasts begin to circulate in the periphery.

The broad regulatory potential of miRNA results from the requirement of only a small degree of complementarity with their target mRNA, thus, a single

miRNA transcript can regulate many different targets[111]. We wanted to explore the prospective mRNA targets of miR-155, one highly enriched miRNA found in AML exosomes. To complement the computational prediction of miRNA targets, we used a biochemical assay designed to identify miRNA targets by combining immunoprecipitation of attenuated RISC-complexes with next generation RNA sequencing. This assay, named the RISCtrap, reveals a panel of novel miR-155 targets that were not predicted using multiple *in silico* algorithms. We then biochemically validate these transcripts to confirm that they are indeed *bona fide* targets of miR-155.

Finally, we aimed to visualize the expansive effects of exogenously delivered miRNA to the transcriptome of recipient cells. To this end we utilized the RISCtrap dataset together with a protein interaction algorithm to create a network of direct and indirect targets of miR-155 that reflects the overall impact of a transferred miRNA on a recipient cell. In total, this work reveals the changes in exosomal cargo as a result of leukemogenesis, how this phenomenon can be leveraged as a diagnostic tool, and illustrates the potential regulatory effects of miRNA trafficking within tumor microenvironments.

2.3 RESULTS

Leukemia exosomes contain discrete, predominantly mature miRNA

In order to identify miRNA transcripts that are specifically upregulated in leukemic exosomes, we made a global comparison of the cellular and exosomal miRNA composition of the AML cell lines HL-60 and Molm-14, and nonmalignant cord blood-derived $CD34^+$ cells. This analysis allowed us to determine the miRNA transcripts that get included and excluded from exosome packaging, and differences in the relative abundancies of these transcript between healthy human HSCs, and leukemic-transformed cell lines. A miRNA microarray evaluation of these samples revealed clear distinctions between both cells and exosomes as well as between malignant and nonmalignant exosomes (Figure 2-1A), a position further strengthened by principal component analysis (Figure 2-1B). These data reinforce the notion that cells conduct active enrichment and exclusion of specific miRNA transcripts into exosomes. Comparing array probes for mature miRNA to those for less-processed pre-miRNA revealed that the vast majority of the miRNA trafficked within exosomes is mature, and could function inside a recipient cell without further processing (Figure 2-1C).

FIGURE 2-1

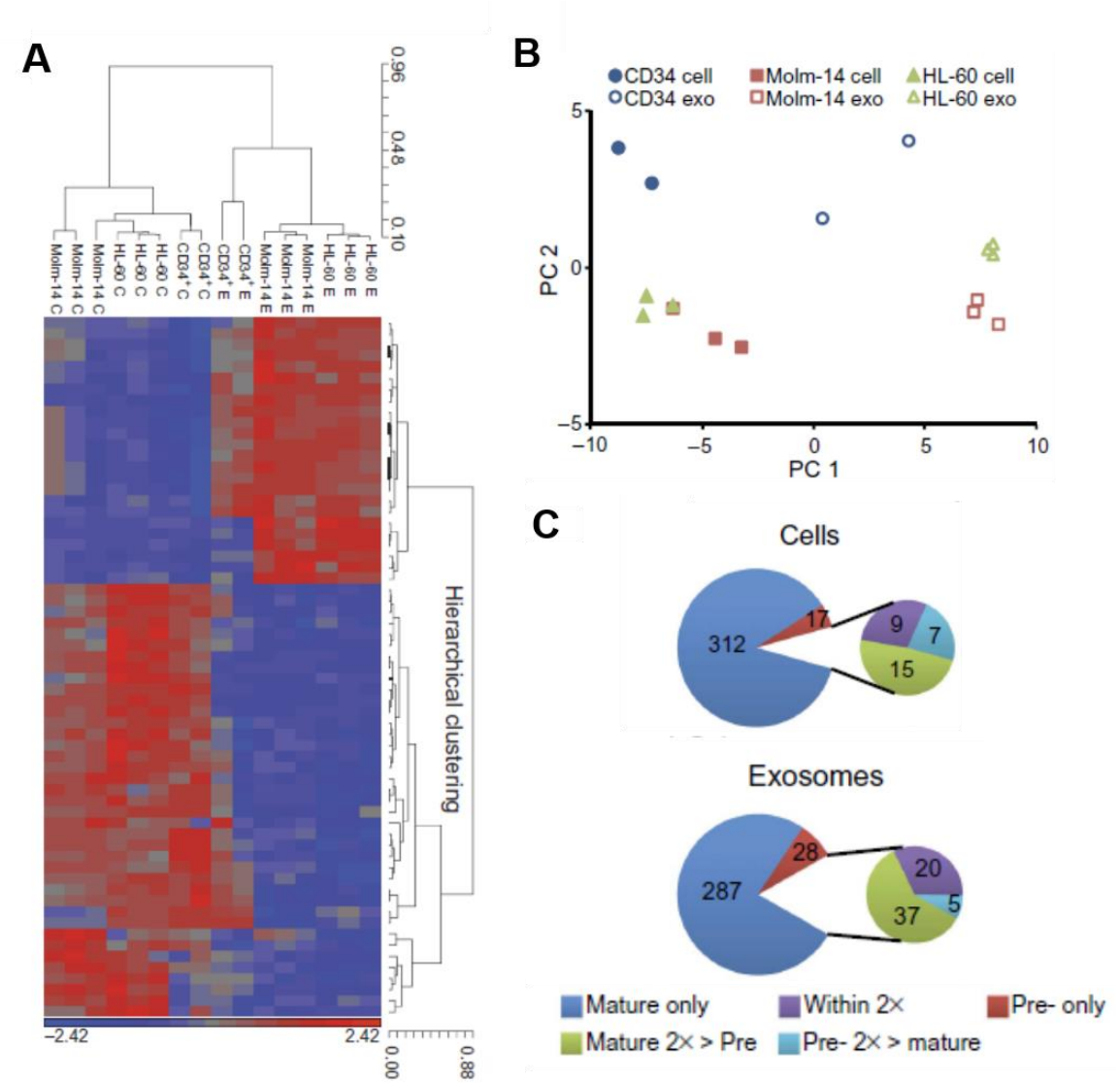

Leukemia Exosomes Suppress HSPC Function and are Enriched with Specific miRNA Transcripts. A. *Microarray comparison of cell, exosome miRNA*. Molm-14, HL-60, and nonmalignant human CD34⁺ cell and exosome microRNA was evaluated using an Affymetrix microRNA microarray. All targets with more than 2-fold mean difference between producing cell and exosome are represented, RMA-corrected and standardized to a mean of 0 and a SD of 1. Dendrogram values are 1 - Pearson's R. **B.** *Principal component analysis*. PCA performed after gene selection for all (63) targets detected in all samples and demonstrating significant (FDR < 0.05) enrichment in leukemic exosomes vs cells. **C.** *Comparison of mature and pre-miRNA levels in Molm-14 cells and exosomes as detected by microarray*. Signal levels of probes for individual miRNA and their associated pre-miRNA measured in Molm-14 cells and exosomes were compared and sorted into categories.

The unique exosomal composition of AML cells provides biomarker potential

To develop an *in vivo* exosome biomarker platform we collected blood from Molm-14 xenograft and control NSG mice and extracted exosomes from the serum. In a series of experiments comprising more than sixty mice, we systematically determined serum levels of four candidate miRNA chosen for their relevance to leukemia[128-130] and incorporation in exosomes miR-150, miR-155, miR-221, and miR-1246 (Figure 2-1A). Using Molm-14-engrafted animals at 14 days (d14) and 21 days (d21) post-engraftment as experimental groups, we compared the levels of these miRNA against unengrafted NSG mice and healthy human CD34+ cell xenografts. In spite of the anticipated substantial inter-animal variability, this panel of miRNA was reproducibly distinguished between cohorts. miR-155 was elevated in Molm-14- and CD34+-engrafted animals but not NSG controls, miR-150 separated Molm-14 from CD34+ engraftment, miR-221 was altered at late but not early leukemia time points, and miR-1246 increased over time in leukemia-, but not nonmalignant CD34+ cell-engrafted mice (Figure 2-2A). To test statistical strength, models of receiver operating characteristic (ROC) were generated by logistic regression. These highlight the added discriminatory capacity conferred by combining the top performing markers (Figure 2-2B). We scored serum exosome miRNA from a separate validation set of animals engrafted with human cord blood-derived $CD34^+$ cells or with Molm-14, then treated with ara-C at 14 days post-engraftment. In order to determine the potential discriminatory capacity of a set cutoff value, we sorted the scores generated by measuring serum exosomal miRNA in the validation set. We then

chose three separate scores (circled in Figure 2-2B) statistically emphasizing sensitivity, specificity, or a balance of the two, based on the observed values in this cohort. Optimizing sensitivity or specificity allowed complete elimination of false negatives or false positives, respectively, while balancing the two in choosing a cutoff value resulted in detection of 8/9 leukemias with only 1/4 controls being scored positive (Figure 2-2C). These results demonstrate both the reproducibility of alterations in serum exosomal miRNA as a marker of leukemia and the independence of this score from both treatment and the level of circulating blasts.

The RISCtrap exposes novel targets of miR-155

The active loading of multiple miRNA species into exosomes suggest that exosomes deliver highly complex cargo to recipient cells. Before delving into the reductionist approach of measuring the consequence of a single miRNA:mRNA interaction (the content of Chapter 3), we evaluated the effects of miR-155 in an effort to identify the entire “targetome” of this miRNA. For these experiments, we chose the RISCtrap for its ability to provide an unbiased target set based on active binding of mRNA by loaded RISC complexes[131]. miRNA targets are identified by immunoprecipitation of a dominant-negative RISC complex co-expressed with the miRNA of interest, extracting and sequencing the complexed mRNA, and comparing results to those obtained using two distinct miRNA (Figure 2-3A).

FIGURE 2-2

A

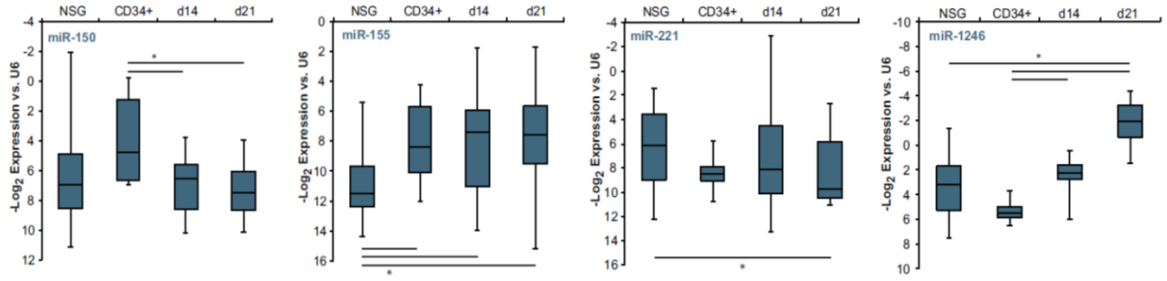

B

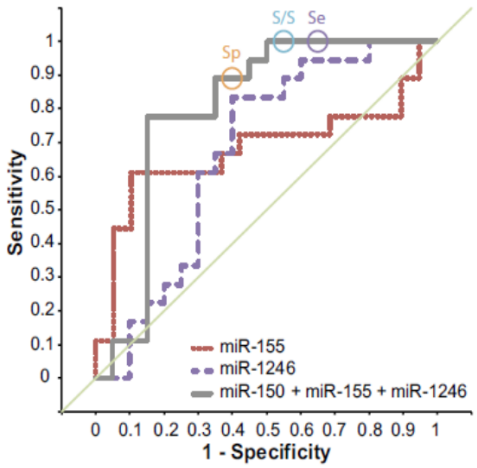

C

For Specificity (Sp):

Cohort	Positive	Negative	%CD45+
CD34+	0/4	4/4	0-0.1%
pre-Tx	4/9	5/9	<0.1%
End of Tx	5/9	4/9	0.1-1.5%
1 wk Post-Tx	5/9	4/9	0.1-23.0%

Balance Sensitivity / Specificity (S/S):

Cohort	Positive	Negative	%CD45+
CD34+	1/4	3/4	0-0.1%
pre-Tx	5/9	4/9	<0.1%
End of Tx	8/9	1/9	0.1-1.5%
1 wk Post-Tx	8/9	1/9	0.1-23.0%

For Sensitivity (Se):

Cohort	Positive	Negative	%CD45+
CD34+	2/4	2/4	0-0.1%
pre-Tx	7/9	2/9	<0.1%
End of Tx	8/9	1/9	0.1-1.5%
1 wk Post-Tx	9/9	0/9	0.1-23.0%

Serum exosome miRNA distinguishes leukemia from homeostatic hematopoiesis. **A.** *Serum miRNA exosome levels*. Exosomes were isolated from peripheral blood of control NSG mice as well as NSG mice engrafted with Molm14 after 14 or 21 days (d14, d21, respectively) or human CD34$^+$ cells. miRNA levels were measured by qRT-PCR. Significance determined by ANOVA and Student's t-test. **B.** *Serum exosome miRNA score performance*. Receiver operator characteristic (ROC) curves are presented for a single miRNA and for the combination of miR-150, -155, and -1246. The circles represent points on the ROC curves whose alpha values were chosen as cutoff values emphasizing specificity, sensitivity, or a balance of the two, respectively. **C.** *Exosome miRNA panel performance*. The cutoff values and the coefficients generated were used to evaluate mice engrafted with Molm-14 and treated with cytarabine, alongside control mice engrafted with human CD34$^+$ cells. Performance for each cohort and cutoff is presented alongside peripheral blood chimerism, determined by flow cytometry analysis of human CD45$^+$ cells in the peripheral blood.

Transcripts significantly enriched in the samples derived from cells transfected with the miRNA of interest are identified through statistical analysis[131]. For this study we compared miR-155 targets against miR-132 and-137. We collected targets from the miR-155 RISCtrap data and compared them to the lists of *in silico*-predicted targets available through miRWalk[132] (Figure 2-3B). The RISCtrap results contained transcripts previously verified as miR-155 targets (including *Bach1*, *Cebpβ*, and *Tab2*[133]), those predicted by miRWalk (including *Abi2* and *Tet1*), and those neither verified nor predicted (such as *Chek2*, *Chordc1*, *Nbea1*, and *Znf431*) which we validated using a dual-luciferase assay designed to quantitatively validate specific miRNA silencing of MRE-containing transcripts (Figure 2-3C).

Exogenous miR-155 has direct and indirect consequences in recipient cells

Intrigued by the broad regulatory potential of many of these targets, we created an overview of the different interconnected pathways that transferred miR-155 could be expected to impact. In order to accomplish this we chose the STRING protein interaction database as a central repository of information about regulatory networks [134]. Using the 100 most enriched mRNA detected in the miR-155 dataset as input (Table 2-1), we collected the set of interactions contained within STRING that involved these proteins. Using Cytoscape software[135], we filtered the dataset for experimentally validated interactions of human proteins, and removed those nodes with only one interaction. This revealed a central network of proteins directly regulated by miR-155, and the

interacting partners of those proteins (Figure 2-3D). Altogether, our analysis yielded compelling insights regarding the activity of miR-155. In addition to its numerous well-studied direct targets, miR-155 may indirectly manipulate the actions of several proteins with established roles in malignancy (TP53, BRCA1, MYC[136-138]) and/or hematopoiesis (CTNNB1, RUNX1, MLL[139-141]). For proof of principle, we demonstrated the indirect effect of exogenous miR-155 activity by analyzing the phosphorylation of p53 in HEK293T cells transfected with miR-155, cel-miR-67, or vehicle. CHEK2 has been shown to activate p53[142] and miR-155-mediated decrease of CHEK2 would therefore reduce phosphorylation on serine-20 of p53. Indeed, exogenous introduction of miR-155 reduces p53 phosphorylation at this residue (Figure 2-3E). Together, these data demonstrate the dynamic activity of miRNA trafficking, and its influence on both direct and indirect targets in recipient cells.

2.4 DISCUSSION

Our microarray investigation demonstrated that both leukemogenesis and exosome production exert dramatic selection bias on miRNA composition. Consistent with a report that exosomes contain elements of the miRNA processing machinery[143], miRNA contained within exosomes were found to be predominantly fully processed, with a minority representation of pre-miRNA. The mechanisms by which selection is accomplished remain under investigation. One group showed that miRNA contain sequence motifs that cooperate with a

FIGURE 2-3

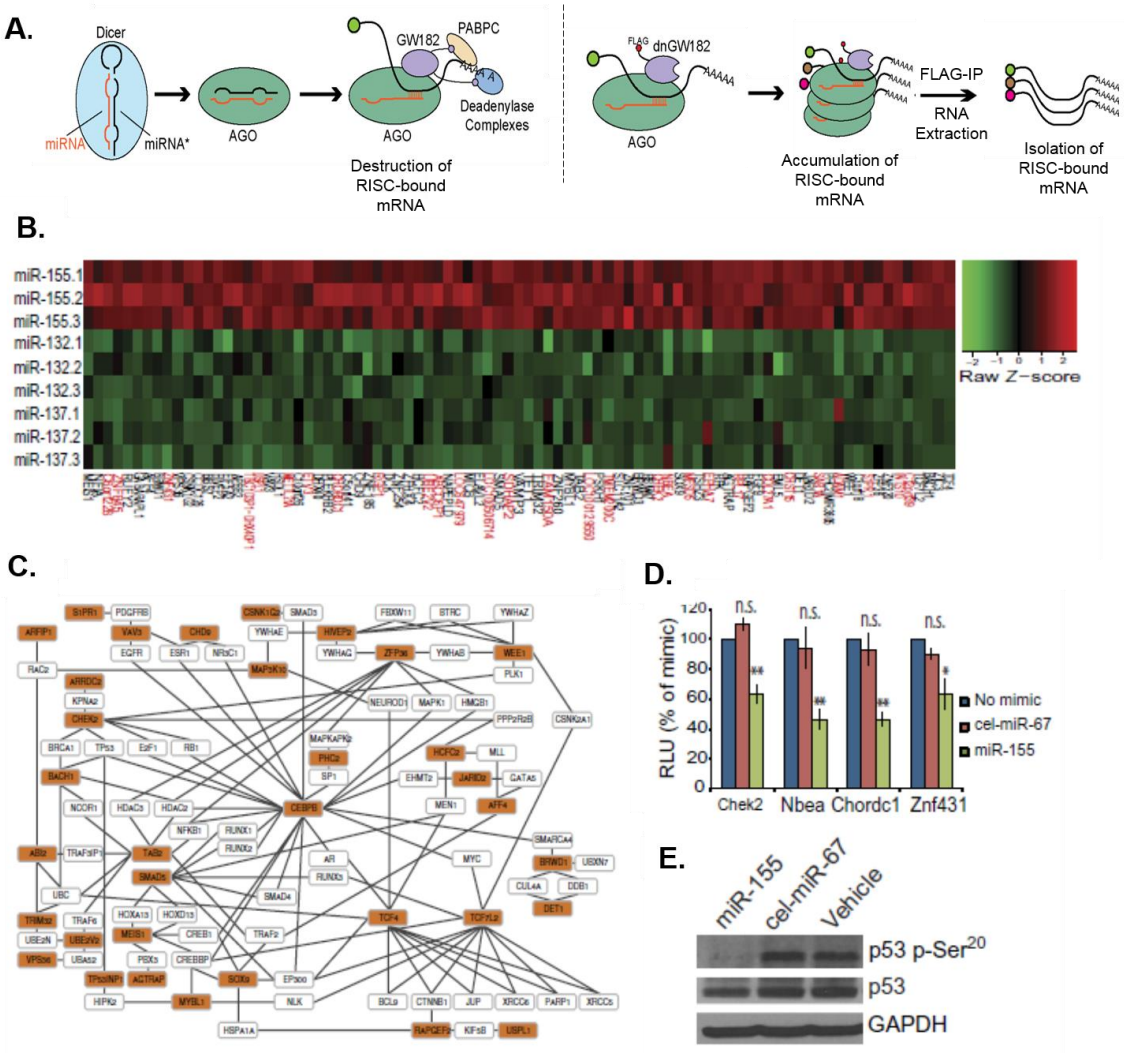

Figure 2-3. Exosome miRNA Target Networks Overlap at Key Hematopoietic Regulators. **A.** *Schematic representation of the RISCtrap assay*. Left: RISC-mediated mRNA silencing. Right: overexpression of dnGW182 (RISCtrap) results in the binding of and accumulation of mRNA in the RISC complex. Immunoprecipitation of FLAG-tag and subsequent RNA extraction enriches for RISC-bound transcripts. **B.** *RISC-Trap identifies both novel and predicted targets of miR-155.* The RISC-Trap assay was performed in HEK-293T cells, comparing miR-155 to miR-132 and -137 as controls. Targets in red were not predicted by any *in silico* prediction algorithms. **C.** *STRING database identifies interacting partners of miR-155 targets*. The targets in (**A**) were used as input for a query to the STRING protein interaction database. The results were filtered by species and interaction detection method, and then leaf nodes were removed. The remaining connected nodes were color-coded and presented. Orange: direct targets of miR-155; white: indirect targets of miR-155. **D.** *Novel targets from the miR-155 RISC-Trap data set were validated with the dual-luciferase assay.* Significance determined by paired t-test. **E.** *miR-155 reduces phosphorylation of p53 indirectly by suppression of CHEK2.* HEK293T cells were transfected with miR-155, cel-miR-67, or vehicle and lysates were generated 48 hours later. Western blots against phosphorylated serine 20 of p53, p53, and GAPDH were performed.

TABLE 2-1

ABCC6P1	FGF9	S1PR1
ABI2	FOXE1	SAR1A
ADAM1	G2E3	SDHAP1
AFF4	GABARAPL1	SDHAP2
AGTRAP	GALT	SDHAP3
APBB2	GOLGA2P5	SLC11A2
ARFIP1	HCFC2	SMAD5
ARL5B	HDAC4	SOX9
ARRDC2	HIVEP2	TAB2
BACH1	HOMEZ	TBC1D14
BBS7	HOXD9	TBRG1
BLZF1	HSDL1	TCF4
BNC2	IER5	TCF7L2
BRWD1	INTS10	TET1
BRWD3	JARID2	TMEM200C
C10orf12	KLHDC5	TMTC2
C10orf26	LOC100129550	TP53INP1
C12orf39	LOC100506714	TRIM32
C2orf18	LOC647979	TRIM36
C3orf18	LRP12	TSHZ3
C5orf41	MAP3K10	UBE2V2
C6orf228	MEIS1	URB2
CCDC126	METTL21A	USP31
CEBPB	MFSD5	USPL1
CHD9	MICB	VAMP3
CHEK2	MYBL1	VAV3
CHORDC1	NAPEPLD	VPS36
CHST15	NBEA	WEE1
CKMT1A	NFIA	YLPM1
CNNM1	NKD1	ZFHX4
COL27A1	NKX3-1	ZFP36
CSNK1G2	PHC2	ZIC3
DCK	PIP5K1B	ZIC5
DET1	PLAG1	ZNF185
DHX40	PLEKHB2	ZNF254
DSG2	PRDM15	ZNF260
EIF5A2	PREX2	ZNF320
ELAVL2	PSKH1	ZNF431
EML5	RAPGEF2	ZNF468
EPHA7	RBM47	ZNF652
ETV3	RFK	ZNF701
FAM150A	RGP1	ZNF845
FAM69A	RUFY2	

The top transcripts identified by the miR-155 RISCtrap assay. Transcripts enriched >2x in the miR-155 RISCtrap assay, in alphabetical order. Targets in green are those not predicted by the miRWalk database, validated genes are circled in red. The transcript encoding c-MYB was identified as a target below the enrichment cutoff threshold used for network analysis.

sumoylated heterogenous ribonucleoprotein A2B1 (hnRNPA2B1) to selectively sort miRNA into exosomes. Similarly, cis elements on mRNA transcripts have also been identified as correlated with exosomal sorting. One study demonstrated the interplay between miRNA and mRNA in the sorting efficiency of transcripts and another study showed the presence of miRNA:RISC complex within exosomes, although advanced techniques for the isolation of exosomes are suggesting that this may not be the case[144,145]. There is broad evidence that sorting is dependent upon both *cis* and *trans* elements, and we speculate that RNA epigenetics may also influence the destination of miRNA transcripts, although this field remains highly understudied.

Sampling of body fluids (e.g. blood, urine, saliva) provide minimally invasive sources of exosomes, allowing more frequent screening, and potentially earlier detection. We propose development of serum exosome miRNA as a platform for a novel, sensitive compartment biomarker for prospective tracking and early detection of AML recurrence. Current methodologies do not perform well at later time points, in part because conventional detection of relapse is based on identifying leukemia at the cellular level[22]. Peripheral blood assays require the presence of leukemic blasts in the circulation, which generally connotes advanced disease burden, while bone marrow aspirates are invasive and rely on a sample from a single physical location. Additionally, both flow cytometry and PCR require the presence of a known leukemia-specific marker. Unlike BCR-ABL1 in chronic myeloid leukemia[43], AML lacks a molecular marker whose detection specifically identifies the malignant cells. Combined, these features have to date precluded the development of a clinically useful and timely prospective surveillance strategy.

While cytokines[146] and circulating cell-free nucleic acids[147,148] have been explored for MRD tracking, and more recently, microRNA (miRNA) have attracted attention as a potential source of novel AML biomarkers[149,150]. MicroRNA expression profiles have been associated with AML subtypes[151], mutations[152], and overall survival[153]. Because exosomes secreted by AML[109], carrying a select panel of cellular RNA and protein[125,154], their potential as biomarkers is beginning to be explored[126,127,155]. Detection of serum exosome miRNA circumvents both the need for an invasive marrow aspiration procedure

and the reliance on the presence of leukemic blasts in the periphery. While the endothelium presents a barrier to leukemia cell egress from the marrow[156], exosomes are able to equilibrate with the bloodstream[157], and thus are detectable in systemic circulation. Based on our findings that AML blasts secrete exosomes that contain a unique miRNA composition, leukemia patient serum should contain exosomes bearing a miRNA profile that could potentially identify AML at early stages of relapse. Accordingly, my experiments demonstrate reproducible miRNA perturbations in peripheral blood exosomes, while less abundant AML-specific mRNA transcripts could not be detected in AML exosomes, even with substantial peripheral blood chimerism. The microarray and qRT-PCR experiments we performed allowed us to derive a panel of miRNA that were not only exported in exosomes by AML, but correlated with the presence of leukemia. These experiments provide a platform for the development of clinical AML biomarkers with the potential to provide improved detection of occult disease in a minimally invasive methodology.

The RISCtrap approach is an ideal tool to dissect the overall impact of leukemic exosomal miRNA on the marrow microenvironment as it captures potential interactions of miRNAs carried in exosomes with endogenous target host cell transcripts. This was powerfully demonstrated by my analysis of the global miR-155 transcript target set, which included several novel targets with regulatory potential that were not bioinformatically predicted[142,158]. These data sets, combined with interaction data from STRING database, created a model that reflects the overall impact of a transferred miRNA on the recipient cell. The

network presented in Figure 2-3C represents one simple approach to assembling such a model. From the arguably limited starting point of the target set of one transferred miRNA, applying informatics provides a broadened perspective, illustrating how the actions of pivotal oncogenes, tumor suppressors, and transcription factors become indirect targets via their interacting partner proteins. Combining this information with transcriptome analysis of the different potential recipient cell types enables the development of predictive algorithms to dissect cell-cell signaling events. The tools described herein can be readily adapted to the systematic analysis of exosomal miRNA regulation in other niche cell populations.

In aggregate, we demonstrate that leukemogenesis drives changes in the composition of exosome cargo, which provides an exploitable opportunity for the development of AML biomarker platform. Combined with the feasibility of isolating exosomal miRNA from small volumes of serum, we predict that with advanced sequencing or miRNA identification techniques will propel the translation of this concept to the clinic, whereby physicians can monitor patients in remission for early signs of relapse, and intervene accordingly. Beyond this biomarker potential, we demonstrate that the miRNA cargo with AML-derived exosomes can have severe influence on recipient cells. This can occur through the direct suppression of critical mRNA targets, or indirectly, by affecting the expression or function of downstream interactors of miRNA-targeted transcripts.

2.5 MATERIALS & METHODS

Cell lines and cell culture

AML cell lines (HL-60, Molm-14, U937) were provided by Dr. Jeffrey Tyner and cultured in RPMI (Invitrogen) with 10% vesicle-free (VF-) FBS. VF-FBS was produced by centrifugation of FBS (Gemini Bio-Products) at 2,000g for 20 min, at 10,000g for 20 min, and at 100,000g for 2 hours.

Mice and xenografts

NOD/SCID/IL-2rγnull mice (NSG) were purchased from The Jackson Laboratory. Animals 6–8 weeks old were used in the experiments. 1×10^5 Molm-14 cells/human cord blood-derived $CD34^+$ cells or 5×10^6 HL-60 cells per animal were engrafted into non-irradiated animals by intravenous tail-vein injection. Retroorbital blood draws were conducted as necessary to obtain serum exosomes or peripheral blood for human CD45 chimerism analysis by flow cytometry. Animals were sacrificed at indicated time points, and peripheral blood, spleen, and bone marrow were collected from each animal. For cytarabine-treated animals, cytarabine was administered by intraperitoneal injection at 300 mg/kg every third day for three total injections48 starting 14d post-engraftment.

Vesicle preparation

Vesicles were isolated from cell lines and primary cells after 48-72 hours in

culture via centrifugation at 300g for 10 min. The supernatant was sequentially centrifuged at 2,000g for 20 min, at 10,000g for 20 min, and at 100,000g for 2 hours. Exosomes from NSG serum were extracted using ExoQuick (System Biosciences). Although polymer-based exosome extraction technologies (such as ExoQuick) may co-precipitate other proteins and vesicles, I selected ExoQuick as a translatable means of obtaining enriched exosome-derived RNA from small-volume biological samples.

RNA analysis, cDNA synthesis, and qRT-PCR

RNA was extracted using miRNeasy (Qiagen) or RNeasy (Qiagen) kits and quantified using a Nanodrop 2000c. RNA integrity was measured using the Agilent Bioanalyzer 'Pico Chip' or 'small RNA Chip' (Agilent). For miRNA quantitation, TaqMan assay kits (Applied Biosystems) were used for both reverse transcription and qRT-PCR, normalized to U6 snRNA.

Microarrays

Microarray assays were performed in the OHSU Gene Profiling Shared Resource. For each sample, 130 ng of total RNA was labeled using the Flash-Tag Biotin HSR miRNA Labeling Kit (Affymetrix) by polyadenylation and ligation with biotinylated 3'DNA dendrimers. Labeled RNA was mixed with hybridization controls and incubated overnight with the GeneChip miRNA 3.0 array (Affymetrix) as per manufacturer recommendations. Arrays were scanned using

the GeneChip Scanner 3000 7G with autoloader (Affymetrix). Image processing was performed using Affymetrix GeneChip Command Console software followed by analysis with Expression Console software (Affymetrix). Array performance and general data quality were assessed using Signal All, mean background intensity, number of detected probe sets, % P, all probe set mean, all probe set standard deviation, all probe set RLE mean, and % species specific small RNA probe sets detected. All arrays passed standard performance quality thresholds.

Microarray statistical analysis and data visualization

Individual array data (.cel files) were uploaded to R software package and analyzed using Bioconductor's Oligo package. Normalization was conducted on all samples in a single set using RMA Background and Quantile Normalization sub-routine. Signal intensities were log2 transformed and probe set values summarized using Median Polish Summarization Method. Final data set included paired samples from exosome and cell samples. Further analysis included 3391 mature and pre-mature human miRNA probe sets. Data visualization tools (e.g., box plot, hierarchical clustering, matrix plots and multi-dimensional scaling) were used to assess general data quality and outliers. To determine differentially expressed miRNA genes, the mixed model was used to assess differences in miRNA probe expression between exosome samples and cell samples. Unadjusted statistical significance was set at $p \leq 0.05$ with FDR correction at $p \leq 0.05$ for multiple testing where relevant. Fold Change values of 2.0 Ire used as a cut-off to identify up- and down-regulated probes.

Normalized log2 transformed signal data for all human mature miRNAs were imported into Partek Genomics Suite 6.6 software and filtered to include only miRNA signal data of interest prior to generating individual heat maps. The Tools Discover Hierarchical Clustering subroutine was invoked to create each clustered heat map. Samples and miRNA Ire clustered using Pearson's Dissimilarity as the measure of distance with complete linkage.

For principal component analysis, normalized log2 transformed signal data was imported into R following gene selection performed based upon significant differences between leukemic cell and exosome samples as described above. This data was used to generate principal component values, which were then exported to Microsoft Excel for visualization.

RISC-Trap

RISC-trap experiments of miR-155, miR-137 and miR-132 and data analyses were performed as previously described)[159], except that reads for each gene were counted by HTSeq[160]. The cutoffs for determining the final list of miR-155 targets were >= 2-fold change and false discovery rate (FDR) <= 15%. The heatmap was plotted using gplots, an R package.

MicroRNA Target Validation

3'UTR of each target was PCR amplified from HEK293T or primary murine c-Kit$^+$ genomic DNA and cloned into pSI-Check2 vector (Promega). 100ng of pSI-Check2 vector and 2nM of microRNA mimic (Dharmacon) were cotransfected into 4x10^5 HEK293 cells that were seeded in a 12-well dish. Cells were washed

in PBS 48 hours post transfection and lysed according to the manufacturer's protocol for Dual Luciferase (Promega). Firefly and Renilla luminescence were measured with a Berthold Centro XS3 LB 960 Luminometer, and relative luminescence was compared to relative luminescence of pSI-Check2 construct transfected without mimic to generate percent knockdown. Technical triplicates were performed for each biological replicate. Error bars represent the SEM from three biological replicates.

CHAPTER 3: AML-Exosome Impact on Hematopoietic Progenitor Cells

Compiled from:

Hornick, N. I., & Doron, B., et al. (2016). "AML suppresses hematopoiesis by releasing exosomes that contain microRNAs targeting c-MYB." Sci Signal 9(444): ra88. PMCID: 27601730

Contributions:

The work in this chapter is derived from our manuscript in *Science Signaling*. The majority of the molecular experiments described here were performed by me. These include the miRNA validation experiments, the clonogenicity assays, and the siRNA electroporations. The generation of xenografts and chimerism analyses were a joint effort by members of the Kurre lab.

3.1 ABSTRACT

Cellular signaling between tumors and their nonmalignant neighbors prompts the development of microenvironments that increase the fitness of the developing cancer. We wanted to explore the direct signaling between AML and HSPCs, and identify link the direct signaling pathway between these populations to the hematopoietic suppression observed in our xenografts and in patients with this disease. Exosomes are paracrine regulators of the tumor microenvironment, but their complex cargo precludes a mechanistic understanding of their action in target cells. Here, we demonstrate that the leukemic erosion of hematopoietic function is conferred by exosome-mediated microRNA trafficking into HSPC, and results from specific translational suppression of the transcription factor c-Myb in HSPCs. Through a series of experiments that segregate microRNA contributions, we show that exosomal delivery of miR-150 and miR-155 impairs HSPC function through translational suppression of c-Myb, an intrinsic regulator of homeostatic HSPC function and differentiation. This work provides mechanistic insight into

how leukemic exosomes regulate the suppression of hematopoiesis through direct signaling with HSPC.

3.2 INTRODUCTION

The progression of AML promotes collateral suppression of normal hematopoiesis, leading to anemia, neutropenia, and thrombocytopenia (collectively known as cytopenia)[36], which are comorbidities that plague patients with the disease. Traditionally, this has been ascribed to successive marrow infiltration by leukemic blasts and resultant overcrowding[161], an explanation that fails to address the occurrence of cytopenias in patients with normal marrow cellularity, or more rarely, in those with exclusively extramedullary AML. Recent experimental work shows that leukemic invasion interferes with residual hematopoietic stem cell (HSPC) function,[162,163] and causes extensive remodeling of the marrow microenvironment[68,164]. Thus, the aggregate clinical and experimental observations suggest active regulation, but the specific mechanisms remain elusive.

Given their selective enrichment in exosomes and broad regulatory potential, exosomal transfer of miRNA directly from leukemic blasts to HSPCs represents a plausible explanation for the observed suppression of hematopoiesis in the leukemic microenvironment.

Here, we demonstrate AML-driven systemic suppression of hematopoiesis through coordinated action of exosomal miRNA trafficking to HSPC. By utilizing the exosomal microarray data (Figure 2-1A), we identify discrete miRNA species that are sufficient to impede hematopoiesis when introduced into HSPC. This reductionist approach provides the mechanistic detail describing the effects of miRNA-mediated suppression of a single target gene. Considering the broad regulatory potential of miRNA (Figure 2-2B), one can appreciate the magnitude of exosomal trafficking of these molecules within homeostatic and malignant niches.

3.3 RESULTS

Systemic Impairment of Hematopoiesis by Leukemia Exosomes

In order to accurately track *in vivo* engraftment and distribution of leukemia, we utilized Molm-14 cells modified to constitutively express both firefly luciferase (*luc*) and myristoylated-GFP (*mGFP*). The myristoylation motif on GFP causes the integration of the fluorophore into the lipid membranes of the producing cell, enabling the tracking of secreted exosomes. Using the expression of luciferase, we quantitated the engraftment of Molm-14 in immunocompromised NSG mice through *in vivo* imaging (Figure 3-1A). Bone marrow aspirates of engrafted mice allowed for correlation of *hsa*-CD45 expression with the luminescence data (Figure 3-1B), as well as the imaging of purified *mmu* c-Kit$^+$, Sca-1$^+$, Lin$^-$ (KSL) HSPC, which contained GFP$^+$ vesicles in the cytosol of these cells (Figure 3-1C). To demonstrate the systemic effects of AML on

hematopoietic function, we exposed murine c-Kit$^+$ HSPC to serum from mice xenografted with either Molm-14 or HL-60. *In vitro* serum exposure significantly reduced clonogenicity in colony forming assays. To implicate the exosomal fraction as the mediator of this phenotype, we exposed c-Kit$^+$ HSPC to exosomes harvested from Molm-14 xenograft serum and observed a similar loss in clonogenicity (Figure 3-1D). Finally, we performed contralateral intrafemoral injections with purified serum exosomes from Molm-14 xenografts into naïve NSG mice. c-Kit$^+$ cells were harvested from each femur 48 hours post injection and a decrease in clonogenicity was observed in the exosome-treated condition. This was observed in mice receiving intravenous injection of HL-60 exosomes, but not Molm14 exosomes, possibly due to systemic dilution within the animal (Figure 3-1E).

Exosome-Delivered miRNA Downregulate Critical Hematopoietic Regulators, Including c-Myb.

To address the hypothesis that exosome delivery of miRNA contributes to the reduction in colony forming capacity of murine HSPC, we examined the relationship between exosome dose and suppression of clonogenicity. We exposed murine HSPC to exosome dilutions prepared from HL-60 cultures. After

FIGURE 3-1

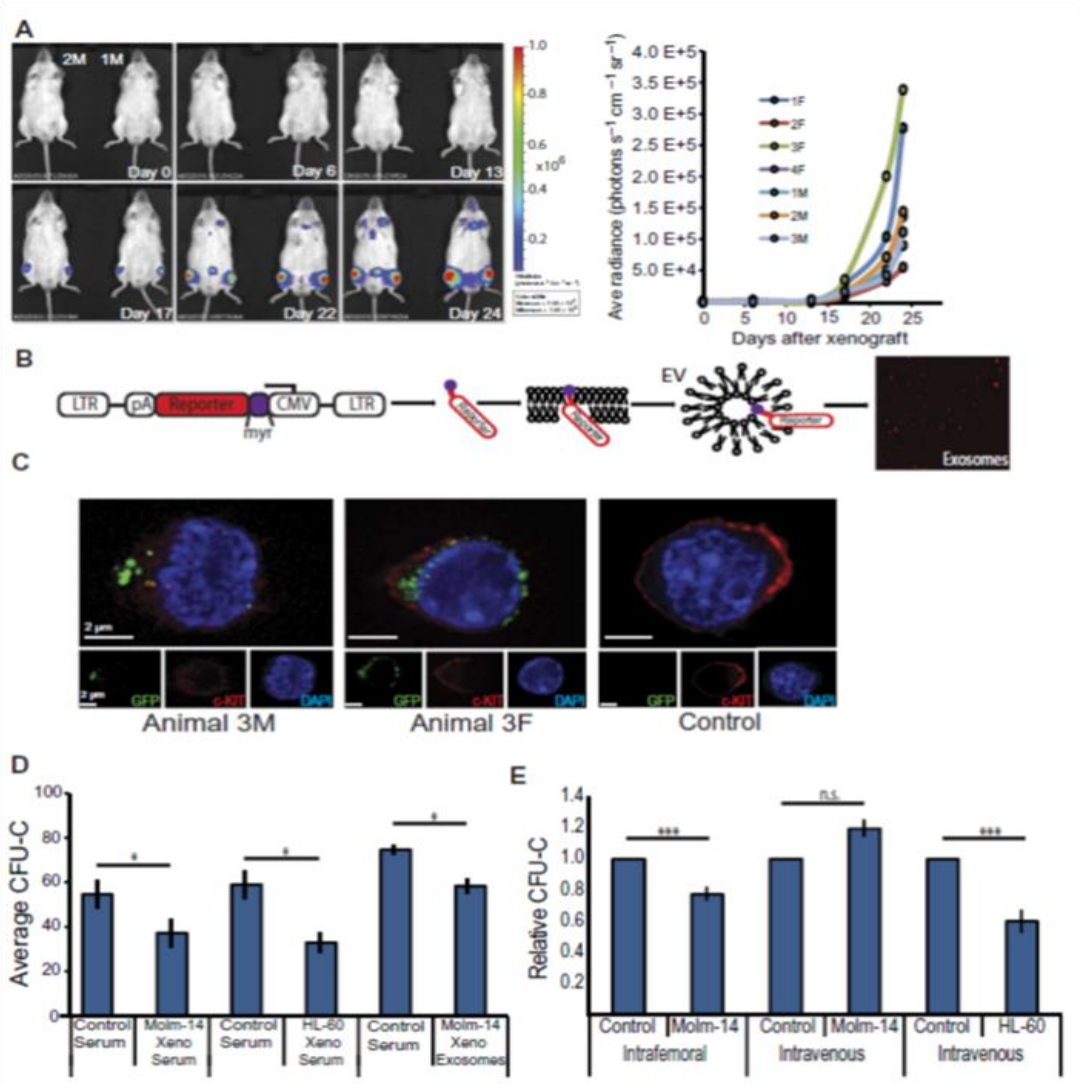

Leukemia Systemically Impairs HSPC Function. A. *Engraftment of luc+ Molm-14 cells were tracked and quantified using in vivo imaging.* Two representative mice (1M and 2M, left and right) were imaged at multiple timepoints following engraftment. Days 0, 6, 13, 17, 22 and 24 are shown. Engraftment was quantitated by radiance as photons/second/cm2/sr. **B.** *HSPC from mice engrafted with mGFP+ Molm-14 contain GFP+ vesicles in their cytosol*. Bone marrow aspirates from control and xenografted mice were sorted for c-Kit+, Sca1+, lin- markers and were imaged by confocal microscopy. **C.** *Serum and exosomes from serum recovered from xenografts exhibits a suppressive effect on HSPC colony formation in vitro*. c-Kit+ cells from C57Bl/6 mice were exposed to serum and serum exosomes collected from healthy and xenografted mice. Exposed cells were then plated in methylcellulose to assay for clonogenicity. **D.** *Serum exosomes impair HSPC in vivo.* NSG mice were exposed to serum exosomes from a xenograft either intravenously, or by contralateral intrafemoral injections. c-Kit+ cells were harvested 48 hours later and assayed for clonogenicity. **E.** Clonogenicity of c-KIT^{+} cells harvested from NSG mice 48 hours after mice were injected with serum exosomes from xenografts. Data are expressed relative to mice injected with control serum. Data are means ± SEM of a representative of cells derived from at least three mice and plated in triplicate. Significance in both (**D**) and (**E**) was determined by Student's t-test. *P<.05, ***P<0.001.

48 hours of exposure, we found that colony counts inversely correlated with the exosome dose (Figure 3-2A). Furthermore, levels of hematopoietic transcripts correlated with amount of exosome exposure (Figure 3-2B). Together, these observations suggested that transferred miRNA may be responsible for regulating hematopoietic transcripts, and consequently for suppression of clonogenicity. We focused on miR-155 due to its overrepresentation in leukemic exosomes[55] along with the relevance of its targets *Cebpβ*, *Tab2*[133,165] and particularly *c-Myb*, given the similarity between the phenotypes observed in *c-Myb*$^{-/-}$ mice and in our exosome-treated HSPC[166]. A search for other miRNA targeting *c-Myb* led us to explore miR-150[167], another highly abundant miRNA within Molm-14 and HL-60 exosomes[55]. Quantitative RT-PCR evaluation of murine HSPC revealed a substantial increase in miR-155 levels after exposure to AML-derived exosomes (Figure 3-2C), supporting transfer of this miRNA to recipient cells. Serum exosomes harvested from xenografts showed a substantial increase in miR-155 when compared to serum exosomes of control mice (Figure 3-2D). Using a dual luciferase reporter system, we verified the targeting of our genes of interest by miR-155, including both human and murine *c-Myb* 3'UTRs. We also validated that miR-150 targets the murine *c-Myb* transcript. (Figure 3-2E). The miRNA-mediated suppression of *c-Myb* was replicated using exosomes in place of transfection of miR-155 mimic (Figure 3-2F), providing the first direct evidence of *c-Myb* suppression by exosome-delivered miRNA.

c-Myb Suppression by Exosomal miR-155 Compromises HSPC Clonogenicity

We then employed an RNAi strategy to demonstrate that translational *c-Myb* suppression is sufficient to impair clonogenicity in murine HSPC. *c-Myb* targeting siRNA were transfected into c-Kit$^+$ cells, and were then assayed for colony-forming capacity, revealing a significant deficit in the *c-Myb*-suppressed cells compared to control siRNA-transfected cells (Figure 3-3A). Quantitative qRT-PCR showed over a tenfold reduction in *c-Myb* transcript levels in the siRNA treated conditions compared to the siRNA-control (normalized to *Gapdh*) (Figure 3-3B). In order to demonstrate the contribution of exosomal miR-155 to this effect in the exosome-exposure paradigm, we electroporated synthetic anti-miRNA oligonucleotides[168] into murine HSPC to protect them from exogenous delivery of miRNA via HL-60 exosomes. HSPC transfected with anti-miR-155 demonstrated partial protection against loss of clonogenicity compared to cells containing the control anti-miRNA. We then electroporated both anti-miRs-155 and -150 into HSPC, which yielded complete protection against the effects of exposure to HL-60 exosomes (Figure 3-3C). *c-Myb* transcript levels were assayed by qRT-PCR at the time of CFU plating, and correlated with the rescue of clonogenicity (Figure 3-3D). These experiments demonstrate that HL-60 exosomes suppress HSPC function through delivery of both miRs-155 and 150. Together, these results indicate that translational suppression of *c-Myb* is sufficient to suppress clonogenicity, and exposure to HL-60 exosomes directly contributes to this in murine HSPC via miRNA-mediated targeting of *c-Myb*.

FIGURE 3-2

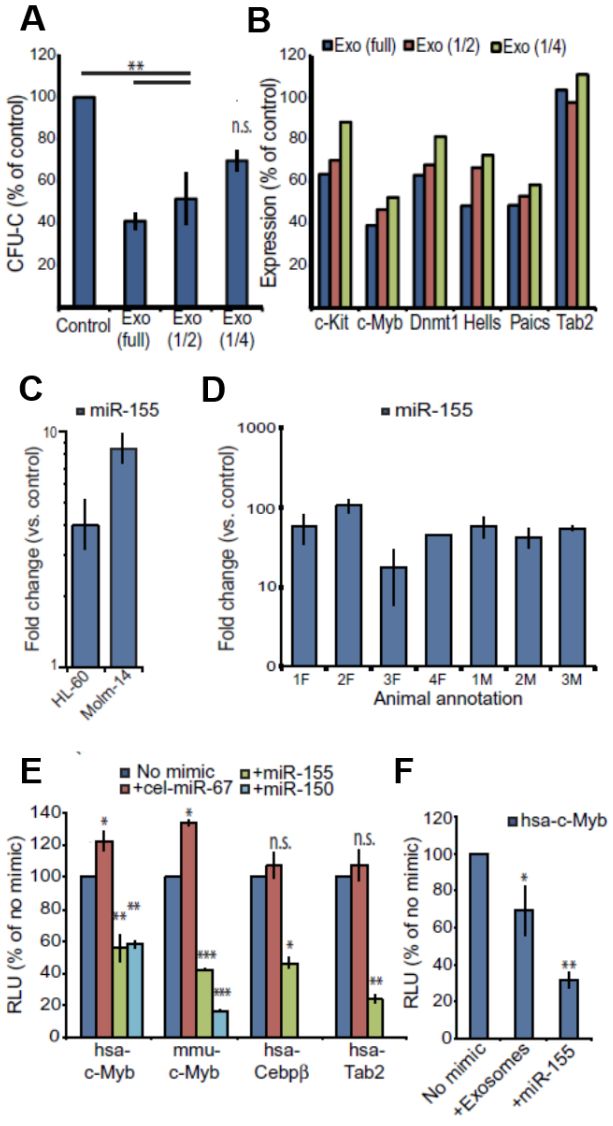

Figure 3-2. Exosome-delivered miR-155 Downregulates Recipient c-Myb. A. *Colony forming capacity is suppressed after exosome exposure*. c-Kit+ cells enriched from murine marrow were cultured with three doses of HL-60 exosomes for 48h and then assayed for clonogenicity. **B.** *Leukemia exosomes suppress the expression of hematopoietic regulators*. c-Kit+ cells were exposed to three doses of exosomes, after which expression of regulatory genes were measured by qRT-PCR, normalized to GAPDH and presented as % of expression to unexposed c-Kit+ cells. **C.** *miR-155 increases after exosome exposure*. c-Kit$^+$ cells were exposed to exosomes isolated from HL-60 or Molm-14, and qRT-PCR was performed. Results are presented as fold change versus c-Kit$^+$ cells without exosome exposure. **D.** *Exosomes in circulation within xenografts contain abundant miR-155*. Exosomes from the serum of xenografts and control mice were measured for levels of miR-155 by qRT-PCR. Results are presented as fold change compared to the average levels of serum exosomal miR-155 from two control mice. **E.** *miR-155 targets the 3'UTR of human and murine c-Myb, human CEPBPb and human TAB2*. Results from dual luciferase assay are presented as % RLU of the no-miRNA control. **F.** *Leukemic exosomes suppress cMYB through 3'UTR targeting*. c-Myb 3' UTR luciferase assay was performed as in (**E**) with the exception that luminescence was read 24 hours after transfection, using HL-60-derived exosomes alongside miR-155 mimic. Significance in (**A**), (**E**), and (**F**) was determined by paired Student's t-tests. *P<.05, **P<0.01.

FIGURE 3-3

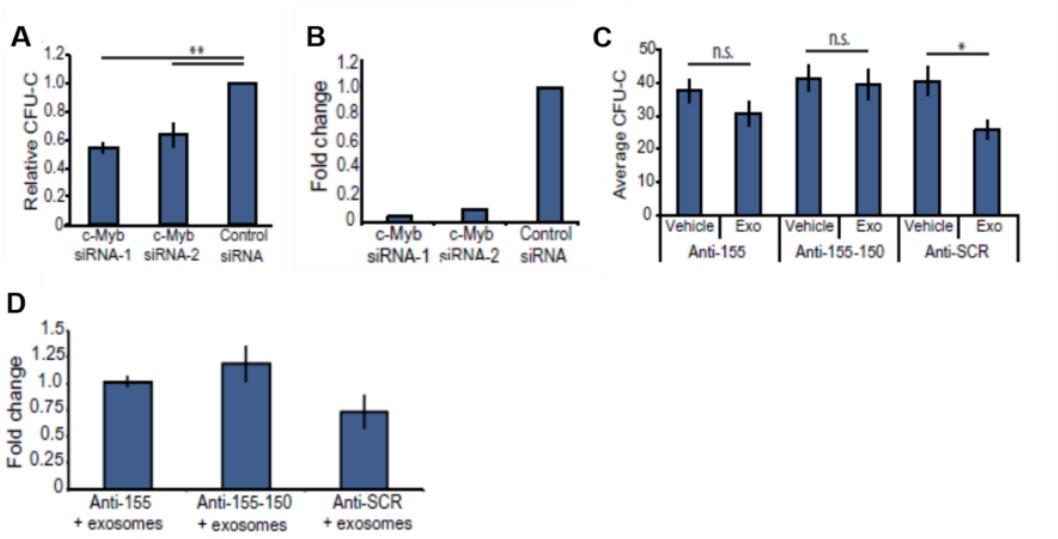

c-Myb Suppression by Exosomal miR-155 Compromises HSPC Clonogenicity. A. *RNAi-mediated suppression of c-Myb reduces clonogenicity*. Murine c-Kit$^+$ cells were transfected with siRNA targeting c-Myb and CFU-C were suppressed when compared to cells transfected with a control siRNA. **B.** *RNAi reduces protein levels of c-Myb*. Reduced protein levels of c-Myb, were confirmed by Western blot against c-Myb from c-Kit$^+$ cell lysates 48 hours after siRNA transfection. **C.** *anti-miR protects cells from loss of clonogenicity from exogenously delivered miRNA*. c-Kit$^+$ cells were transfected with anti-miR-155, anti-miR-155 and -150, or anti-miR-control, and then exposed to either HL-60 derived exosomes or vehicle. **D.** RNA was extracted from cells from (**C**) and qRT-PCR analysis revealed protection against the reduced mRNA levels found in exosome-exposed cells containing the anti-miR-scramble. Significance in both (**A**) and (**C**) was determined by paired Student's t-test. *P<.05, **P<0.01.

3.4 DISCUSSION

The failure of the residual HSPC pool to meet the demand for adequate blood cell production creates significant morbidity for patients with AML. A compelling explanation for this erosion of hematopoiesis has remained elusive, even as residual nonmalignant HSC are retained within the marrow, but unable to produce progenitors and their progeny[68,162-164]. When removed from the

marrow environment, these HSC regained their hematopoietic potential, supporting the hypothesis that leukemia actively exerts suppressive effects, but the response is transient, at least in HSPCs[83]. We demonstrate the systemic and transferable nature of HSPC suppression in experiments involving the transfer of serum and serum exosomes from xenografted animals *in vitro* and *in vivo*. Our findings show that AML constrains HSPC function systemically via the circulation. To clarify the role of regulatory non-coding RNA, we examined our miRNA microarray dataset (Figure 2-1A) in detail, with a particular interest in the targeting of transcripts with the potential reduce hematopoietic function.

The microarray investigation demonstrated that both leukemogenesis and tumor evolution exerts dramatic selection bias on miRNA composition in both intracellular and exosome-destined compartments. We began a more mechanistic investigation with emphasis on the leukemia- and exosome-enriched miR-155, as it has established connections to both hematopoiesis and leukemia[137]. Several groups have shown that the transcription factor *c-Myb* is a direct target of miR-155, with *c-Myb* suppression providing a phenocopy of the reduced clonogenic phenotype[169]. While miR-155 was sufficient to impair clonogenicity in exosome-treated HSPC, full protection was only conferred when both exosome-carried suppressors of *c-Myb*, miR-150 and -155, were blocked. In total, the experiments described here provide support for a model in which AML exerts systemic control over hematopoiesis through distribution of selected miRNA in trafficked exosomes. Conceptually, this work extends our

understanding of the coordinate regulation of the leukemic marrow. We show that the changes in the miRNA profile that occur during leukemogenesis result in the secretion of exosomes containing molecules that reduce the potential of competing healthy HSPCs in the niche. During the evolution of these cancers, they subverted the growth-prohibitive miR-155 transcripts to exosomes, and in doing so reduce the suppressive effects of miR-155 intrinsically. While this makes sense in the context of leukemic expansion, these tumors could have also epigenetically silenced miR-155 expression, or degraded the MVBs containing miR-155 with the lysosomal machinery. Perhaps the “weaponized” outcome (miR-155 loaded in HSPC-bound exosomes) was evolutionarily advantageous during the development of these leukemias by suppressing competing hematopoietic cells in the niche.

3.5 MATERIALS & METHODS

Cell Culture and Exosome Preparation

HL-60 and Molm-14 cells were obtained from the laboratory of Dr. Jeff Tyner, and were cultured in RPMI (Gibco) with 10% FBS (GemCell) and 1X Pen-Strep (Gibco) at 37°C, 5% CO_2 and >95% humidity. Exosomes were isolated by differential centrifugation as described previously. AML cells were cultured for 48 hours, the culture media was spun at 300xg for 10 min to remove cells, and then the supernatant was spun at 2,000xg for 20 min and 10,000xg for 20 min to remove cellular debris. The supernatant was centrifuged at 100,000xg for 2

hours. Exosomes were either resuspended in PBS or used for RNA extraction. RNA was extracted from exosomes or cells using RNeasy or miRNeasy kits (Qiagen) according to manufacturer's instructions.

Colony Forming Unit in Culture (CFU-C) Assay

Marrow cells were harvested from NSG or C57BL/6 mice as described previously[170]. Briefly, bone marrow was flushed from femurs and tibia using IMDM media. Progenitor c-kit$^+$ cells were then isolated using EasySep mouse PE selection kit (StemCell Technologies) following the protocol described by the manufacturer. Murine c-Kit$^+$ cells were cultured in IMDM with 10% VF FBS and supplements of 50ng/ml mouse IL-3 and SCF (R&D System). About 1x10^6 cells were incubated with exosomes harvested from 60-70x10^6 HL-60 cells for 48 hours. IMDM media was used as the control. Mouse Methylcellulose Complete media (R&D Systems) was used for CFU assays. The plating concentration was 5,000 treated c-Kit$^+$ cells per 35-mm dish. Cells were incubated for 7 days at 37°C with 5% CO_2 and ≥95% humidity. Colonies Were counted at day 7, the results averaged from triplicate plates per condition.

qRT-PCR

RNA was extracted from exosomes and cells using miRNeasy or RNeasy kits and quantified using a Nanodrop 2000c (Thermo). RNAs were converted into cDNA using the SuperScript III First Strand Synthesis Kit (Invitrogen) with oligo-dT priming, followed by RT-PCR analysis. SYBR Green PCR kit (Applied

Biosystems) was used for qRT-PCR analysis. Relative quantification was calculated using the ΔΔCT algorithm with Gapdh as the endogenous control. For miRNA quantification, TaqMan assay kits (Applied Biosystems) were used for reverse transcription and qRT-PCR, using U6 snRNA as the endogenous control.

Microarrays

Microarray assays were performed in the OHSU Gene Profiling Shared Resource. Sample quality assessment: RNA quantity and purity was measured by UV absorbance on the NanoDrop 1000 spectrometer (Thermo Scientific). RNA integrity and size distribution were determined by running each sample on an RNA 6000 Nano chip and a Small RNA chip (Agilent Technologies). Target labeling: Total RNA (130 ng) was prepared for hybridization using the Flash-Tag Biotin HSR miRNA Labeling Kit (Affymetrix) following manufacturer recommendations. Array hybridization and processing: Hybridization solutions were prepared according to Affymetrix recommendations and injected into a GeneChip miRNA 3.0 Array cartridge (Affymetrix), followed by incubation at 48^{o}C for 18 hours. Arrays were processed according to Affymetrix recommendations and scanned on a GeneChip Scanner 3000 7G with autoloader (Affymetrix). Image processing was performed using Affymetrix GeneChip Command Console software, followed by array analysis in Expression Console (Affymetrix) to evaluate array performance and general data quality. All arrays passed performance quality thresholds in the core lab.

Statistical analysis

The results are presented as mean ± SEM. Student's *t*-test was used for comparison between samples derived from the same source (cell or exosome) but subjected to different conditions. For comparisons between parental cell and exosomes the paired *t*-test was conducted to correct for sample relatedness. Unadjusted statistical significance was set at $p \leq 0.05$ followed by implementation of an FDR at $p \leq 0.10$ to correct for multiple testing where relevant.

MicroRNA Target Validation

3'UTR of each target was PCR amplified from HEK293T or primary murine c-Kit$^+$ genomic DNA and cloned into pSI-Check2 vector (Promega). 100ng of pSI-Check2 vector and 2nM of microRNA mimic (Dharmacon) were cotransfected into $4x10^5$ HEK293 cells that were seeded in a 12-Ill dish. Cells were washed in PBS 48 hours post transfection and lysed according to the manufacturer's protocol for Dual Luciferase (Promega). Firefly and Renilla luminescence were measured with a Berthold Centro XS3 LB 960 Luminometer, and relative luminescence was compared to relative luminescence of pSI-Check2 construct transfected without mimic to generate percent knockdown. Technical triplicates were performed for each biological replicate. Error bars represent the SEM from three biological replicates.

siRNA Knockdown of c-Myb

c-Kit$^+$ cells were enriched as described above. Immediately following enrichment, 5x10^4 were electroporated using an Amaxa 4D-Nucleofector X system (Lonza) following the manufacturers guidelines for CD34$^+$ cells. The transfection used an optimized setting determined by pilot electroporation with a GFP expressing vector. The siRNA (Origene) included two siRNA targeting *c-Myb* and a negative control siRNA which was used as the comparative control. A final concentration of 20nM of siRNA was electroporated into cells, and transfection efficiency was compared to cells electroporated with a GFP expressing vector in parallel. 48 hours after electroporation 5,000 cells were plated in methylcellulose and CFUs were determined as described above.

Western blot

Western blots were performed as described in [109]. GAPDH (Novus Biologicals), p53 (Cell Signalling Technology), and p53 phospho-ser-20 antibody (Cell Signalling Technology).

anti-miR electroporation

A final concentration of 20nM of anti-miR were electroporated into c-Kit$^+$ cells as described above. Cells recovered in IMDM with 10% VF FBS and supplements of 50ng/ml mouse IL-3 and SCF (R&D System) for two hours. Cells were then exposed to either HL-60 exosomes or vehicle. 48 hours later 5,000 cells were plated in methylcellulose and CFUs were determined as described above.

CHAPTER 4: Transmissible ER Stress via Extracellular Vesicles Reconfigures the AML Bone Marrow Microenvironment

Compiled from: Ben Doron, Sherif Abdelhamed, John T. Butler, Saman K. Hashmi, Terzah M. Horton and Peter Kurre. *Transmissible ER Stress via Extracellular Vesicles Reconfigures the AML Bone Marrow Microenvironment*. Unpublished

Contributions

The work in this chapter is derived from our manuscript in progress. The majority of the experiments described herein were performed by me, with the exception of the microscopy and protein analysis of patient samples. The generation of xenografts and chimerism analyses were a joint effort by members of the Kurre lab.

4.1 ABSTRACT

The successive functional adaptation of the bone marrow (BM) stroma from homeostatic microenvironment to self-reinforcing leukemic niche is an integral aspect of leukemogenesis. Here, we set out to model the events that reshape the compartment and alter healthy BM function in acute myeloid leukemia (AML). Our studies in an AML xenograft model revealed systematic changes in stroma composition with gains in the fraction of BM mesenchymal stromal cells (MSC) and promotion of osteogenic lineage differentiation. We further showed that differentiation resulted from widespread induction of endoplasmic reticulum (ER) stress in BM MSC, and coincided with an unfolded protein response (UPR) in the AML xenograft itself. These results were further corroborated in AML patient cells. We next tested the hypothesis of an underlying transmissible UPR response, and found that AML derived extracellular vesicles (EV) trafficked to MSC, where they preferentially localized at the ER. Indeed, EV proved to be a source of BMP2 and trafficking between AML cells and stroma was sufficient for UPR induction. This is the first demonstration of UPR transfer via EVs and

supports a model whereby AML cells dynamically adjust EV cargo and utilize cell-cell trafficking to re-configure composition and alter the function of the BM compartment.

4.2 INTRODUCTION

Hematopoiesis occurs in operationally defined niches in the bone marrow (BM) and is regulated through reciprocal signaling between hematopoietic and stromal tissue components[60-63,81,171]. Leukemia cells, including Acute Myeloid Leukemia (AML), actively compete with hematopoietic stem cells (HSC) for niche occupancy. The successive tumor growth in turn affects resident hematopoietic- and stromal cell function, and results in reduced chemotherapeutic efficacy as well as impaired blood formation[83,162,172,173]. These observations do not appear to be AML subtype-specific, and similar defects have been described in murine models of CML[68,164]. Evidence from several groups indicates that remodeling and secretory conversion of the microenvironment accounts for the role of the BM as a sanctuary site for residual, drug resistant disease and relapse[35,50]. This notion is further consistent with observations that AML patient-derived mesenchymal stem cells (MSCs) exhibit an altered secretion of cytokines with reduced hematopoietic support and a more chemoprotective phenotype[174-176]. Murine congenic and xenograft models additionally add *in vivo* context and provide further insight into distinct immunophenotypically defined stromal populations[47,61,68,83,177].

AML cells are typically located at endosteal areas of the bone[178]. To better understand leukemia induced changes in the composition of the AML BM compartment, we decided to focus on two critical mesenchymal populations within the endosteal niche: MSCs, which maintain the potential to differentiate along adipo-, chondro-, and osteolineages; and Osteoblastic Progenitor Cells (OPCs), a population of osteolineage committed progeny that will mature into osteoblasts[68]. Both populations contribute to hematopoietic homeostasis, or -conversely- their functional disruption can lead to myelodysplastic growth and clonal evolution[84,179]. We were particularly interested in understanding the reciprocal crosstalk in the AML niche that would spur osteogenic differentiation bias, previously implicated during AML expansion[48,68,164,180], and associated with changes in the release of soluble factors that regulate growth and adhesion[181].

The studies herein identify significant compositional changes in the niche of AML xenograft animals associated with osteogenic MSC differentiation bias. We also show that the underlying mechanism relies on transmissible ER stress (TERS)[182,183], and identify AML derived extracellular vesicles (EVs) as contributory factor in conferring a stromal unfolded protein response (UPR), a known stimulus for altering secretion and inducing osteogenic differentiation[118,120,184].

4.3 RESULTS

AML remodels the endosteal niche

To examine BM niche composition and function *in vivo* we used NOD-*scid* IL2R □ ^{null} (NSG) xenografts[83,162,173] with tail-vein grafting and without conditioning irradiation to ascertain undisturbed niche function[117,185]. To avoid expansion artifacts during *in vitro* cell culture of MSCs and OPCs, we isolated endosteal MSC and OPC populations directly from mice using fluorescence activated cell sorting (FACS)[186] (Figure 4-1A). Specifically, we excluded hematopoietic and endothelial cells (CD45 and TER119, and CD31, respectively) to sort the two immunophenotypically distinct mesenchymal populations critical for HSC support: SCA-1$^+$/CD51$^+$ MSCs and SCA-1$^-$/CD51$^+$ OPCs[68,187] (Figure 4-1B). We analyzed cells sorted from long bones for morphological differences, clonogenic growth, and extracted RNA to perform qRT-PCR and transcriptionally validate differential expression of genes characteristically expressed in either population (Figure 4-1C). We also confirmed the anticipated distinct morphological differences in day 10 adherent cells *in vitro* (Figure 4-1D). With this strategy in place, we generated several xenograft cohorts *via* intravenous injection of three human AML cell lines Molm-14, U937, and HL60. Chimerism was tracked by the percentage of human CD45$^+$ cells over time in the peripheral blood and at time of harvest in the bone marrow. We included xenografts with a marrow chimerism > 60% in this study to simulate niche remodeling effects during advanced disease[55]. Functionally, we observed reduced fibroblastic colony forming (CFU-F) potential in both MSCs and OPCs from all three AML

xenograft cohorts (Figure 4-1E). Strikingly, we also observed a significant shift in the proportion of the two populations (Figure 4-1F), with increased MSC/OPC ratios, signifying a compositional change within the BM niche.

MSCs and OPCs exhibit differential fates in the leukemic bone marrow

We hypothesized that the altered proportion of MSCs and OPCs may be due to increased apoptotic turnover of OPCs, as Osterix-expressing progenitor cells have been previously shown to be sensitive to AML-induced apoptosis[47,188]. Indeed, isolated OPCs exhibited increased apoptosis within xenografts as measured by increases in Annexin V positivity and Ser-15 phosphorylated p53, but not overall p53 (Figure 4-2A). These OPC differences were significant in Molm-14 and U937 xenografts, but did not reach statistical significance for HL60 xenografts. Xenograft- derived MSC on the other hand did not show evidence of apoptosis or p53 engagement under these conditions (Figure 4-2B). Rather, we observed significant induction of osteolineage differentiation in MSC from AML xenografts. In all three xenograft models, MSCs showed increased expression of Runx2, Osterix, and Dkk1, whereas markers of late osteoblastic development, Col1α1 and Spp1, were significantly reduced (Figure 4-2C). Consistently, Molm-14 xenograft-derived MSCs displayed an increased propensity for osteogenic differentiation and a reduction in adipolineage differentiation following in vitro differentiation assays, as evidenced by the retention of Alizarin Red S and Oil Red O following incubation in osteogenic or adipogenic differentiation media, respectively (Figure 4-2D-E). Together, the data indicate that leukemia cells

provide extrinsic cues that promote osteogenic MSC differentiation and increased apoptosis in OPCs, resulting in aggregate changes in the overall composition of the BM compartment in vivo.

FIGURE 4-1

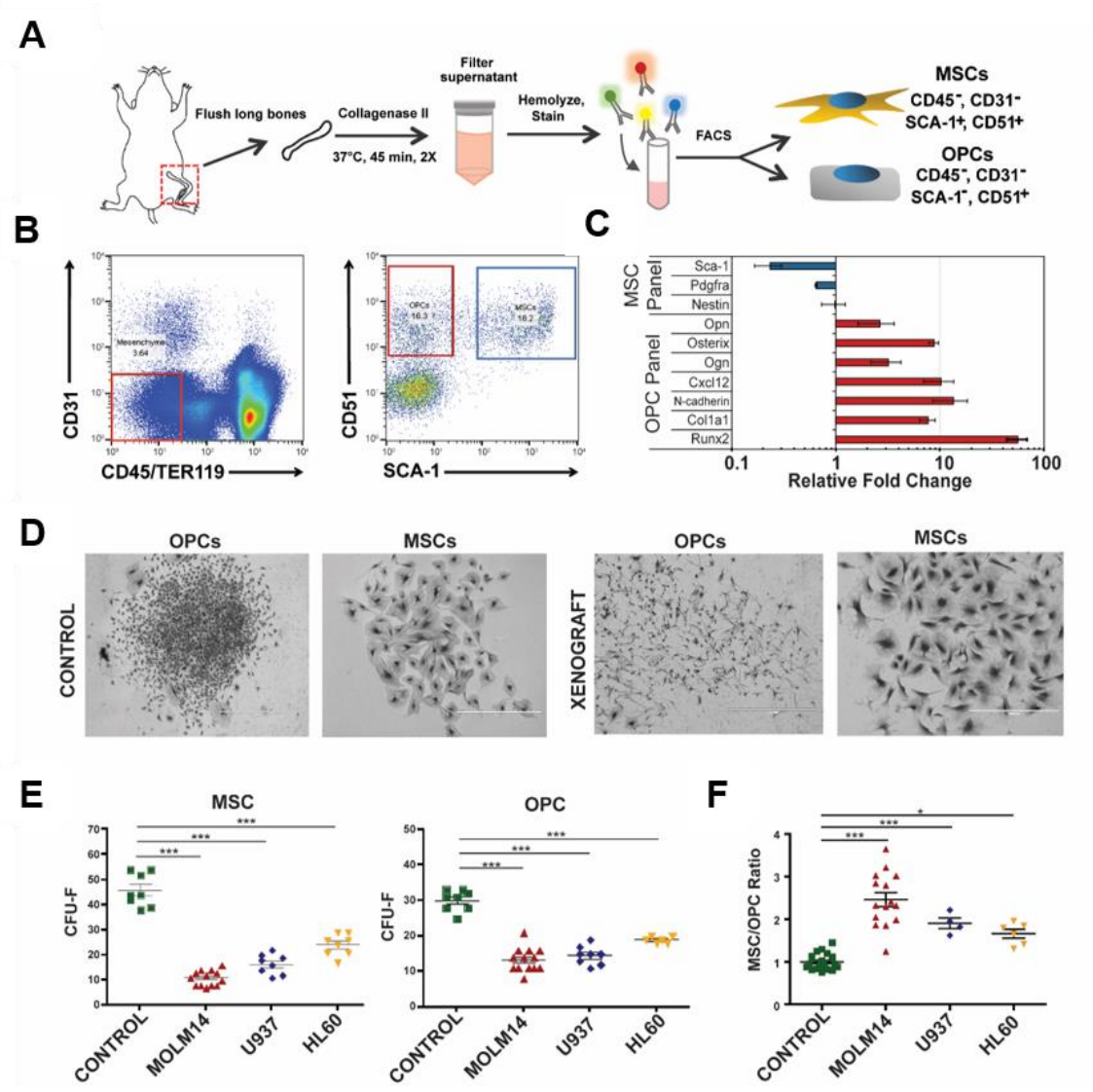

AML negatively impacts the endosteal niche. A. MSC and OPC harvest workflow. Long bones from control and xenografted mice are removed, flushed, crushed, and incubated in Collagenase II. Disadhered cells are then filtered, stained with antibodies, and sorted via FACS. **B.** Gating strategy for MSC and OPC. Following gating on live, single cells, the mesenchyme population is gated on the absence of hematopoietic (CD45 and TER119) or endothelial (CD31) markers. Within this gate MSCs are gated on CD51+ and SCA-1+, and OPCs on CD51+ and SCA-1-. **C.** MSCs and OPCS express genes relevant to their function. Gene expression analysis of a panel of MSC and OPC relevant genes. Fold change determined by $2^{-\Delta\Delta Ct}$ of OPCs against MSCs. Error bars are Standard Error of the mean from three independent experiments. **D.** Images of colonies from CFU-F reveal morphological changes between MSC and OPC, as well as across control and xenograft conditions. Scale bars are 1000μm. **E.** CFU-F assay of MSCs and OPCs derived control and AML xenografted animals. Error bars are standard error of the mean from (n=8, 13, 8, 8) animals per condition. **F.** The ratio of MSCs / OPCs in control and AML xenograft animals. Error bars are standard error of the mean from (n= 22, 14, 4, 6) animals per condition. Significance in (**E**) and (**F**) was determined using ANOVA and Bonferroni correction. **P<.05, ***P<0.001.

Stromal UPR induction in AML xenografts

Both the increasing translational burden within the ER during osteogenic differentiation[189] and the XBP1 dependent upregulation of Osterix, a master regulator of osteogenesis[120], led us to consider the involvement of the UPR. We therefore assembled a RT-PCR survey panel to screen core components of this pathway. Results showed broad engagement of the UPR in xenograft-derived MSC and OPC populations compared to those from control mice. Both populations exhibited significant upregulation of *Grp78*, a core regulatory component of the UPR, as well as marked increases in the spliced isoform of *Xbp1* and upregulation of *Chop* (Figure 4-3A-B). The fact that the UPR can also promote osteogenesis[190] was supported by increased *Runx2* and *Osterix* gene expression after exposure of MSCs to the UPR inducer thapsigargin (Figure 4-3C). By contrast, hematopoietic progenitor cells, identified by the expression of c-Kit, Sca-1, and the absence of lineage markers (KSL) did not exhibit induction of the UPR, signifying a stroma-specific response to AML influence (Figure 4-3D).

FIGURE 4-2

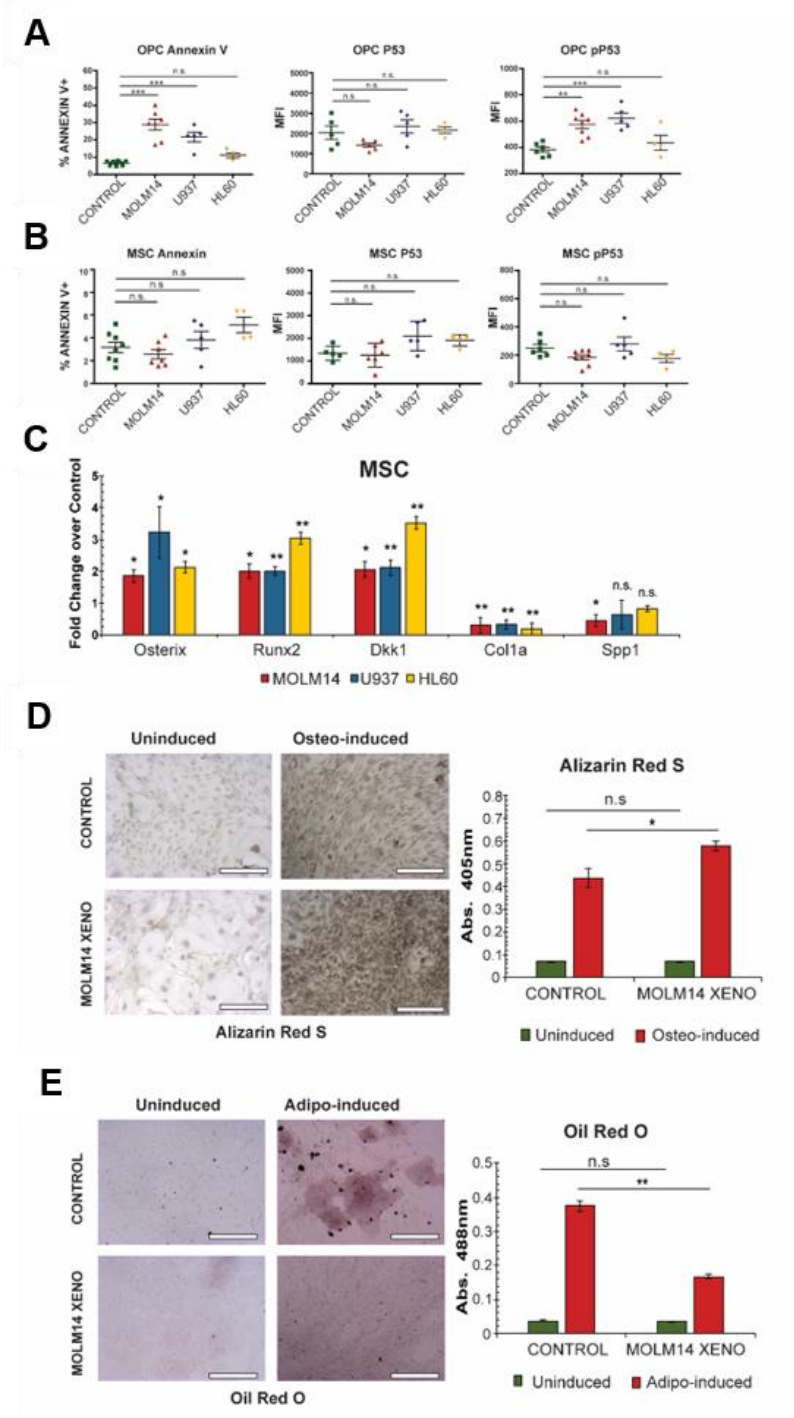
A
OPC Annexin V
OPC P53
OPC pP53
% ANNEXIN V+
MFI
CONTROL
MOLM14
U937
HL60
B
MSC Annexin
MSC P53
MSC pP53
C
MSC
Fold Change over Control
Osterix
Runx2
Dkk1
Col1a
Spp1
MOLM14 U937 HL60
D
Uninduced
Osteo-induced
CONTROL
MOLM14 XENO
Alizarin Red S
Abs. 405nm
n.s
Uninduced Osteo-induced
E
Uninduced
Adipo-induced
Oil Red O
Abs. 488nm
Uninduced Adipo-induced

MSCs and OPCs exhibit differential fates in the leukemic bone marrow. A-B. Analysis of apoptosis in stromal populations. The percentage of Annexin V+ cells, and the MFI of P53 and Ser-15 phosphorylated P53 in control and xenografted animals within OPC (**A**) and MSC (**B**) gates. Error bars are standard error of the mean from (n= 8, 7, 5, 4) animals for Annexin V dataset and (n= 5, 6, 5, 4) for the pP53 and P53 experiments. Significance in (**A**) and (**B**) was determined using ANOVA and Bonferroni correction. **P<.01, ***P<0.001. **C.** Expression analysis of genes involved in early and late osteogenesis of xenograft-derived MSCs compared to control MSCs. Fold change determined by $2^{-\Delta\Delta Ct}$ in pairwise analysis against control MSCs. Error bars are standard error of the mean from four animals per condition. Significance was determined by ANOVA and Student's t-test. *P<.05, **P<.01, ***P<0.001. **D.** Osteogenic differentiation potential of MSCs from control and Molm-14 xenografted animals. Osteogenesis was quantified based on Alizarin Red S staining (left). Scale bars are 100μm. Quantification of stain retention was measured by absorbance at 405nm of culture extracts (right). Significance was determined by Student's t-test. **E.** Adipogenic differentiation potential of MSCs from control and Molm-14 xenografted animals. Adipogenesis was quantified based on Oil Red O staining (left). Scale bars are 100μm. Quantification of stain retention was measured by absorbance at 488nm of culture extracts. Error bars are standard error of the mean from three biological replicates. Significance was determined by Student's t-test. *P<.05 **P<.01.

To further implicate the UPR in the increase in apoptosis within the OPC population, we sorted for Annexin V^+ OPCs and Annexin$^-$ populations from both Molm-14 xenografts and controls (Figure 4-3E). Specifically, we reasoned that the UPR should preferentially be induced in Annexin V^+ cells, and indeed we observed significant upregulation of *Grp78*, *Chop*, *XBP1* and *sXBP1* genes in Molm14 xenograft derived Annexin V^+ cells compared with those from controls (Figure 4-3F). Altogether, the data suggest that ER stress in the AML niche contributes to the adaptive changes in BM stromal fate and composition. The data indicate that ER stress in the AML niche alters the stromal composition and uniquely affects the different cell populations in the compartment.

FIGURE 4-3

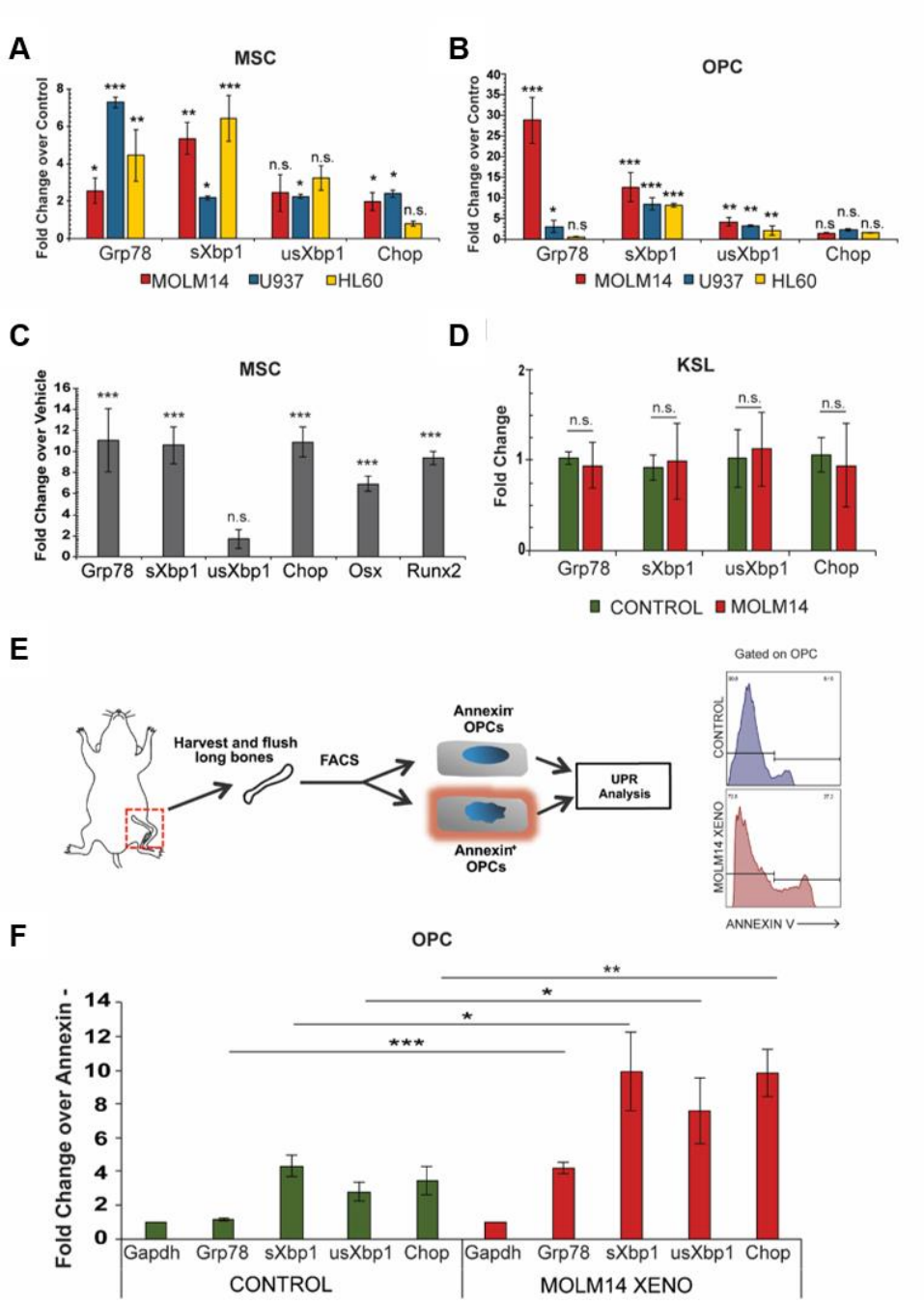
A
MSC
Fold Change over Control
Grp78
sXbp1
usXbp1
Chop
MOLM14
U937
HL60
B
OPC
Fold Change over Contro
Grp78
sXbp1
usXbp1
Chop
MOLM14
U937
HL60
C
MSC
Fold Change over Vehicle
Grp78
sXbp1
usXbp1
Chop
Osx
Runx2
D
KSL
Fold Change
Grp78
sXbp1
usXbp1
Chop
CONTROL
MOLM14
E
Harvest and flush long bones
FACS
Annexin⁻ OPCs
Annexin⁺ OPCs
UPR Analysis
Gated on OPC
CONTROL
MOLM14 XENO
ANNEXIN V
F
OPC
Fold Change over Annexin -
Gapdh
Grp78
sXbp1
usXbp1
Chop
CONTROL
MOLM14 XENO

MSCs and OPCs exhibit increased ER stress. A-B. Expression analysis of genes involved in the UPR from xenograft-derived MSCs (**A**) and OPCs (**B**). Fold change determined by $2^{-\Delta\Delta Ct}$ in pairwise analysis against control MSC and OPCs, respectively. Error bars are standard error of the mean from four animals per condition. Significance was determined by ANOVA and Student's t-test. *P<.05, **P<.01, ***P<0.001. **C.** Expression analysis of genes involved in the UPR and osteogenesis in MSCs cultured in 5ng/mL thapsigargin compared to vehicle-treated MSCs. Fold change determined by $2^{-\Delta\Delta Ct}$ against control cells. Error bars are standard error of the mean from three biological replicates. Significance was determined by Student's t-test. ***P<0.001. **D.** Expression analysis of UPR genes in hematopoietic stem cells (c-KIT+, SCA-1+, lin-; KSL) from Molm-14 xenografts. Fold change determined by $2^{-\Delta\Delta Ct}$ against KSL from control animals. Error bars are standard error of the mean from three animals per condition. Significance was determined by Student's t-test. **E.** Experimental workflow of OPC Annexin V sort. OPCs were sorted based on Annexin V status, and cells from the same animal were compared against each to measure UPR status. **F.** Expression analysis of UPR genes between Annexin V+ and Annexin V- OPCs from control and Molm-14 xenografts. Fold change determined by $2^{-\Delta\Delta Ct}$ against Annexin V- OPCs. Error bars are standard error of the mean from four animals per condition. Significance was determined by Student's t-test. *P<.05, **P<.01, ***P<0.001.

Uptake of AML-derived EV into endosteal cells in vivo and in vitro

We and others previously demonstrated that AML-derived EVs enter into $CD45^-$ / plastic-adherent stromal cells *in vitro*[117,173]. To more specifically visualize MSC and OPC uptake of AML-derived EVs *in vivo* we generated Molm-14 cells stably expressing myristoylated GFP (Molm-14-*mGFP*), which functions as a lipid membrane label. Molm-14 cells release brightly labels EV into tissue culture and enable us to detect circulating EVs in the peripheral blood (Figure 4-4A), or map *in vivo* tissue dissemination and cellular uptake of EV from the Molm14 xenograft *in vivo*[185]. Here, we performed live-cell microscopy of FACS-purified MSC and OPC. At animal sacrifice, the sorted cells are transferred to culture dishes and labeled with Hoechst nuclear stain and Cellmask, a lipophilic dye used to mark the cytoplasm. Results reveal that both MSCs and OPCs from Molm-14 xenografts, but not control animals, contained discrete $mGFP^+$ vesicles (Figure 4-

4B). For quantification of mGFP$^+$ vesicle uptake, we next scored mGFP$^+$ foci in both cell types. The MSCs and OPCs from xenografted animals (day 21 sacrifice) were found to contain GFP$^+$ vesicles in 55% and 34% of cells respectively (Figure 4-4C). In both cell types the total number of internalized foci ranged from one to thirty EVs (Figure 4-4D). To do this, the Cellmask staining marking the outer membrane was used to determine the volume of the cells. Within this volume, individual mGFP$^+$ voxels and their respective grey value were summated to determine EV numbers. We repeated these imaging studies in MSCs and OPCs expanded in culture to EVs harvested from Molm-14-*mGFP in vitro* and confirmed vesicle uptake using confocal live-cell microscopy (Figure 4-4E) Finally, we were interested in determining spatial distribution of EVs inside recipient cells and found that MSCs and OPCs not only uptake AML derived EVs *in vitro,* but that most of the EV localize at the ER, as shown by both DIC and ER Tracker co-staining (Figure 4-4E-F), consistent with previous observations of EV fate [191]. Altogether, the imaging data indicate that AML-derived EVs traffic to both MSC and OPC populations and co-localize intracellularly at the ER. Because UPR induction generally leads to an increase in size of the ER compartment [192,193], we visualized ER size and morphology of MSCs and OPCs exposed to Molm-14-derived EVs (not labeled in this experiment) *in vitro* using ER-Tracker [194]. EV-treated cells displayed a dilated ER, similar to cells treated with thapsigargin [193] (Figure 4-4G).

FIGURE 4-4

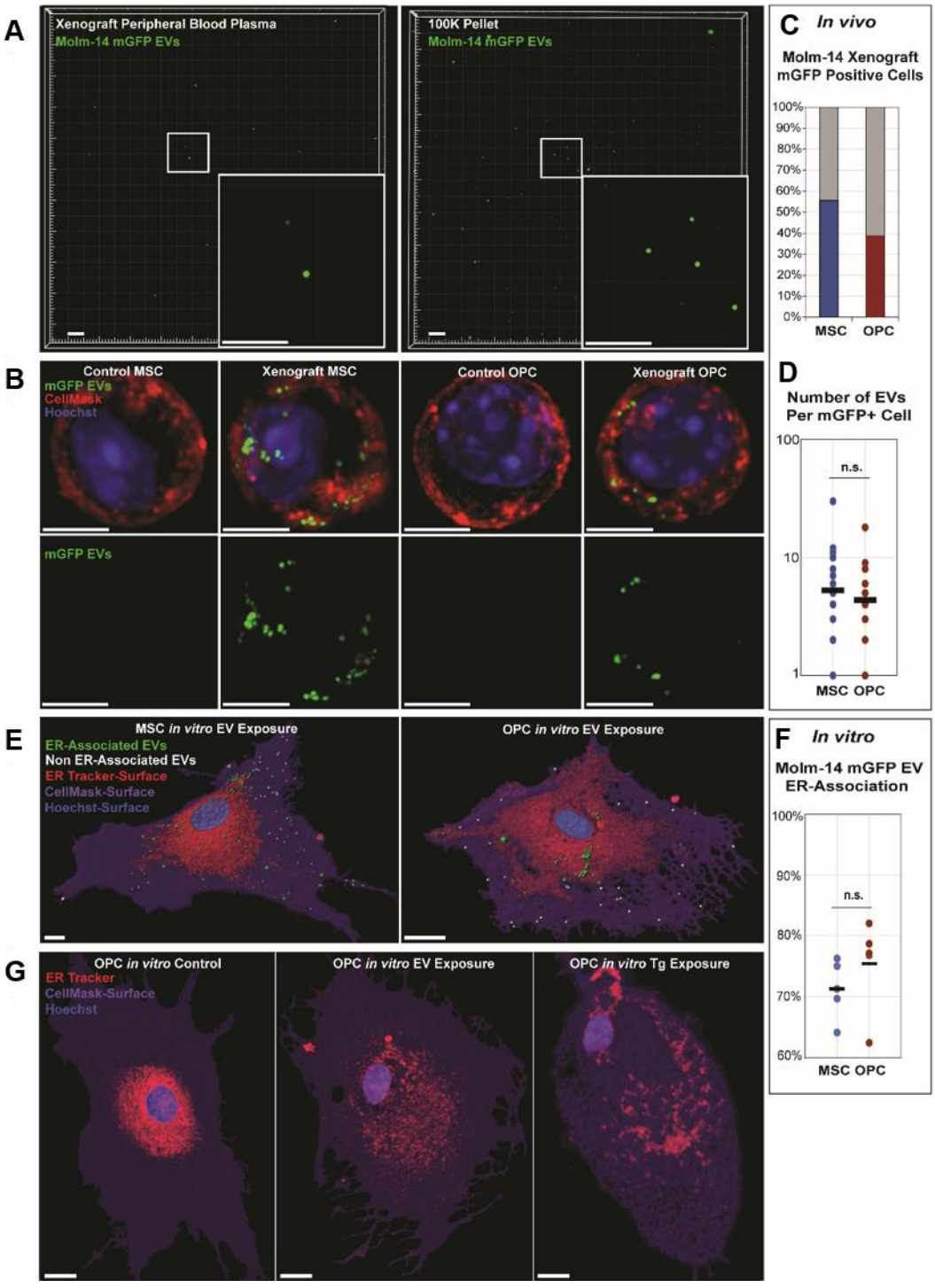
A
Xenograft Peripheral Blood Plasma
Molm-14 mGFP EVs
100K Pellet
Molm-14 mGFP EVs
B
Control MSC
Xenograft MSC
Control OPC
Xenograft OPC
mGFP EVs
CellMask
Hoechst
mGFP EVs
C In vivo
Molm-14 Xenograft
mGFP Positive Cells
100%
90%
80%
70%
60%
50%
40%
30%
20%
10%
0%
MSC
OPC
D
Number of EVs
Per mGFP+ Cell
100
10
1
n.s.
MSC OPC
E
MSC in vitro EV Exposure
ER-Associated EVs
Non ER-Associated EVs
ER Tracker-Surface
CellMask-Surface
Hoechst-Surface
OPC in vitro EV Exposure
F In vitro
Molm-14 mGFP EV
ER-Association
100%
90%
80%
70%
60%
n.s.
MSC OPC
G
OPC in vitro Control
ER Tracker
CellMask-Surface
Hoechst
OPC in vitro EV Exposure
OPC in vitro Tg Exposure

AML EVs traffic to the ER of MSCs and OPCs. A. Solid capture imaging of mGFP+ EVs from peripheral blood of Molm-14-mGfp xenografts (left) and from in vitro Molm-14-mGfp cells (right). Scale bars are 5μm. **B.** Live-cell imaging of MSCs and OPCs derived from control and Molm-14-mGfp xenografts. mGFP: green, Cellmask: red, Hoechst: blue. Scale bars are 5μm. **C.** Quantification of Molm-14-mGfp xenograft-derived MSCs and OPCs containing mGFP+ vesicles. # of animals, data is representative of 60 cells analyzed per condition. **D.** Quantification of mGFP+ vesicles per MSC and OPC derived from Molm-14-mGfp xenografts. Error bars are standard error of the mean from 8 animals per condition. Significance determined by paired Students t-test. **E.** Representative images of live-cell, confocal microscopy of in vitro expanded MSCs (left) and OPCs (right) exposed to EVs harvested from Molm-14-mGfp cells. Green: ER-localized mGFP+ vesicles, white: cytosol-localized mGFP+ vesicles, red: ER surface, purple: plasma membrane surface, blue: Hoechst. Scale bars are 5μm. **F.** Quantification of ER-localization of internalized mGFP+ vesicles in in vitro expanded MSCs and OPCs. Error bars are standard error of the mean. Significance determined by paired Student's t-test. **G.** Representative images of live-cell, confocal microscopy of in vitro expanded OPCs exposed to vehicle (left), Molm-14-derived EVs (center), or 10ng/mL thapsigargin. Red: ER surface, purple: plasma membrane surface, blue: Hoechst.

AML EVs induce the UPR in MSCs and OPC in vivo

The observation that EVs traffic to and promote dilation of the ER in recipient cells prompted us to systematically test if EVs transmit ER stress, accounting for UPR activation and alterations in MSC and OPC differentiation [195-197]. To test this hypothesis, we performed contralateral intrafemoral injections, delivering dose-matched, purified EVs from in vitro cultured Molm-14 cells versus healthy human bone marrow-derived $CD34^+$ cultures (Figure 4-5A), an approach previously reported [185]. Animals were sacrificed 48 hours later and MSCs and OPCs were sorted directly into RNA extraction buffer for subsequent examination of UPR induction by qRT-PCR (Figure 4-5B). OPCs, but not MSCs exhibited an increase in Grp78 and spliced Xbp1 expression when exposed to AML-derived, but not healthy $CD34^+$ cell-derived, EVs. For confirmation of EV-mediated UPR induction we expanded MSCs and OPCs in vitro and again observed a

persistent, but more moderate increase of the UPR in both cell types 48 hours post EV-exposure (Figure 4-5C). Recent reports also indicate a non-cell-autonomous, transmissible ER stress response (TERS) between cancer and bystander cells in pancreatic and breast tumor microenvironments[182,183]. To test the possibility of TERS from AML cells to stroma, we first measured UPR induction in FACS-purified Molm-14 cells explanted from AML xenografts at sacrifice, and during subsequent in vitro propagation at 48 and 96 hours. Remarkably, when compared against Molm-14 cells grown in vitro, we found initially robust, but rapidly diminishing transcriptional activity of several key UPR components over time in cell culture (Figure 4-5D). Next, we had the opportunity to test blasts enriched from AML patients at diagnosis and compared their UPR status to healthy controls. Among a set of 38 samples available to use, we found that ~20% exhibited a robust UPR illustrated by the upregulation of GRP78 and phosphorylated eIF2α protein levels in five AML patients and two controls (Figure 4-5E). To better correlate the magnitude of UPR induction in patients with our xenograft results, we performed an additional transcriptional analysis of GRP78, s/usXBP1, and CHOP expression and found highly significant differences between patients and controls (Figure 4-5F). Consistent with the UPR induction found in the three cell lines used in our xenograft studies, UPR induction occurred independently of AML subtype. With the availability of peripheral blood plasma from AML patients, we next purified plasma-derived EVs by serial ultracentrifugation and performed intrafemoral injections into recipient mice, with contralateral vehicle controls and harvest of MSCs and OPCs 48hrs later. We

then analyzed UPR induction by qRT-PCR and confirmed that serum EVs from patients with AML blasts induce UPR in bone marrow MSC and OPC, whereas serum-EVs from healthy donors failed to do so (Figure 4-5G). TERS has not been previously considered in the extrinsic remodeling of the AML niche but our experiments suggest that ER stress in the AML niche results from a leukemia-derived, transmissible, EV-bound factor.

FIGURE 4-5

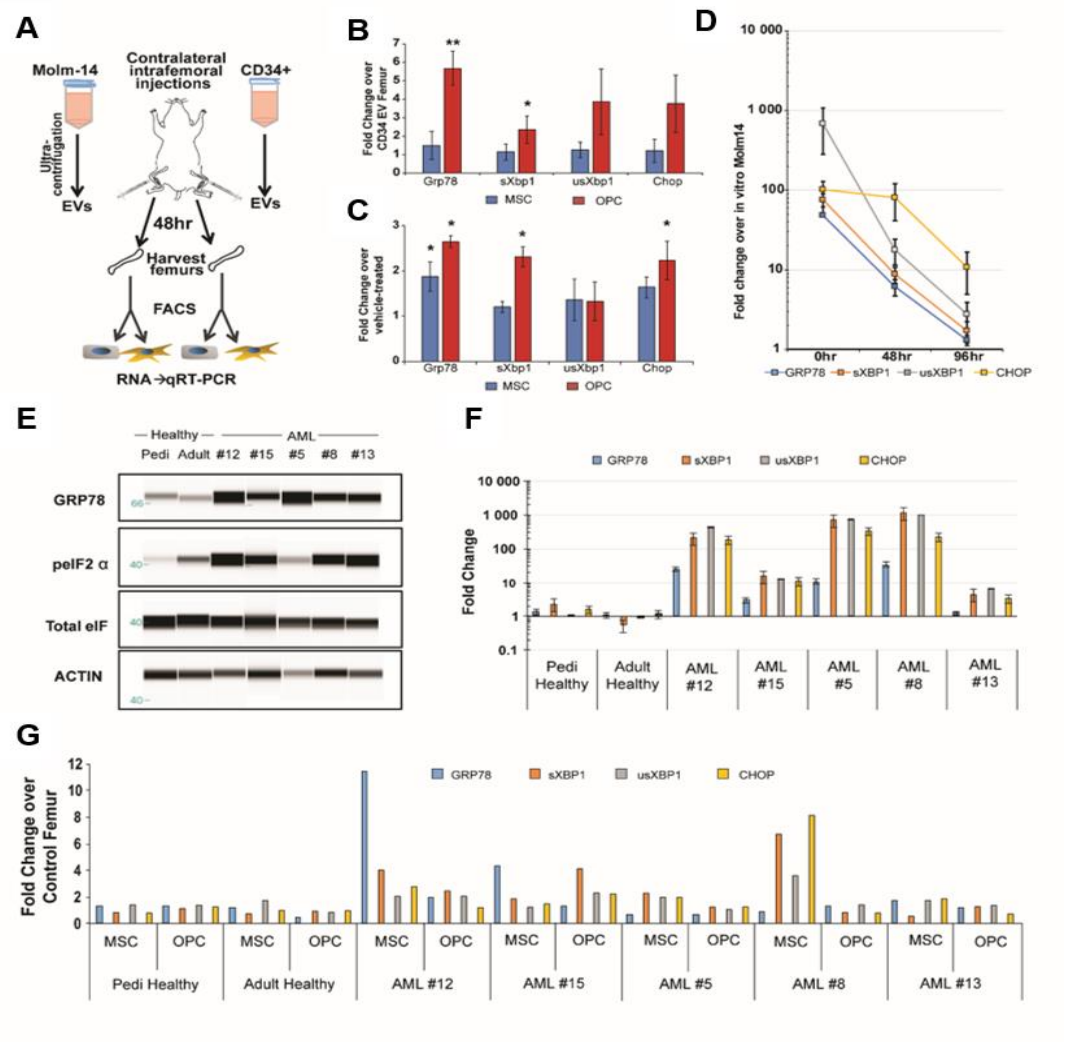

AML cells exhibit an UPR *in vivo*. A. Experimental outline for intrafemoral injections. EVs from Molm-14 cells and healthy CD34+ cells were injected contralaterally into femurs of recipient mice. Femurs were harvested 48hrs later, MSCs and OPCs were sorted into RNA extraction buffer for gene expression analysis. **B.** Expression analysis of UPR genes from MSCs and OPCs from Molm-14 EV injected femurs. Fold change was determined by $2^{-\Delta\Delta Ct}$ against respective cells from CD34+ EV injected femurs. Error bars are standard error of the mean from three animals per condition. **C.** Expression analysis of UPR genes from in vitro cultured MSCs and OPCs exposed to Molm-14 EVs. Fold change determined by $2^{-\Delta\Delta Ct}$ against vehicle-treated cells. Error bars are standard error of the mean from three separate experiments. Significance in (**B**) and (**C**) was determined by Student's t-test, *P<.05, **P<.01. **D.** Timecourse of UPR gene expression in explanted Molm-14. Molm-14 cells were sorted out of xenograft bone marrow based on human CD45 expression and cultured ex vivo. RNA was extracted from cells directly from the sort (0hr) or 48 and 72hrs in normal culture media in vitro. Fold change determined by $2^{-\Delta\Delta Ct}$ against in vitro cultured Molm-14 cells. Error bars are standard error of the mean from three separate experiments. **E.** UPR status was determined by protein levels of GRP78, and phosphorylated eIF2α in AML-patient samples and healthy pediatric and adult controls. **F.** Expression analysis of UPR genes from blasts from AML patients samples. Fold change determined by $2^{-\Delta\Delta Ct}$ in pairwise analysis against control samples. Error bars are standard error of the mean. **G.** Expression analysis of UPR genes from MSCs and OPCs from serum EV-injected femurs. Serum EVs from healthy donors or AML patients were harvested and intrafemoraly injected. Fold change was determined by $2^{-\Delta\Delta Ct}$ against respective cells from vehicle-injected femurs.

UPR induction alters EV cargo

To corroborate the observations that AML cells experiencing an UPR could more readily transfer ER stress and induce UPR in stromal cells, we decided to analyze EV cargo. Intriguingly, BMP signaling via leukemic blasts has been shown to promote osteogenic bias in MSCs[180]. Accordingly, we tested EVs for BMP2 content. Indeed, thapsigargin treatment significantly induced the expression of the BMP family of genes in Molm-14 cells (Figure 4-6A). *Ex vivo* analysis of the BMP family of proteins revealed that these genes are also significantly upregulated *in vivo*, and propagation in culture decreases their expression over time (Figure 4-6B). This gene set was also upregulated in patient-derived samples (Figure 4-6C). AML patients have been reported to

harbor increased concentration of circulating BMP2. We performed a BMP2 ELISA on EVs harvested from Molm-14 cells and found a significant increase in BMP2 protein contained within EVs derived from thapsigargin-treated cells compared to vehicle treated cells (Figure 4-6D). Intriguingly, there was no detectable change in vesicle free BMP2 (that is, not contained in EVs). These data suggest a model, supported by data from in both xenografts and patients, that AML blasts utilize UPR in the BM niche to adapt to metabolic ER stress, while dynamically adjusting their EV secretome for extrinsic transmission and UPR induction in recipient cells. This promotes the subsequent remodeling of stromal composition within the endosteal AML niche (Figure 4-6E).

4.4 DISCUSSION:

While circulating blasts are rapidly eliminated by conventional chemotherapy, at least 40% of AML patients relapse with drug resistant disease that persists in the BM. The adaptive changes that foster the survival of AML clones in the BM niche not only coincide with disease progression, but may play a causative role in drug resistance and hematopoietic suppression[50,198]. Accordingly, the crosstalk between tumor cells and the microenvironment that adapts stroma function represents a critical gap in our understanding of AML leukemogenesis. We and others previously demonstrated the trafficking of AML derived EVs to BM stroma[106,109,117,173], and the work herein further implicates EVs in the regulation of BM niche function, specifically via transmission of ER

FIGURE 4-6

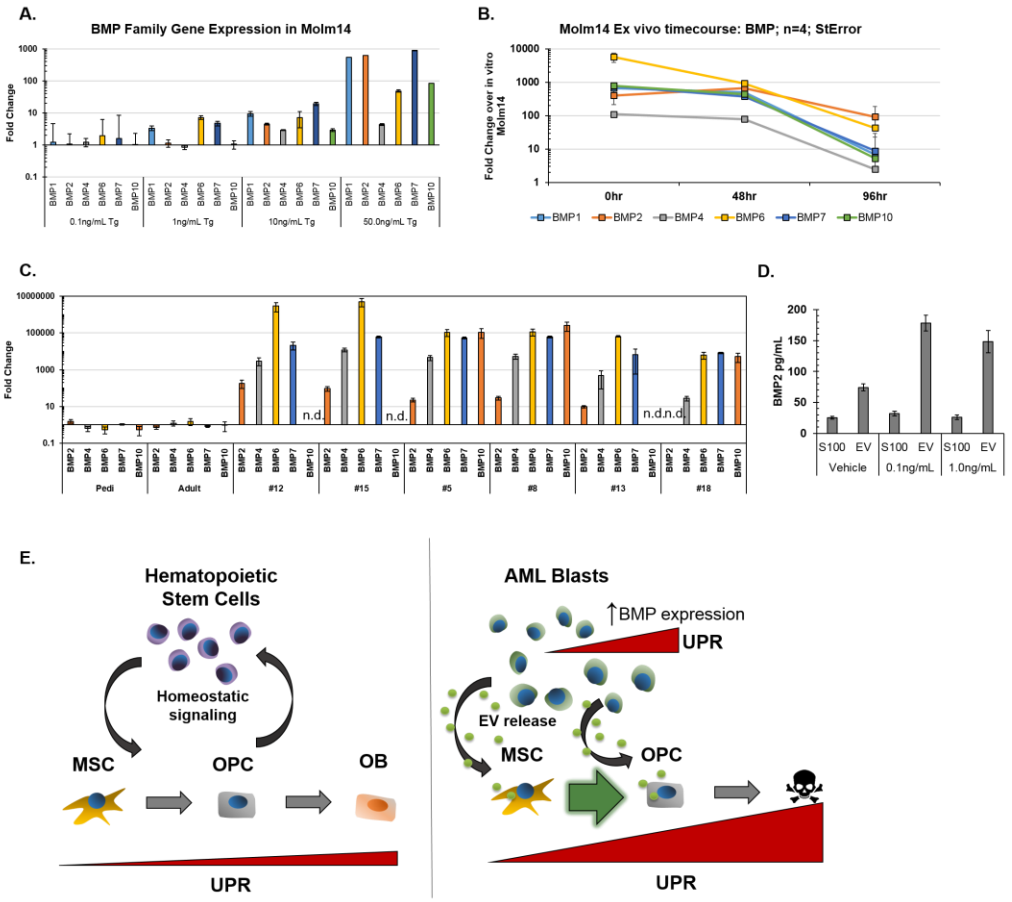

AML cells alter their EV cargo upon UPR induction. A. Expression analysis of BMP genes in Molm-14 cells cultured in thapsigargin. Fold change determined by 2-ΔΔCt against vehicle-treated cells. Error bars are standard error of the mean from (n=4, two separate experiments). **B.** Timecourse of BMP gene expression in explanted Molm-14. Molm-14 cells were sorted out of xenograft bone marrow based on human CD45 expression and cultured *ex vivo*. RNA was extracted from cells directly from the sort (0hr) or 48 and 72hrs in normal culture media *in vitro*. Fold change determined by $2^{-\Delta\Delta Ct}$ against *in vitro* cultured Molm-14 cells. Error bars are standard error of the mean from (n=7, two separate experiments). **C.** Expression analysis of BMP genes from AML patient samples. Fold change determined by $2^{-\Delta\Delta Ct}$ in pairwise analysis against control samples. Error bars are standard error of the mean. **D.** Concentration of BMP2 protein in the supernatant (SN) and pellet (EV) from EV harvest of Molm-14 cells cultured in thapsigargin. ELISA was used to determine protein concentration.**D.** *UPR stress promotes packaging of BMP2 into EVs.* Molm-14 cells were treated with vehicle or two doses of thapsigargin and the amount of BMP2 protein packaged into EVs was compared with an ELISA assay. **E**. Model for the alterations that occur within the endosteal niche in AML. Homeostasis is maintained via reciprocal signaling between stroma and hematopoietic stem cells (Chapter 1). During leukemic progression, AML blasts exhibit UPR induction, leading to an increase in BMP expression and packaging into EVs. EV trafficking to recipient MSCs and OPCs promotes an UPR and contributes to the enhanced osteogenesis in MSCs and apoptosis in OPCs.

stress, as a mechanism by which AML cells can actively shape the BM composition and alter the MSC phenotype.

To better understand the cell-cell signaling that alters and coopts the BM during AML invasion, we relied on a xenograft model that does not require host radiation and we prioritized the direct *ex vivo* analysis of immunophenotypically defined cell populations without tissue culture propagation in an unmanipulated microenvironment. First, we set out to undertake an unbiased survey of stroma composition with emphasis on the two key populations involved in endosteal niche function, where AML preferentially localizes[50,178]. Using validated immunophenotyping strategy, we observed a systematic shift in the proportion of MSCs and OPC that proved to be highly reproducible across different AML xenograft cell lines and correlated directly with suppression of clonal fibroblast expansion (CFU-F) and a p53 mediated pro apoptotic response in the case of OPC. We were particularly intrigued by the stromal cell type specific regulation whereby MSC simultaneously experienced a broad and significant induction of osteogenesis with a reduction in adipogenesis in the AML microenvironment.

Others previously showed that AML blasts similarly undergo a UPR to adjust to ER stress[199,200]. In addition there is more recent evidence that ER stress can be transmitted between cells in a tissue compartment, a known mechanism of drug resistance in pancreatic and breast cancer[182,183]. Here, we reasoned that

osteogenic MSC differentiation to a more secretory phenotype might provoke ER stress and engage one of three branches of the UPR as an adaptive mechanism to adjust protein folding and secretory load[120,184,201]. Our observations not only confirm those studies, but demonstrate that AML cells transfer ER stress that elicits a strong stimulus for osteogenic differentiation of MSC[118]. Thus, transmission of UPR responses from AML cells to both MSC and OPC contributes to the functional adaptation of the endosteal niche, but the rapid loss in expression of central UPR components *GRP78* and spliced *XBP1* in tissue culture suggests that this is highly-context dependent.

We previously showed that AML cells produce EVs that enter bystander cells in the AML niche and deliver protein and RNA regulatory cargo[173,185]. While often viewed as effectors of poorly defined phenotypic changes, EV trafficking can be a narrowly specific signaling paradigm, as in the case of suppressed colony formation via EV miRNA targeting of the c-Myb transcription factor that is highly expressed in hematopoietic progenitors, but not in HSC, MSC or OPC[185]. In other words, EVs are multicomponent signaling devices and the outcomes in different target cells differ based on target cell identity. Accordingly, while hematopoietic progenitors are regulated by EV contained miR-155, MSC appear to respond to BMP2 trafficking. The data certainly does not exclude mechanisms other that BMP trafficking in EV-mediated stromal UPR induction[202], and other cargo may modulate ER stress responses and subsequent phenotypic changes in BM stroma further. It is tempting to speculate that intracellular localization and cargo

deposition at ER membranes[191] may also be involved in the translational suppression via miRNA by ER resident components of the RISC complex[203,204].

The osteogenic differentiation of MSC in the AML niche echoes similar recent reports in patient-derived MSCs[47,48,180,188]. However, one study in particular caught our attention as it directly linked BMP2 release by AML blasts with MSC differentiation and leukemia promotion. Our data now indicate that EVs are the predominant carriers of BMP2 in tissue culture and in patient plasma, and are sufficient to elicit a UPR response and osteogenic differentiation in MSC. Importantly, upregulated EV production, increased BMP2 release, and UPR responses rely on specific environmental conditions found *in vivo*. Alternatively, inhibition of the Wnt signaling pathway has been previously described in a recent study as a mechanism driving the remodeling of bone marrow stroma[173]. In this study the authors show that AML-derived EVs are sufficient to upregulate Dkk1 expression. Intriguingly, Dkk1 is a known osteogenic inhibitor and instead has been linked to promotion of adipogenesis[205], a result opposing the results of this work. One reason for this discrepancy could arise from the different cell lines used (Molm-14, U937, and HL60 versus KG1A, MV411 and NB4) as well as the stromal isolation strategies which rely on different surface epitopes used to purify the stromal populations. This notion further supports the idea that the heterogeneity of AML may be reflected in the response of cells affected by AML EV signaling, as well as the recipient cell-type.

Finally, reciprocal signaling in the bone marrow microenvironment contributes to AML pathogenesis and the successive emergence of a more leukemia-permissive stroma environment can be viewed as a part of leukemogenesis[47,48,50,86,206-208]. However, unlike the disease heterogeneity among patients, BM stroma effects seem remarkably similar among different AML subtypes, indeed among different leukemias. This should provide strong motivation to uncover the durability of the observed changes, determine their impact on drug resistance, and develop adjuvant therapies that increase treatment efficacy without further escalating toxicity.

In aggregate, we demonstrate that AML EVs contribute to changes in BM stromal composition through ER stress transfer. We believe that these studies tie together several disparate observations in patients and murine models to support a model whereby AML EV trafficking of BMP2, transmits a stromal UPR and induces osteogenic differentiation of MSC.

4.5 MATERIALS AND METHODS:

Mice and xenografts

NOD-*scid* IL2R □ ^{null} mice were purchased from The Jackson Laboratory (Bar Harbor, ME, USA). Animals 6 to 8 weeks old were used in the experiments. Molm-14 cells (1×10^5 per animal), HL-60 cells (5×10^6 per animal), or U937 (2×10^5 per animal) were engrafted into nonirradiated animals by tail vein injection.

No randomization process was used. Chimerism was determined by flow cytometry on marrow plugs using a human CD45 antibody and/or mGFP expression. Animals were sacrificed at indicated time point and bone marrow from femurs and tibias were collected from each animal. Mouse care and experimental procedures were performed in accordance with federal guidelines and protocols approved by the Institutional Animal Care and Use Committee at Oregon Health & Sciences University.

Cell culture and EV preparation

Molm-14, HL60, and U937 cells were obtained from the laboratory of J. Tyner and were cultured in RPMI (Invitrogen/Gibco, Waltham, MA, USA) with 10% fetal bovine serum (FBS) (Gemini, West Sacramento, CA, USA) and 1X penicillin/streptomycin (Invitrogen/Gibco) at 37°C, 5% CO_2, and >95% humidity. Cell lines are routinely checked for *Mycoplasma* contamination using the MycoAlert Plus assay (Lonza, Switzerland). For imaging experiments, AML cells were transduced with lentivirus harboring the mGFP transgene (Addgene Plasmid #17481) and then purified using flow cytometry. Human $CD34^+$ bone marrow progenitors were purchased from ATCC and cultured in X-Vivo medium (Lonza) supplemented with BIT 9500 Serum Substitute (STEMCELL Technologies, Vancouver, BC, Canada), FMS-like tyrosine kinase 3 ligand (50 ng/ml), G-CSF (10 ng/ml), IL-3 (10 ng/ml), IL-6 (10 ng/ml), stem cell factor (SCF) (50 ng/ml), and thrombopoietin (25 ng/ml) (Peprotech, Rocky Hill, NJ, USA). EVs were isolated by differential centrifugation as described previously[185]. Briefly,

cells were cultured for 48 hours, the culture medium was spun at 300*g* for 10 min to remove cells, and then the supernatant was spun at 2000*g* for 20 min and at 10,000*g* for 20 min to remove cellular debris. The supernatant was centrifuged at 100,000*g* for 2 hours. EVs were either resuspended in phosphate-buffered saline (PBS) or media, depending on the experiment.

MSC and OPC isolation

Long bones were isolated and marrow plugs flushed as previously described [185]. Bones were then broken into small pieces with surgical scissors and incubated in Collagenase II (Sigma Aldrich) buffer (DMEM, 2% FBS, 1% Penicillin/Streptomycin, 2mg/mL Collagenase II) for one hour at 37°C and 200 RPM. The solution was then filtered through a 70µm filter, and then washed with Hemolytic Buffer. Hemolyzed cells were then filtered into Cell-Strainer tubes (Corning, Corning, NY, USA) and resuspended in FACS Wash (DPBS, 2%FBS), stained with antibodies, and then sorted/analyzed using flow cytometry. *In vitro* cultured cells were propagated in MSC media (MEMα, 15% FBS, 1X penicillin/streptomycin) at 37°C, 5% CO_2, and >95% humidity.

Intrafemoral injections of cell line and serum-derived EVs

Animals were anesthetized using isoflurane (1.5-2.0%) and carefully shaved at the injection site using an electric razor. The shaved area were disinfected and sterilized by alternate scrubbing with 1% betadine and 70% ethanol three times.

The injected leg was positioned so that it is bent at the knee at a 90˚ angle keeping the femur vertical. The injected femur was cored by gently twist using a 25-gauge needle at the patellar groove into the femoral cavity. The coring needle was carefully removed and another 27-gauge injection needle was inserted into the femoral cavity to slowly inject 50 µl of the sample suspended in PBS.

Patient and control samples

Peripheral blood samples were collected from pediatric patients with histologically confirmed, newly diagnosed AML treated at Texas Children's Hospital, Houston TX between 2009 and 2013. Informed consent was obtained from patients or their guardian in accordance with the US National Cancer Institute (NCI), and institutional policies before entry onto this study. Samples were collected in Cell-Save preservation tubes from patients with an absolute blast count of at least 1000 blasts/µL. Peripheral blood mononuclear cells (PBMCs) were isolated from peripheral blood using sucrose centrifugation. Magnetic bead separation (Miltenyi Biotech, Germany) was used to separate tumor cells from non-malignant cells. Anti-CD3 and anti-CD19 antibodies were used to enrich AML cells. B-isolation and T-isolation beads were used to isolate these tumor fractions. Tumor cells were frozen as pellets for immunoblotting and lysates made for Western blots and Simple Western (WesTM) analyses as previously described [209]. Negative controls were obtained from peripheral blood collected from healthy siblings of bone marrow transplant recipients and from

healthy adult volunteers. Patients were treated using either standard therapy or protocol-specific drugs as noted in Supplemental Table 1.

Chemicals and AML cell lines

Our control cell lines included U937 and THP1. ER stress was induced in cell lines using tunicamycin or thapsigargin. Cells were harvested pre-treatment, at 3hrs, 6hrs and 24hrs post treatment.

Protein detection

Capillary electrophoresis immunoblotting was performed using ProteinSimple Wes (ProteinSimple, San Jose, CA, USA). Minimum concentration of samples loaded for detection was optimized at 1mg/ml. Antibodies were used at the following concentrations: Grp78 (BD Pharmingen, Franklin Lakes, NJ, USA; 610978; 1:500), Actin (Sigma Aldrich, St. Louis, MO, USA; A5441; 1:250), phospho-eIF2α (Cell Signaling 9721; 1:50), total eIF (Cell Signaling, Danvers, MA, USA; 9722; 1:50) and IRE1 (Cell Signaling 3294; 1:50). UPR protein expression was quantified using the area under the curve (AUC) for the peak on the electropherogram for the protein of interest (ProteinSimple Compass software v2.7). The AUC for the UPR protein was normalized to the AUC for endogenous control actin for the same patient sample. UPR induction post chemotherapy was defined as more than 2 fold increase from baseline expression of the UPR protein.

RNA isolation and qRT-PCR

MSCs, OPCs, and KSL cells were sorted directly into 350μL of Buffer RLT (Qiagen, Germany). RNA was extracted using the manufacturers protocol from the RNeasy kit (Qiagen) and quantified using a NanoDrop 2000c spectrophotometer (Thermo Scientific, Waltham, MA, USA). RNA was converted into complementary DNA using the SuperScript III First-Strand Synthesis kit (Invitrogen) with oligo(dT) priming, followed by RT-PCR analysis using TaqMan. Relative quantification was calculated using the ΔΔCT algorithm with *Gapdh*/*GAPDH* as the endogenous control when appropriate.

Live cell microscopy of cells sorted from Xenografts

MSCs and OPCs were sorted into 2 ml Eppendorf tubes containing 1 ml of MSC media (as described above). Freshly sorted cells were centrifuged at 1000xg for 10 minutes at 4C and resuspended in fresh phenol-free media, before being replated onto Matrigel (growth factor reduced/phenol free) diluted 1:9 in 35mm live cell culture chambers with 4 well inserts and #1.5 polymer coverslip bottom (Ibidi, Germany). Cells were then incubated at 37°C 5% CO2 for 45 minutes to allow for attachment to Matrigel coated chamber. Cells were then stained with Hoechst (250ng/ml; ThermoFisher) and Cellmask Deep Red (1ul/ml; ThermoFisher) for 15 minutes at 37°C and gently washed twice with warmed phosphate buffered saline (1X) before adding fresh media. Cells were then

imaged using a Deltavision CoreDV/Olympus IX71 microscope, equipped with 60X Plan Apo N 1.49 objective, 7-color solid state LED illumination, motorized stage, Nikon Coolpix HQ CCD camera, and live cell chamber supplying 37°C/5% CO2. 3D Z-stacks were acquired in 3 channels using a 200nm Z-step through the entire cell volume to maximize capture speed while maintaining adequate axial resolution. Exposure times and laser intensity were held constant between conditions. To identify non-specific background for the 488 channel (GFP), z-stacks of MSCs and OPCs from non-xenografted NSG mice were captured to determine thresholding value. Images were deconvolved using SoftworXs and analyzed using Imaris Bitplane.

Live cell microscopy in vitro UPR stress experiments

FACS sorted MSCs and OPCs were expanded for one week in culture on Matrigel (1:11 dilution) coated Ibidi gridded culture slides with #1.5 coverglass. Cells were then treated with either 1ng/ml Thapsigargin, $1x10^8$ Molm-14 mGFP EVs or vehicle at 0 and again at 24 hours. At hour 36, cells were washed in 37°C phosphate buffered saline, stained with ER-Tracker (500nM in Hank's Balanced Salt Solution) for 1 hour, rinsed and stained with Cell Mask and Hoechst (as described above). Cells were then imaged in live cell conditions using a Nikon TiE microscope equipped with Yokogawa CSU-W1 Spinning Disk confocal, 100X Plan Apo TIRF 1.49 objective, 4-channel laser excitation, motorized stage, Nikon CCD camera, and live cell chamber supplying 37C/5% CO2. Z-stacks were acquired at 100nm Z-step using 50nm pinhole through the total volume of the cell

with exposure times and laser power held constant across conditions. Images were analyzed using imaris bitplane. To measure mGFP foci and their association with the ER territory, Imaris functions *Spots* and *Surfaces* were used to identify, count and differentially pseudo-color internal mGFP foci based on colocalization with ER tracker signal.

EV imaging and concentration determination

For vesical imaging, EVs were mounted in solid capture by embedding Molm-14 mGFP EVs into a solid hydrogel to prevent Brownian motion. To embed vesicles, EVs were resuspended up to 100ul in phenol-free media, shaken over night at 4C, then added on ice to Matrigel in a 1:6 v/v ratio with pre-cooled pipet tips. The ice-cold EV/Matrigel mixture is vortexed and immediately pipetted with pre-cooled pipet tips into a well of a 96-well imaging plate with #1.5 bottom (Ibidi) and incubated at 37C for 4 hours. Following incubation, solid gels containing mGFP-labled EVs are imaged by using a Nikon Yokogawa CSU-W1 Spinning Disk confocal as described above, and counted using Imaris Bitplane. Concentrations are determined by acquiring 3D Z-stacks with a known volume (100µm x 100µm x 10µm = $1x10^{-7}$ ml) using 488 laser excitation. Images of known volume were thresholded to remove non-specific background which calculated by imagining embedded non-fluorescently labeled Molm-14 EVs. Individual mGFP foci are counted in 5 fields of known volume using Imaris Surfaces function. The count average (n) is then multiplied by the dilution factor (df) and number of volume equivalents (V) per milliliter as shown.

$(n\ x\ df)\left(\frac{1\ ml}{V}\right) = EVs/ml$. To validate resolution of sub-diffraction level structure size, 34nm, 100nm and 180nm reference beads (ThermoFisher) were utilized to determine detection limit and relative signal point-spread estimation. Using a 100X Plan Apo 1.49 TIRF objective and 50nm pinhole, signals from all three beads were detectable with consistent size and intensity, with a point-spread roughly 4-fold larger than the actual size of the respective reference bead. This ensured that detection of particles in the EVs size range is possible using our microscopy system. To further validate accuracy and precision of counting individual foci within Z-stacks, 100nm Tetraspeck Beads (ThermoFisher) of known concentration.

CFU-F assay

One thousand MSCs and OPCs from NSG mice were sorted directly into 6-well plates containing MSC media (MEMα, 15% FBS, 1X penicillin/streptomycin) and cultured at 37°C, 5% CO_2, and >95% humidity for 14 days, replacing half of the media every three days. On day 15, cells were gently washed in PBS and then fixed in methanol. Cells were then incubated with Giemsa (EMD Millipore, Burlington, MA, USA) for one hour. Stain was removed and cells washed with water. CFU-Fs were counted and only colonies containing >50 cells were scored.

Osteo- and adipogenic differentiation assays

Sorted MSCs were allowed to reach confluency in culture (2-3 weeks) in MSC media prior to induction. For osteogenic differentiation, cells were cultured in

MSC media containing 100 nmol/L dexamethasone, 10 mmol/L beta-glycerophosphate, and 0.05 mmol/L L-ascorbic acid-2-phosphate for 3 weeks. Cells were fixed in 4% PFA and calcium mineralization of osteoblasts was detected by alizarin red staining and staining intensity was quantified by colorimetric detection of reextracted alizarin red at 405nm using a plate reader. For adipogenic differentiation, cells were incubated in MSC media containing 1µM dexamethasone, 1µM indomethacin, 500 µM 3-isobutyl-1-methylxantine (IBMX) and 10 µg/ml human recombinant insulin for 3 weeks. Cells were fixed in 4% PFA and lipid vacuoles were detected using oil red O staining and staining intensity was quantified by colorimetric detection of reextracted stain at 488nm using a plate reader.

ELISA

EVs were generated as previously described, and resuspended in manufacturer's diluent solution containing 1% Triton-X. Supernatant (SN) from the EV prep was used to detect vesicle free BMP2. Experiment was conducted per manufacturer's instructions (AbCam, United Kingdom; BMP2 detection kit, ab119581). Samples and standards were read using a SyngeryH1 plate reader (BioTek, Winooski, VT, USA). BMP2 concentrations were generated using a standard curve.

Statistical analysis

All experiments were replicated at least three times in the laboratory with the exception of the intrafemoral injections of patient-derived plasma (Figure 4-5G). Comparisons between two groups were performed with a two-tailed Student's *t*-test. One-way analysis of variance (ANOVA) was utilized when comparing more than two groups. T-tests with Bonferonni correction were used to determine p-values. An N of at least three animals or biological replicates was used in all analyses. Error bars represent ± Standard Error of the Mean. For qRT-PCR analyses, a pairwise comparison of fold change ($2^{-\Delta\Delta CT}$) between control and xenograft-derived cells, or between vehicle-treated and EV-treated cells was performed. P-values were determined by two-tailed Student's T-test following one-way ANOVA. An N of at least four were used in these analyses. Statistical analyses were performed using the PRISM software for Windows produced by Graphpad Software Inc. (La Jolla, CA, USA) For all experiments, statistical significance was set at *= p-val <0.05, **=p-val <.01, and ***=p-val <.001. No statistical test was used to determine the sample size. No randomization was used to allocate animals to particular groups; age and sex-matched recipients were used for transplantation experiments. The investigators were not blinded to experimental groups during analysis.

CHAPTER 5: Conclusions and Future Directions

Compiled in part from:

Doron, B., et al. (2017). "Concise Review: Adaptation of the Bone Marrow Stroma in Hematopoietic Malignancies: Current Concepts and Models." Stem Cells. PMID: 29235199

5.1 FUTURE DIRECTIONS

This dissertation work can be divided into two major sections: AML's influence on the hematopoietic stem cell niche, and its influence on the mesenchymal stem cell niche. While each project reached a fairly reasonable stopping point, there is plenty of work to be done.

The work published in *Science Signaling* in 2016 focuses on the how AML exosomes reduce the clonogenicity of c-Kit$^+$ HSPCs. This author would consider this result, while robust, to still be incredibly broad. The bone marrow cells within the c-Kit$^+$ population represent a spectrum of hematopoietic stem and progenitor cells, and the data we generated may only represent what is occurring in a majority subpopulation of this population. Currently, the effects of AML-derived exosomes on more stringently defined HSPC populations is underway in the Kurre lab, and we are learning that AML trafficking to these cells induces more discrete and nuanced responses. Further, the development of biomarkers based on the miRNA profile of serum-derived exosomes could benefit from additional follow-up in other miRNA species present in AML-derived exosomes. Alternatively, this system could be used to monitor for signs of relapse during remission, and the miRNA biomarkers could be based on the serum miRNA signature that is present during primary disease. This would require generating a patient-specific miRNA panel, and an easier way to sequence or detect miRNA. Currently, this is not cost effective, but hopefully the future of advanced medicine will not be hindered by the price tag of therapies.

The project described in Chapter 4 regarding AML's influence on the MSC niche in the bone marrow has certainly opened up more questions than it has answered. For one, how does the compositional shift between MSCs and OPCs result in a more pro-leukemic niche? Work from others indicate that OPCs secrete factors that promote leukemic growth and proliferation[180,210], and preliminary observation we have made suggest that in the early stages of leukemic burden there is an increase in the proportion of OPCs. This makes sense considering the osteogenic promotion of MSCs by AML. There is perhaps a window of time during which the leukemia can trigger osteogenesis in MSCs, but not induce the apoptosis in OPCs that is observed during advanced disease burden. This may have to do with the "dose" of UPR induction, which, as discussed in Chapter 4, is sufficient to drive osteogenesis and apoptosis in either population, respectively. If the transfer of UPR is dependent on the amount of AML in the bone marrow, then it seems reasonable that the niche is shaped differently during early and late disease progression, as the UPR dose is relatively low when chimerism is around 20%, and high when chimerism is over 70%, which is the window we looked through for this project. Considering that UPR is a stress pathway that can be triggered by a variety of external stressors such a hypoxia and nutrient deprivation, an overcrowded marrow bursting with leukemic clones might contain a different proteotoxic signature than in earlier stages of disease.

One major experimental avenue that did not reach fruition meant to explore how AML accomplishes stable remodeling of stromal cell function.

Despite the selection pressures provided by standard treatment regimens which shape residual leukemic cells to become hyper-aggressive in relapse, there is also stromal element contributing to AML relapse. While stroma can be actively manipulated by leukemia to support malignant cells at the expense of normal hematopoiesis[174], this author speculates that these changes are reinforced by epigenetic mechanisms within the stromal cells themselves. This would result in stably remodeled niches that provide the fertile soil for residual leukemic seeds to flourish into aggressive relapse. This is a relatively unexplored concept in AML biology, and may provide a common thread through the heterogeneous background of AML, with the hope that this idea could lead to adjuvant therapies that reduce the incidence of relapse.

This idea was spawned by the data generated in preliminary experiments, as well as thorough investigation of the current literature. Primarily, observations made in the Konopleva lab demonstrated that the expression of pro-survival cytokine secretion by AML patient stromal cultures persisted through multiple passages *ex vivo*, rather than returning to normal expression levels[211]. These observations show that AML-exposed mesenchymal cells cultured *in vitro* maintain a pro-leukemic transcriptional signature over time in the absence of any leukemic influence. We have also generated preliminary data demonstrating that AML can actively dysregulate several genes involved in epigenetic remodeling, particularly enzymes involved in controlling DNA methylation. Dysregulation of these enzymes has been implicated in multiple disease states due to the resultant genome-wide aberrant gene expression. While DNA methylation is a

major contributor to the leukemia epigenome[212], it has not been determined how AML manipulates this ubiquitous process in nonmalignant bone marrow cells. Our interpretation of these data has informed this proposed model: AML cells signal to mesenchymal cells in the bone marrow, shifting their supportive role away from hematopoiesis towards the leukemic cells. These changes in gene expression are reinforced by endogenous epigenetic machinery, which may also be actively manipulated by the leukemia. The result of this process is a bone marrow microenvironment that has been stably remodeled to support leukemia. Importantly, this process would prime the bone marrow for disease relapse, either from residual AML blasts or from a secondary neoplasm.

Unfortunately, technical issues surrounding the whole genome bisulfite sequencing experiment prevented us from getting the resolution of CG methylation required to pursue this hypothesis. Despite this, global analysis of the data supported the notion that both MSCs and OPCs were epigenetically distinct, and MSCs and OPCs derived from xenografted mice were also epigenetically distinct from their counterparts in healthy mice. This could have been powerful data, as we would have been able to describe the DNA methylation state of distinct stromal cell types, as well as identify pathways dysregulated and epigenetically reinforced by AML. This author would strongly urge Peter to pursue this, as this study could potentially have important implications for the treatment of AML, and even other types of cancers. Study showing reversion of stromal function can inhibit, or at least reduce the growth of

leukemia, implicating that the development of stroma-targeted adjuvant therapies would reduce the rate of relapse and increase the efficacy of targeted therapies[51,83,213].

This author hopes that the dissertation work has opened up avenues of future research, including translation into the clinic in some form, whether that be in building on the exosomal miRNA biomarker platform or looking into stroma-targeted adjuvant therapies. Below are outlined a few key issues that may have introduced artifacts into the data, as well as alternative routes of analysis. Importantly, concrete scientific data is only generated at the level at which we can resolve phenomena, or to put it another way: we can only measure what we can see. Beyond this lies theoretical science, which provides the roadmap to future studies and informs technological developments that will increase our limits of detection.

5.2 DISEASE MODELING

Xenografts

As described in the introduction, the use of the NSG mouse strain has provided the opportunity to study human AML experimentally *in vivo*. Additionally, xenograft models also allow the role of stroma in disease propagation to be addressed [49,50], as well as the use of patient-derived xenograft (PDX) models which been used to study of primary cancer tissue, especially in understanding

disease progression and evaluating drug responses [52,53]. Recent work by the Bhatia lab has demonstrated that NSG mice grafted with HLA mismatched patient AML cells and healthy human control hematopoietic cells can further refine the study of interactions between healthy and malignant hematopoietic cells *in vivo.* Despite these promising developments, the lack of a functional immune system and inconsistencies of engraftment in PDX models remain obstacles in the study of human AML *in vivo*. To alleviate these shortcomings, new strategies of grafting include the use of humanized mice, which provide an immune system and express specific human hematopoietic supportive factors to enhance engraftment success[214]. Alternative efforts to generate a humanized bone marrow niche in mice are moving towards the use of bioengineered scaffolds. Three dimensional extramedullary scaffolds can mimic human bone marrow niches and provide a viable environment for modeling human cancer[215,216]. These human MSC-derived structures support the ectopic engraftment and proliferation of AML cells[215,217], reducing concerns about species-specific interactions between stroma and leukemia[216,218,219].

Transgenic models of AML

Current techniques in genetic engineering have generated a number of murine leukemia models using transgenic mice with tissue specific loss- or gain-of-function phenotypes intended to mimic common genetic lesions encountered in patients. Genetically Engineered Mouse Models (GEMM) provide faithful alterations to genes of interest with a high degree of disease penetrance, as well

as an intact immune system. Recently developed GEMMs utilize tissue specific approaches to dysregulate gene expression in specific cell types or tissues, and provide temporal control of Cre-recombinase mediated excision and disease onset [38]. These allow for the study of tumor initiation and provide an intact microenvironment that contains stromal and immune populations more representative of disease propagation in patients[39,40]. An important step in the translation of this dissertation work would be to perform parallel analyses using the *MLL-AF9 FLT3-ITD* syngeneic mouse model, which reflects the biology of the Molm-14 cell line quite accurately.

5.3 BONE MARROW POPULATION ISOLATION

The use of antigen and genetic labeling techniques to identify and isolate discrete populations has provided an enormous impetus to the study of the role of cells within bone marrow niches. While this technique pushed tissue biology beyond the confines of morphological analyses[220], it is important to understand that this is an *enrichment* technique. The increasing ability to analyze biological phenomena at greater and greater resolutions has shown that these enriched populations contain a relatively large amount of heterogeneity. The cKIT^{+} population of cells analyzed in Chapter 3 contain long-term and short-term HSCs, as well as early progenitors. Increasing the stringency by eliminating progenitors using SCA-1 and lineage markers further enriches for stem cells (termed KSL cells). This can be taken even further by also including the SLAM markers

CD150, CD48, CD229, and CD244 to look at four more populations within the KSL population. This problem is even more prevalent in stromal populations which lack the immunophenotypic resolution found in hematopoietic tissue. Indeed, my “MSC” and “OPC” populations are groups of cells containing true MSCs and OPCs, but there must be a spectrum of cell types that express the same surface markers. It is becoming obvious that single-cell analysis will provide paradigm-shifting insights into the properties of cells within a tissue[221-223].

5.4 EXOSOME ISOLATION

The majority of the exosomes used in this study were isolated from the supernatant of cells growing in monoculture using ultracentifugation. This generates two potential pitfalls when interpreting the results of experiments utilizing vesicles prepared in this way: the exosomal composition may not accurately reflect the content of exosomes generated by the same cells *in vivo*; and ultracentrifugation alone only *enriches* for exosomes, with both debris and other vesicles such apoptotic bodies and microvesicles present in the preparation. The former presents a challenging obstacle, as purification of AML-derived exosomes from a xenograft in sufficient abundancy would be extremely difficult. This could potentially be accomplished, and efforts should be made to make this a reality. The use of *mGFP*-expressing AML lines generates GFP^+ vesicles that are detectable in xenograft serum[185], which could then be purified using flow cytometry or imaged with fluorescent microscopy[224]. Flow cytometric

isolation of exosomes shows promise as a method for purifying exosomes based on either genetic labeling (*mGFP*) or via antibody staining of common exosome surface markers such as TSG101 or CD63[96,101]. This technique could also be utilized to address the second pitfall of exosome preps by either forgoing ultracentifugation, or used as a secondary purification of exosomes from spun-down preparations. Multiple groups have also utilized sucrose gradients to further isolate exosomes based on density, and some have even further combine ultracentrifugation with sucrose gradients and immune-affinity enrichment for CD63[144,145]. As the techniques for exosome isolation become more sophisticated, we will see an increase in both the dynamic biology of these vesicles, and a retraction of aspects of exosome biology that resulted from artifacts in crude exosome preparations.

5.5 CONCLUSIONS

Prior to entering the Programs in Molecular and Cellular Biosciences PhD program, I worked in a lab studying a fungal pathogen of oats, and then a lab studying a bacterial lung pathogen of humans. This experience provided me with insight into the “Evolutionary Arms Race” between pathogen and host, which is one of my favorite biological concepts. My initial conversations with Peter and Noah about exosome trafficking in the leukemic niche sparked the notion that cancer, in a sense, is a pathogen. At a seminar a few months later[†], an almost

[†] I unfortunately have forgotten who the speaker was.

offhand comment by the speaker along the lines of “cancer is Darwinian Evolution within tissues” made everything click, and galvanized my philosophy on cancer biology. I still try to keep an open mind on this however, as recent work conducted in the Sears lab at OHSU suggest a “Lamarkian” mechanism of tumor evolution through the exploitation of epigenetic plasticity[225]. A fascinating concept that I also hope to explore in my career.

My work in collaboration with Noah concerning the use of AML-derived exosomes as biomarkers for disease introduced me to exosome biology and protocols, miRNA biology and analysis, and the Molm-14 xenograft model. With Noah’s guidance, I analyzed the miRNA profile of exosomes isolated from the serum of mice using qRT-PCR designed to measure miRNA abundance, as the oilgo-dT method of cDNA synthesis is incompatible with miRNA transcripts, and he leveraged these data to generate the statistical analysis required for biomarker studies. Our work showed that AML-derived exosomes contain a unique miRNA profile compared to exosomes derived from healthy $CD34^+$ cells. We then showed that this phenomenon could be exploited to generate a biomarker platform based on sequencing miRNA from exosomes in the peripheral blood. Importantly, this system promises the ability to detect relapse at an early stage in patients in remission. This is due to the lack of circulating AML blasts during initial relapse, which instead hide within the bone marrow, yet can still secrete exosomes into the periphery.

The recently deflated hypothesis that overcrowding in the marrow was responsible for the inhibition of hematopoiesis[162] provided the motivation to seek

out a transferred molecule that was responsible for causing this comorbidity. Our attention then shifted to the biological consequences of miRNA trafficking to HSPCs. Working off of the foundation we built in our biomarker experiments, we then dissected the contributions of exogenously delivered miR-150 and -155 in HSPCs. In a two pronged approach that emphasized our individual strengths we demonstrated that miR-155 is sufficient to cause the hematopoietic suppression common in this disease. We then conducted the RISC-trap experiment with miR-155. This experiment, in collaboration with the Goodman lab, yielded data that Noah was able to computationally analyze, which I then subsequently validated experimentally. The data we generated in this study provided much need insight into how AML induces cytopenias, demonstrating that miRNA trafficking via exosomes directly from AML to HSPC could sufficiently modulate HSPC function. The summation (or rather a good stopping point) of this work is embodied in our joint 2016 publication in *Science Signaling*.

The next stage of my dissertation proved to be quite difficult. I wanted to explore the stromal contributions to leukemic progression, particularly concerning the stable remodeling of stromal function by which the bone marrow maintains a pro-leukemic phenotype through remission, and thus contributes to the aggressive nature of relapse. Inferential evidence for the potential durability of abnormal function comes from the sustained impairment of patient-derived MSCs to support hematopoietic cells after serial passages *in vitro*, and epigenetic changes in patient MSC [35,206,226].

To approach this, I developed a protocol to isolate MSCs and OPCs based on their immunophenotypic signatures, and validated their roles in the NSG mouse. One sentence summarizing the eventual success of this endeavor following the months of troubleshooting, frustration, and despair did not feel justified; so I included this one. After getting this protocol finalized, I was able to study AML's effects in MSCs and OPCs with a high degree of resolution and reproducibility. Using this method, I have demonstrated that not only does AML negatively affect these cells, but these cells have unique responses to AML influence. This is an important, if nuanced observation. Current studies of patient-derived MSCs rely on expansion on plastic, incubating primary cells *in vitro* for days prior to analysis. While this generates a uniform stromal population maintaining differential potential and surface markers that denote human MSCs[227,228], it remains unclear how representative these MSCs are from their *in vivo* counterparts[229,230]. This is where the mouse model shines, the allowance of fresh isolation of rare stromal cells, provides data more illustrative of the *in vivo* interactions between AML and stroma. While this work is ongoing as I write this, it appears that AML can induce the UPR in MSCs and OPCs, and this is at least partially mediated by exosome trafficking. The exogenous UPR stimulation prompts differential fates in these two population, with the implications that this is a mechanism that contributes to bone marrow remodeling and the synthesis of pro-leukemic niches[35,49,50,180,206,231].

In addition to my contributions to the hematology field, I feel like my experience in graduate school has made me a stronger and more humble person. There were times that really tested my resolve and perseverance. In talking with graduate students and recent graduates, I have come to the conclusion that to get through graduate school, one must suffer in some way or another. Learning how to keep pushing forward, to let disappointment and failure inform the next move rather than hamper it, are important attributes for life as well as work as a scientist. This is one last thank you to everyone else who helped guide me along the way.

Ben Doron

2705 SW Spring Garden St, Portland, OR 97239 | 503-309-4456 |
ben.doron.888@gmail.com
LinkedIn: https://www.linkedin.com/in/ben-doron-71b75760

EDUCATION

2010 Oregon State University
BS Biology, Chemistry Minor

2013-2018 Oregon Health Sciences University
PhD in Molecular and Cellular Biosciences: Cancer Biology
Dissertation: "Exosome-Mediated Remodeling of Hematopoietic and Mesenchymal Stem Cell
Niches in the Leukemic Bone Marrow"

AWARDS

2012 Best Poster at OHSU MMI Annual Retreat. "*Legionella pneumophila requires the IcmSW chaperones for the export of a subset of effector proteins"*

2015 Nicholas L. Tartar Trust Fellowship Award – *This was awarded following a submitted research proposal. This award was used to fund the purchase of equipment related to my studies.*

2016 Best Poster at OHSU CDCB Retreat. "*Systemic trafficking of leukemia-derived exosomes impairs hematopoiesis through miRNA action on c-Myb*"

2017 Knight Cancer Institute Sponsored Graduate Student Stipend – *This was awarded following a submitted research proposal. This award will cover my stipend for one year.*

2017 Winner, OHSU Three Minute Thesis Competition, People's Choice Award- "*Acute Myeloid Leukemia: BAD TO THE BONE"*, Portland, OR.

2017 Finalist, State of Oregon Three Minute Thesis Competition- "*Acute Myeloid Leukemia: BAD TO THE BONE"*, Eugene, OR.

2017 OHSU Cancer Biology Student Stipend Award- *This grant was awarded following submission of a written research proposal. The award funded my student stipend for an entire year.*

RESEARCH EXPERIENCE

2007-2009 Oregon State University Plant Pathology Clinic
Molecular Diagnostician
I performed diagnostic PCR on plant material for pathogen detection and reported the results to the clinic. This job was my introduction to lab work, and I learned a lot of basic lab skills including, aseptic technique, diligent note taking, setting up properly controlled assays, and reporting data and results clearly.

2009-2011 Oregon State University Plant Pathology Dept.
Undergraduate Researcher, Research Assistant II
I worked in Dr. Tom Wolpert's laboratory using biochemical and molecular techniques aimed at understanding *C. victoriae* (Victoria Blight) pathogenesis. I was involved in experimental design and execution of an independent research project involving the interactions of two proteins involved in the plant innate immune system, and their response to Victorin toxin. I performed protein-interaction assays, plant culture, genetic manipulation of *Arabidopsis* and *Nicotiana* species, toxin purification via HPLC, data analysis, and presentation of my work.

2011-2013 OHSU Molecular Microbiology and Immunology Dept.
Research Assistant II
I worked in Dr. Eric Cambronne's laboratory and used biochemical and molecular biological experimentation aimed at understanding *L. pneumophila* (Legionairre's Disease) pathogenesis. I was responsible for multiple research projects involved in identifying chaperone proteins responsible for the controlled secretion of effector proteins involved in host-cell manipulation. I also worked on identifying host-dependent signaling factors that altered effector protein expression. I contributed to the generation of a new protocol for harvesting phagocytosed bacteria, and gene expression profiling of *L. pneumophila* harvested from various protozoan and mammalian host cells. I identified chaperone-dependent effector proteins, and presented my work at multiple conferences.

2013-2018 OHSU Pediatrics and Cancer Biology Departments
PhD Candidacy Research
I am in Dr. Peter Kurre's laboratory using biochemical, genetic, and molecular biological experimentation aimed at understanding how Acute Myeloid Leukemia influences the bone marrow microenvironment. I have two projects, each related to how leukemia influences the nonmalignant resident cells of the bone marrow. My early project involves understanding how AML-derived extracellular vesicles deliver specific microRNA molecules to hematopoietic stem and progenitor cells, and the effects on hematopoietic function. This project utilizes both in vitro assays and in vivo xenografting modeling of human AML. My second project involves analyzing the long-term effects of AML on the mesenchymal stem cells (MSCs) and early osteoblastic progenitor cells (OPCs) of the bone marrow. This project involves the use of xenografted animals and studying how the physiological changes in these stroma cells persist in the absence of leukemia. To this end I

am utilizing whole-genome bisulfite sequencing on AML-exposed MSCs and OPCs, as well as a novel model of AML remission.

TEACHING EXPERIENCE

2015 Murdock Scholar Mentor.
I guided an undergraduate Murdock Scholar in laboratory practice including experimental design, safe and sterile technique, cloning, the CRISPR/Cas9 system, and data analysis.

2016 Instructor for OHSU Nanocourse: "Exosomes".
I worked with three OHSU professors to construct a curriculum and lecture to students, technicians, and post-docs to cover the current advances in exosome and microvesicle biology.

2017 Guest Lecture at University of Oregon Honors College: "Cell Signaling, Extracellular Vesicles, and Implications in Leukemia".
I created a curriculum aimed at describing our work in exosome and leukemia biology to students with a mixed background in molecular biology. This lecture covered basic cellular signaling mechanisms and then delved into leukemogenesis and the role of exosomes in the bone marrow.

PUBLICATIONS

2013 Drennan, S. L., Lama, A., Doron, B., & Cambronne, E. D. (2013). Tractable mammalian cell infections with protozoan-primed bacteria. *J Vis Exp*(74). doi:10.3791/50300. PMC.

2015 Doron B., Kurre P. *Encyclopedia of Cancer: Exosomes*. Springer Publishing Group. Springer.
This entry was written to cover the basic concepts of exosome biogenesis and the role these vesicles play in cancer biology.

2016 Hornick NI, Huan J, Doron B, Goloviznina NA, Lapidus J, Chang BH, Kurre P. (2015) Serum Exosomes MicroRNA as a Minimally Invasive Early Biomarker of AML. *Scientific Reports*. PubMed.
This manuscript provides a platform for a less invasive method of monitoring patients in remission from AML by measuring the miRNA profile of serum-derived exosomes. I performed serum-exosome enrichment and subsequent miRNA analysis, and contributed to writing the manuscript.

2016 Hornick NI*, Doron B*, Huan J, Harrington CA, Shen R, Cambronne XA, Kurre P. (2016) AML Exosomes Suppress Hematopoiesis through miRNA Action on the Transcription Factor c-Myb. *Science Signaling*. *these authors contributed equally to this work. PubMed.
Within this manuscript we describe the role and mechanism of exosome mediated hematopoietic suppression. We identify novel targets of microRNA-155 and additional pathways that are dysregulated by exogenous delivery of this microRNA. I contributed to the experimental design, performed experiments, generated figures, and wrote the manuscript.

2017 Doron B, Handu M, Kurre P. (2017). Concise Review: Adaptation of the Bone Marrow Stroma in Hematopoietic Malignancies: Current Concepts and Models. *Stem Cells*. PubMed.
This review covers current topics in the leukemia microenvironment, specifically the stromal conversion by leukemia and the resulting aberrant signaling within the niche. This article discusses the advantages and limitations of available experimental model system and emphasizes open scientific questions and opportunities.

PRESENTATIONS

2013 Poster Presentation at OHSU Molecular Microbiology and Immunology Retreat. Portland, OR. "*Legionella pneumophila requires the IcmSW chaperones for the export of a subset of effector proteins*"

2013 Poster Presentation at American Society of Microbiology Annual Meeting. Denver, CO "*Legionella pneumophila requires the IcmSW chaperone complex for the export of a subset of effector proteins*"

2013 Oral Presentation at OHSU Molecular Microbiology and Immunology Seminar Series. Portland, OR. "*Chaperone proteins and their role in the Type IV secretion system of Legionella pneumophila*"

2013 Poster Presentation at OHSU PMCB Retreat. Welches, OR. "*AML selectively packages miRNA for exosomal delivery to hematopoietic cells*"

2014 Ten Minute Talk at OHSU Research Week. Portland, OR. "*RISC-y Business: miRNA mediated suppression of hematopoiesis*"

2016 Poster Presentation at Keystone Conference: Tumor Microenvironment. Breckinridge, CO. "*Systemic trafficking of leukemia-derived exosomes impairs hematopoiesis through miRNA action on c-Myb*"

2016 Oral Presentation at OHSU CDCB Seminar Series, Portland, OR. "*AML-exosome mediated suppression of hematopoiesis"*

2016 Oral Presentation at OHSU CDCB Seminar Series, Portland, OR. "*AML mediates bone marrow stromal remodeling"*

2017 Oral Presentation at OHSU and State Three Minute Thesis Competition, Portland, OR and Eugene OR. "*Acute Myeloid Leukemia: BAD TO THE BONE"*

2017 Poster presentation at CABTRAC annual retreat

2017 Poster presentation at ASH conference.

2018 Dissertation Defense at OHSU: "A Tale of Two Niches: Exosome-Mediated Remodeling of Hematopoietic and Mesenchymal Stem Cell Niches in the Leukemic Bone Marrow", Portland, OR

CONTRIBUTIONS TO SCIENCE

2015 Reviewed Manuscript for *PLOS One*

2015 Reviewed Manuscript for *Cancer Letters*

2015 Reviewed Manuscript for *PLOS One*

2016 Reviewed manuscript for *Leukemia*

REFERENCES

1. Ayala FJ. "Nothing in biology makes sense except in the light of evolution": Theodosius Dobzhansky: 1900-1975. J Hered 1977;68:3-10.
2. Baym M, Lieberman TD, Kelsic ED, et al. Spatiotemporal microbial evolution on antibiotic landscapes. Science 2016;353:1147-51.
3. Greaves M. Evolutionary determinants of cancer. Cancer Discov 2015;5:806-20.
4. Hanahan D, Weinberg RA. The hallmarks of cancer. Cell 2000;100:57-70.
5. Hanahan D, Weinberg RA. Hallmarks of cancer: the next generation. Cell 2011;144:646-74.
6. Hoggatt J, Kfoury Y, Scadden DT. Hematopoietic Stem Cell Niche in Health and Disease. Annu Rev Pathol 2016;11:555-81.
7. Pietras EM, Warr MR, Passegue E. Cell cycle regulation in hematopoietic stem cells. J Cell Biol 2011;195:709-20.
8. Weissman IL, Shizuru JA. The origins of the identification and isolation of hematopoietic stem cells, and their capability to induce donor-specific transplantation tolerance and treat autoimmune diseases. Blood 2008;112:3543-53.
9. Iveson-Iveson J. Anatomy and physiology: the blood. Nurs Mirror 1979;148:35.
10. Matarraz S, Lopez A, Barrena S, et al. The immunophenotype of different immature, myeloid and B-cell lineage-committed CD34+ hematopoietic cells allows discrimination between normal/reactive and myelodysplastic syndrome precursors. Leukemia 2008;22:1175-83.
11. Lowenberg B, Downing JR, Burnett A. Acute Myeloid Leukemia. New Engl J Med 1999;341:1051-62.
12. Renneville A, Roumier C, Biggio V, et al. Cooperating gene mutations in acute myeloid leukemia: a review of the literature. Leukemia 2008;22:915-31.
13. De Kouchkovsky I, Abdul-Hay M. 'Acute myeloid leukemia: a comprehensive review and 2016 update'. Blood Cancer J 2016;6:e441.
14. Howlader N NA, Krapcho M, Neyman N, Aminou R, Waldron W, Altekruse SF, Kosary CL, Ruhl J, Tatalovich Z, Cho H, Mariotto A, Eisner MP, Lewis DR, Chen HS, Feuer EJ, Cronin KA, Edwards BK (eds). SEER Cancer Statistics Review, 1975-2008. 2011 ed. Bethesda, MD: National Cancer Institute; 2010.
15. Meyers J, Yu Y, Kaye JA, Davis KL. Medicare fee-for-service enrollees with primary acute myeloid leukemia: an analysis of treatment patterns, survival, and healthcare resource utilization and costs. Appl Health Econ Health Policy 2013;11:275-86.
16. Faulk K, Gore L, Cooper T. Overview of therapy and strategies for optimizing outcomes in de novo pediatric acute myeloid leukemia. Paediatric drugs 2014;16:213-27.

17. Sill H, Olipitz W, Zebisch A, Schulz E, Wolfler A. Therapy-related myeloid neoplasms: pathobiology and clinical characteristics. Br J Pharmacol 2011;162:792-805.
18. Patel JP, Gonen M, Figueroa ME, et al. Prognostic relevance of integrated genetic profiling in acute myeloid leukemia. N Engl J Med 2012;366:1079-89.
19. Knudson AG, Jr. Mutation and cancer: statistical study of retinoblastoma. Proc Natl Acad Sci U S A 1971;68:820-3.
20. Hasserjian RP. Acute myeloid leukemia: advances in diagnosis and classification. Int J Lab Hematol 2013;35:358-66.
21. Takahashi S. Current findings for recurring mutations in acute myeloid leukemia. J Hematol Oncol 2011;4:36.
22. Dohner H, Estey EH, Amadori S, et al. Diagnosis and management of acute myeloid leukemia in adults: recommendations from an international expert panel, on behalf of the European LeukemiaNet. Blood 2010;115:453-74.
23. Park SH, Chi HS, Min SK, Park BG, Jang S, Park CJ. Prognostic impact of c-KIT mutations in core binding factor acute myeloid leukemia. Leuk Res 2011;35:1376-83.
24. Port M, Bottcher M, Thol F, et al. Prognostic significance of FLT3 internal tandem duplication, nucleophosmin 1, and CEBPA gene mutations for acute myeloid leukemia patients with normal karyotype and younger than 60 years: a systematic review and meta-analysis. Ann Hematol 2014;93:1279-86.
25. Levis M. FLT3 mutations in acute myeloid leukemia: what is the best approach in 2013? Hematology Am Soc Hematol Educ Program 2013;2013:220-6.
26. Druker BJ, Tamura S, Buchdunger E, et al. Effects of a selective inhibitor of the Abl tyrosine kinase on the growth of Bcr-Abl positive cells. Nat Med 1996;2:561-6.
27. Advani AS. FLT3 and acute myelogenous leukemia: biology, clinical significance and therapeutic applications. Curr Pharm Des 2005;11:3449-57.
28. Tallman MS. Acute myeloid leukemia; decided victories, disappointments, and detente: an historical perspective. Hematology / the Education Program of the American Society of Hematology American Society of Hematology Education Program 2008:390.
29. Barrett A, Barrett AJ, Powles RL. Total body irradiation and marrow transplantation for acute leukaemia. The Royal Marsden Hospital experience. Pathologie-biologie 1979;27:357-9.
30. Dicke KA, Zander AR, Spitzer G, et al. Autologous bone marrow transplantation in relapsed adult acute leukemia. Experimental hematology 1979;7 Suppl 5:170-87.
31. Forman SJ, Rowe JM. The myth of the second remission of acute leukemia in the adult. Blood 2013;121:1077-82.
32. Yin JA, O'Brien MA, Hills RK, Daly SB, Wheatley K, Burnett AK. Minimal residual disease monitoring by quantitative RT-PCR in core binding factor AML allows risk stratification and predicts relapse: results of the United Kingdom MRC AML-15 trial. Blood 2012;120:2826-35.

33. Dohner H, Estey EH, Amadori S, et al. Diagnosis and management of acute myeloid leukemia in adults: recommendations from an international expert panel, on behalf of the European LeukemiaNet. Blood 2010;115:453-74.
34. Ding L, Ley TJ, Larson DE, et al. Clonal evolution in relapsed acute myeloid leukaemia revealed by whole-genome sequencing. Nature 2012;481:506-10.
35. Duan CW, Shi J, Chen J, et al. Leukemia propagating cells rebuild an evolving niche in response to therapy. Cancer Cell 2014;25:778-93.
36. Lehrnbecher T, Sung L. Anti-infective prophylaxis in pediatric patients with acute myeloid leukemia. Expert Rev Hematol 2014;7:819-30.
37. Geyh SR-P, M.; Khandanpour, C.; Cadeddu, R.P.; Jäger, P.; Zilkens, C.; Dührsen, U.; Wilk, C.M.; Fenk, R.; Gattermann, N.; Germing, U.; Kobbe, G.; Lyko, F.; Haas, R.; Schroeder, T. Functional Inhibition of Mesenchymal Stem and Progenitor Cells (MSPC) Significantly Contributes to Hematopoietic Insufficiency with Acute Myeloid Leukemia (AML). 56th ASH Annual Meeting and Exposition. San Francisco, CA2014.
38. Heyer J, Kwong LN, Lowe SW, Chin L. Non-germline genetically engineered mouse models for translational cancer research. Nat Rev Cancer 2010;10:470-80.
39. Hasegawa K, Tanaka S, Fujiki F, et al. An Immunocompetent Mouse Model for MLL/AF9 Leukemia Reveals the Potential of Spontaneous Cytotoxic T-Cell Response to an Antigen Expressed in Leukemia Cells. PLoS One 2015;10:e0144594.
40. Bresin A, D'Abundo L, Narducci MG, et al. TCL1 transgenic mouse model as a tool for the study of therapeutic targets and microenvironment in human B-cell chronic lymphocytic leukemia. Cell Death Dis 2016;7:e2071.
41. Basova P, Pospisil V, Savvulidi F, et al. Aggressive acute myeloid leukemia in PU.1/p53 double-mutant mice. Oncogene 2014;33:4735-45.
42. Beurlet S, Omidvar N, Gorombei P, et al. BCL-2 inhibition with ABT-737 prolongs survival in an NRAS/BCL-2 mouse model of AML by targeting primitive LSK and progenitor cells. Blood 2013;122:2864-76.
43. Daley GQ, Van Etten RA, Baltimore D. Induction of chronic myelogenous leukemia in mice by the P210bcr/abl gene of the Philadelphia chromosome. Science 1990;247:824-30.
44. Bijl J, Sauvageau M, Thompson A, Sauvageau G. High incidence of proviral integrations in the Hoxa locus in a new model of E2a-PBX1-induced B-cell leukemia. Genes Dev 2005;19:224-33.
45. Carofino BL, Ayanga B, Justice MJ. A mouse model for inducible overexpression of Prdm14 results in rapid-onset and highly penetrant T-cell acute lymphoblastic leukemia (T-ALL). Dis Model Mech 2013;6:1494-506.
46. Xiao P, Heshmati Y, Bouderlique T, et al. Mesenchymal Stromal Cells, Instigator or Suppressor for the Development of MLL-AF9 Induced Acute Myeloid Leukemia? Blood 2016;128:1488-.
47. Frisch BJ, Ashton JM, Xing L, Becker MW, Jordan CT, Calvi LM. Functional inhibition of osteoblastic cells in an in vivo mouse model of myeloid leukemia. Blood 2012;119:540-50.

48. Lim M, Pang Y, Ma S, et al. Altered mesenchymal niche cells impede generation of normal hematopoietic progenitor cells in leukemic bone marrow. Leukemia 2016;30:154-62.
49. McMillin DW, Negri JM, Mitsiades CS. The role of tumour-stromal interactions in modifying drug response: challenges and opportunities. Nat Rev Drug Discov 2013;12:217-28.
50. Ishikawa F, Yoshida S, Saito Y, et al. Chemotherapy-resistant human AML stem cells home to and engraft within the bone-marrow endosteal region. Nat Biotechnol 2007;25:1315-21.
51. Li X, Guo H, Duan H, et al. Improving chemotherapeutic efficiency in acute myeloid leukemia treatments by chemically synthesized peptide interfering with CXCR4/CXCL12 axis. Sci Rep 2015;5:16228.
52. Hidalgo M, Amant F, Biankin AV, et al. Patient-derived xenograft models: an emerging platform for translational cancer research. Cancer Discov 2014;4:998-1013.
53. Cogle CR, Goldman DC, Madlambayan GJ, et al. Functional integration of acute myeloid leukemia into the vascular niche. Leukemia 2014;28:1978-87.
54. Ivanov M, Baranova A, Butler T, Spellman P, Mileyko V. Non-random fragmentation patterns in circulating cell-free DNA reflect epigenetic regulation. BMC Genomics 2015;16 Suppl 13:S1.
55. Hornick NI, Huan J, Doron B, et al. Serum Exosome MicroRNA as a Minimally-Invasive Early Biomarker of AML. Sci Rep 2015;5:11295.
56. Anatomy and Physiology. Med Chir J Rev 1818;5:65-7.
57. Birnie GD. The HL60 cell line: a model system for studying human myeloid cell differentiation. Br J Cancer Suppl 1988;9:41-5.
58. Rowley JD, Golomb HM, Dougherty C. 15/17 translocation, a consistent chromosomal change in acute promyelocytic leukaemia. Lancet 1977;1:549-50.
59. Dreyling MH, Martinez-Climent JA, Zheng M, Mao J, Rowley JD, Bohlander SK. The t(10;11)(p13;q14) in the U937 cell line results in the fusion of the AF10 gene and CALM, encoding a new member of the AP-3 clathrin assembly protein family. Proc Natl Acad Sci U S A 1996;93:4804-9.
60. Chitteti BR, Cheng YH, Poteat B, et al. Impact of interactions of cellular components of the bone marrow microenvironment on hematopoietic stem and progenitor cell function. Blood 2010;115:3239-48.
61. Mendez-Ferrer S, Michurina TV, Ferraro F, et al. Mesenchymal and haematopoietic stem cells form a unique bone marrow niche. Nature 2010;466:829-34.
62. Jung Y, Song J, Shiozawa Y, et al. Hematopoietic stem cells regulate mesenchymal stromal cell induction into osteoblasts thereby participating in the formation of the stem cell niche. Stem Cells 2008;26:2042-51.
63. Morrison SJ, Scadden DT. The bone marrow niche for haematopoietic stem cells. Nature 2014;505:327-34.
64. Rashidi NM, Scott MK, Scherf N, et al. In vivo time-lapse imaging shows diverse niche engagement by quiescent and naturally activated hematopoietic stem cells. Blood 2014;124:79-83.

65. Boyd AL, Bhatia M. Bone marrow localization and functional properties of human hematopoietic stem cells. Curr Opin Hematol 2014;21:249-55.
66. Calvi LM, Adams GB, Weibrecht KW, et al. Osteoblastic cells regulate the haematopoietic stem cell niche. Nature 2003;425:841-6.
67. Arai F, Hirao A, Ohmura M, et al. Tie2/angiopoietin-1 signaling regulates hematopoietic stem cell quiescence in the bone marrow niche. Cell 2004;118:149-61.
68. Schepers K, Pietras EM, Reynaud D, et al. Myeloproliferative neoplasia remodels the endosteal bone marrow niche into a self-reinforcing leukemic niche. Cell Stem Cell 2013;13:285-99.
69. Park D, Spencer JA, Koh BI, et al. Endogenous bone marrow MSCs are dynamic, fate-restricted participants in bone maintenance and regeneration. Cell Stem Cell 2012;10:259-72.
70. Yavropoulou MP, Yovos JG. Osteoclastogenesis--current knowledge and future perspectives. J Musculoskelet Neuronal Interact 2008;8:204-16.
71. Frenette PS, Pinho S, Lucas D, Scheiermann C. Mesenchymal stem cell: keystone of the hematopoietic stem cell niche and a stepping-stone for regenerative medicine. Annu Rev Immunol 2013;31:285-316.
72. Greenbaum A, Hsu YM, Day RB, et al. CXCL12 in early mesenchymal progenitors is required for haematopoietic stem-cell maintenance. Nature 2013;495:227-30.
73. Nilsson SK, Johnston HM, Whitty GA, et al. Osteopontin, a key component of the hematopoietic stem cell niche and regulator of primitive hematopoietic progenitor cells. Blood 2005;106:1232-9.
74. Sugiyama T, Kohara H, Noda M, Nagasawa T. Maintenance of the hematopoietic stem cell pool by CXCL12-CXCR4 chemokine signaling in bone marrow stromal cell niches. Immunity 2006;25:977-88.
75. van Beijnum JR, Rousch M, Castermans K, van der Linden E, Griffioen AW. Isolation of endothelial cells from fresh tissues. Nat Protoc 2008;3:1085-91.
76. Kisanuki YY, Hammer RE, Miyazaki J, Williams SC, Richardson JA, Yanagisawa M. Tie2-Cre transgenic mice: a new model for endothelial cell-lineage analysis in vivo. Dev Biol 2001;230:230-42.
77. Winkler IG, Barbier V, Nowlan B, et al. Vascular niche E-selectin regulates hematopoietic stem cell dormancy, self renewal and chemoresistance. Nat Med 2012;18:1651-7.
78. Ding L, Saunders TL, Enikolopov G, Morrison SJ. Endothelial and perivascular cells maintain haematopoietic stem cells. Nature 2012;481:457-62.
79. Guezguez B, Campbell CJ, Boyd AL, et al. Regional localization within the bone marrow influences the functional capacity of human HSCs. Cell Stem Cell 2013;13:175-89.
80. Xie Y, Yin T, Wiegraebe W, et al. Detection of functional haematopoietic stem cell niche using real-time imaging. Nature 2009;457:97-101.
81. Mendez-Ferrer S, Chow A, Merad M, Frenette PS. Circadian rhythms influence hematopoietic stem cells. Curr Opin Hematol 2009;16:235-42.

82. Zhou BO, Yu H, Yue R, et al. Bone marrow adipocytes promote the regeneration of stem cells and haematopoiesis by secreting SCF. Nat Cell Biol 2017;19:891-903.
83. Boyd AL, Reid JC, Salci KR, et al. Acute myeloid leukaemia disrupts endogenous myelo-erythropoiesis by compromising the adipocyte bone marrow niche. Nat Cell Biol 2017;19:1336-47.
84. Raaijmakers MH, Mukherjee S, Guo S, et al. Bone progenitor dysfunction induces myelodysplasia and secondary leukaemia. Nature 2010;464:852-7.
85. Wang L, Zhang H, Rodriguez S, et al. Notch-dependent repression of miR-155 in the bone marrow niche regulates hematopoiesis in an NF-kappaB-dependent manner. Cell Stem Cell 2014;15:51-65.
86. Raaijmakers MH. Niche contributions to oncogenesis: emerging concepts and implications for the hematopoietic system. Haematologica 2011;96:1041-8.
87. Blank U, Karlsson S. TGF-beta signaling in the control of hematopoietic stem cells. Blood 2015;125:3542-50.
88. Fleming HE, Janzen V, Lo Celso C, et al. Wnt signaling in the niche enforces hematopoietic stem cell quiescence and is necessary to preserve self-renewal in vivo. Cell Stem Cell 2008;2:274-83.
89. Yamazaki S, Iwama A, Takayanagi S, et al. Cytokine signals modulated via lipid rafts mimic niche signals and induce hibernation in hematopoietic stem cells. EMBO J 2006;25:3515-23.
90. van Niel G, Porto-Carreiro I, Simoes S, Raposo G. Exosomes: a common pathway for a specialized function. J Biochem 2006;140:13-21.
91. Johnstone RM. Exosomes biological significance: A concise review. Blood Cells Mol Dis 2006;36:315-21.
92. Yanez-Mo M, Siljander PR, Andreu Z, et al. Biological properties of extracellular vesicles and their physiological functions. J Extracell Vesicles 2015;4:27066.
93. Colombo M, Raposo G, Thery C. Biogenesis, secretion, and intercellular interactions of exosomes and other extracellular vesicles. Annu Rev Cell Dev Biol 2014;30:255-89.
94. Smith ZJ, Lee C, Rojalin T, et al. Single exosome study reveals subpopulations distributed among cell lines with variability related to membrane content. J Extracell Vesicles 2015;4:28533.
95. Ostrowski M, Carmo NB, Krumeich S, et al. Rab27a and Rab27b control different steps of the exosome secretion pathway. Nat Cell Biol 2010;12:19-30; sup pp 1-13.
96. Willms E, Johansson HJ, Mager I, et al. Cells release subpopulations of exosomes with distinct molecular and biological properties. Sci Rep 2016;6:22519.
97. Raposo G, Stoorvogel W. Extracellular vesicles: exosomes, microvesicles, and friends. J Cell Biol 2013;200:373-83.
98. Becker A, Thakur BK, Weiss JM, Kim HS, Peinado H, Lyden D. Extracellular Vesicles in Cancer: Cell-to-Cell Mediators of Metastasis. Cancer Cell 2016;30:836-48.
99. Kucharzewska P, Christianson HC, Welch JE, et al. Exosomes reflect the hypoxic status of glioma cells and mediate hypoxia-dependent activation of

vascular cells during tumor development. Proc Natl Acad Sci U S A 2013;110:7312-7.
100. Schey KL, Luther JM, Rose KL. Proteomics characterization of exosome cargo. Methods 2015;87:75-82.
101. Kowal J, Arras G, Colombo M, et al. Proteomic comparison defines novel markers to characterize heterogeneous populations of extracellular vesicle subtypes. Proc Natl Acad Sci U S A 2016;113:E968-77.
102. Hanson PI, Cashikar A. Multivesicular body morphogenesis. Annu Rev Cell Dev Biol 2012;28:337-62.
103. Perez-Hernandez D, Gutierrez-Vazquez C, Jorge I, et al. The intracellular interactome of tetraspanin-enriched microdomains reveals their function as sorting machineries toward exosomes. J Biol Chem 2013;288:11649-61.
104. Record M, Carayon K, Poirot M, Silvente-Poirot S. Exosomes as new vesicular lipid transporters involved in cell-cell communication and various pathophysiologies. Biochim Biophys Acta 2014;1841:108-20.
105. van Meer G, Vaz WL. Membrane curvature sorts lipids. Stabilized lipid rafts in membrane transport. EMBO Rep 2005;6:418-9.
106. Valadi H, Ekstrom K, Bossios A, Sjostrand M, Lee JJ, Lotvall JO. Exosome-mediated transfer of mRNAs and microRNAs is a novel mechanism of genetic exchange between cells. Nat Cell Biol 2007;9:654-9.
107. Chen Y JR, Konopleva M, Garzon R, Croce C, Andreef M. CXCR4 downregulation of let-7a drives chemoresistance in acute myeloid leukemia. J Clin Invest 2013;123:2395-407.
108. Crescitelli R, Lasser C, Szabo TG, et al. Distinct RNA profiles in subpopulations of extracellular vesicles: apoptotic bodies, microvesicles and exosomes. J Extracell Vesicles 2013;2.
109. Huan J, Hornick NI, Shurtleff MJ, et al. RNA trafficking by acute myelogenous leukemia exosomes. Cancer Res 2013;73:918-29.
110. Ambros V. The functions of animal microRNAs. Nature 2004;431:350-5.
111. Friedman RC, Farh KK, Burge CB, Bartel DP. Most mammalian mRNAs are conserved targets of microRNAs. Genome research 2009;19:92-105.
112. Ha M, Kim VN. Regulation of microRNA biogenesis. Nature reviews Molecular cell biology 2014;15:509-24.
113. Yates LA, Norbury CJ, Gilbert RJ. The long and short of microRNA. Cell 2013;153:516-9.
114. Braun JE, Huntzinger E, Fauser M, Izaurralde E. GW182 proteins directly recruit cytoplasmic deadenylase complexes to miRNA targets. Molecular cell 2011;44:120-33.
115. Huntzinger E, Izaurralde E. Gene silencing by microRNAs: contributions of translational repression and mRNA decay. Nature reviews Genetics 2011;12:99-110.
116. Waldman SA, Terzic A. A study of microRNAs in silico and in vivo: diagnostic and therapeutic applications in cancer. FEBS J 2009;276:2157-64.
117. Huan J, Hornick NI, Goloviznina NA, et al. Coordinate regulation of residual bone marrow function by paracrine trafficking of AML exosomes. Leukemia 2015;29:2285-95.

118. Horiuchi K, Tohmonda T, Morioka H. The unfolded protein response in skeletal development and homeostasis. Cell Mol Life Sci 2016;73:2851-69.
119. Oyadomari S, Mori M. Roles of CHOP/GADD153 in endoplasmic reticulum stress. Cell Death Differ 2004;11:381-9.
120. Tohmonda T, Miyauchi Y, Ghosh R, et al. The IRE1alpha-XBP1 pathway is essential for osteoblast differentiation through promoting transcription of Osterix. EMBO Rep 2011;12:451-7.
121. Hu CC, Dougan SK, McGehee AM, Love JC, Ploegh HL. XBP-1 regulates signal transduction, transcription factors and bone marrow colonization in B cells. EMBO J 2009;28:1624-36.
122. Scadden DT. Rethinking stroma: lessons from the blood. Cell Stem Cell 2012;10:648-9.
123. Howlader N NA, Krapcho M, Miller D, Bishop K, Kosary CL, Yu M, Ruhl J, Tatalovich Z, Mariotto A, Lewis DR, Chen HS, Feuer EJ, Cronin KA. SEER Cancer Statistics Review, 1975-2014, National Cancer Institute, Bethesda, MD. https://seercancergov/csr/1975_2014/, 2017;based on November 2016 SEER data submission, posted to the SEER web site, April 2017.
124. Cheng L, Sun X, Scicluna BJ, Coleman BM, Hill AF. Characterization and deep sequencing analysis of exosomal and non-exosomal miRNA in human urine. Kidney Int 2014;86:433-44.
125. Thery C, Zitvogel L, Amigorena S. Exosomes: composition, biogenesis and function. Nat Rev Immunol 2002;2:569-79.
126. Manterola L, Guruceaga E, Gallego Perez-Larraya J, et al. A small noncoding RNA signature found in exosomes of GBM patient serum as a diagnostic tool. Neuro Oncol 2014;16:520-7.
127. Hong CS, Muller L, Whiteside TL, Boyiadzis M. Plasma exosomes as markers of therapeutic response in patients with acute myeloid leukemia. Front Immunol 2014;5:160.
128. Fayyad-Kazan H, Bitar N, Najar M, et al. Circulating miR-150 and miR-342 in plasma are novel potential biomarkers for acute myeloid leukemia. J Transl Med 2013;11:31.
129. Rommer A, Steinleitner K, Hackl H, et al. Overexpression of primary microRNA 221/222 in acute myeloid leukemia. BMC Cancer 2013;13:364.
130. Spinello I, Quaranta MT, Riccioni R, et al. MicroRNA-146a and AMD3100, two ways to control CXCR4 expression in acute myeloid leukemias. Blood Cancer J 2011;1:e26.
131. Cambronne XA, Shen R, Auer PL, Goodman RH. Capturing microRNA targets using an RNA-induced silencing complex (RISC)-trap approach. Proc Natl Acad Sci U S A 2012;109:20473-8.
132. Dweep H, Gretz N, Sticht C. miRWalk database for miRNA-target interactions. Methods Mol Biol 2014;1182:289-305.
133. Muylkens B, Coupeau D, Dambrine G, Trapp S, Rasschaert D. Marek's disease virus microRNA designated Mdv1-pre-miR-M4 targets both cellular and viral genes. Arch Virol 2010;155:1823-37.

134. Franceschini A, Szklarczyk D, Frankild S, et al. STRING v9.1: protein-protein interaction networks, with increased coverage and integration. Nucleic Acids Res 2013;41:D808-15.
135. Shannon P, Markiel A, Ozier O, et al. Cytoscape: a software environment for integrated models of biomolecular interaction networks. Genome Res 2003;13:2498-504.
136. Pinto EM, Ribeiro RC, Figueiredo BC, Zambetti GP. TP53-Associated Pediatric Malignancies. Genes Cancer 2011;2:485-90.
137. Elton TS, Selemon H, Elton SM, Parinandi NL. Regulation of the MIR155 host gene in physiological and pathological processes. Gene 2013;532:1-12.
138. Delgado MD, Albajar M, Gomez-Casares MT, Batlle A, Leon J. MYC oncogene in myeloid neoplasias. Clin Transl Oncol 2013;15:87-94.
139. Artinger EL, Mishra BP, Zaffuto KM, et al. An MLL-dependent network sustains hematopoiesis. Proc Natl Acad Sci U S A 2013;110:12000-5.
140. Koh CP, Wang CQ, Ng CE, et al. RUNX1 meets MLL: epigenetic regulation of hematopoiesis by two leukemia genes. Leukemia 2013;27:1793-802.
141. Scheller M, Huelsken J, Rosenbauer F, et al. Hematopoietic stem cell and multilineage defects generated by constitutive beta-catenin activation. Nat Immunol 2006;7:1037-47.
142. Ou YH, Chung PH, Sun TP, Shieh SY. p53 C-terminal phosphorylation by CHK1 and CHK2 participates in the regulation of DNA-damage-induced C-terminal acetylation. Molecular biology of the cell 2005;16:1684-95.
143. Melo SA, Sugimoto H, O'Connell JT, et al. Cancer exosomes perform cell-independent microRNA biogenesis and promote tumorigenesis. Cancer Cell 2014;26:707-21.
144. Shurtleff MJ, Temoche-Diaz MM, Karfilis KV, Ri S, Schekman R. Y-box protein 1 is required to sort microRNAs into exosomes in cells and in a cell-free reaction. Elife 2016;5.
145. Shurtleff MJ, Yao J, Qin Y, et al. Broad role for YBX1 in defining the small noncoding RNA composition of exosomes. Proc Natl Acad Sci U S A 2017;114:E8987-E95.
146. Rickmann M, Macke L, Sundarasetty BS, et al. Monitoring dendritic cell and cytokine biomarkers during remission prior to relapse in patients with FLT3-ITD acute myeloid leukemia. Ann Hematol 2013;92:1079-90.
147. Xiao B, Wang Y, Li W, et al. Plasma microRNA signature as a noninvasive biomarker for acute graft-versus-host disease. Blood 2013;122:3365-75.
148. Lim SH, Becker TM, Chua W, et al. Circulating tumour cells and circulating free nucleic acid as prognostic and predictive biomarkers in colorectal cancer. Cancer Lett 2014;346:24-33.
149. Raghavachari N, Liu P, Barb JJ, et al. Integrated analysis of miRNA and mRNA during differentiation of human CD34+ cells delineates the regulatory roles of microRNA in hematopoiesis. Exp Hematol 2014;42:14-27 e1-2.
150. Morris VA, Zhang A, Yang T, et al. MicroRNA-150 expression induces myeloid differentiation of human acute leukemia cells and normal hematopoietic progenitors. PLoS One 2013;8:e75815.

151. Marcucci G, Radmacher MD, Maharry K, et al. MicroRNA expression in cytogenetically normal acute myeloid leukemia. N Engl J Med 2008;358:1919-28.
152. Garzon R, Garofalo M, Martelli MP, et al. Distinctive microRNA signature of acute myeloid leukemia bearing cytoplasmic mutated nucleophosmin. Proc Natl Acad Sci U S A 2008;105:3945-50.
153. Wang Y, Li Z, He C, et al. MicroRNAs expression signatures are associated with lineage and survival in acute leukemias. Blood Cells Mol Dis 2010;44:191-7.
154. Skinner AM, O'Neill SL, Kurre P. Cellular microvesicle pathways can be targeted to transfer genetic information between non-immune cells. PLoS One 2009;4:e6219.
155. Liu J, Sun H, Wang X, et al. Increased exosomal microRNA-21 and microRNA-146a levels in the cervicovaginal lavage specimens of patients with cervical cancer. Int J Mol Sci 2014;15:758-73.
156. Bazarbachi A, Abou Merhi R, Gessain A, et al. Human T-cell lymphotropic virus type I-infected cells extravasate through the endothelial barrier by a local angiogenesis-like mechanism. Cancer Res 2004;64:2039-46.
157. Taylor DD, Gercel-Taylor C. MicroRNA signatures of tumor-derived exosomes as diagnostic biomarkers of ovarian cancer. Gynecol Oncol 2008;110:13-21.
158. He Z, Cai J, Lim JW, Kroll K, Ma L. A novel KRAB domain-containing zinc finger transcription factor ZNF431 directly represses Patched1 transcription. The Journal of biological chemistry 2011;286:7279-89.
159. Cambronne XA, Shen, R., Auer, P. L. & Goodman, R. H. Capturing microRNA targets using an RNA-induced silencing complex (RISC)-trap approach. Proceedings of the National Academy of Sciences of the United States of America 2012;109:20473-8.
160. Anders S PP, Huber W. HTSeq--a Python framework to work with high-throughput sequencing data. Bioinformatics 2015;31:166-9.
161. Lowenberg B, Downing JR, Burnett A. Acute myeloid leukemia. N Engl J Med 1999;341:1051-62.
162. Miraki-Moud F, Anjos-Afonso F, Hodby KA, et al. Acute myeloid leukemia does not deplete normal hematopoietic stem cells but induces cytopenias by impeding their differentiation. Proc Natl Acad Sci U S A 2013;110:13576-81.
163. Huan J, Hornick NI, Goloviznina NA, et al. Coordinate regulation of residual bone marrow function by paracrine trafficking of AML exosomes. Leukemia 2015.
164. Zhang B, Ho YW, Huang Q, et al. Altered microenvironmental regulation of leukemic and normal stem cells in chronic myelogenous leukemia. Cancer Cell 2012;21:577-92.
165. Yin Q, McBride J, Fewell C, et al. MicroRNA-155 is an Epstein-Barr virus-induced gene that modulates Epstein-Barr virus-regulated gene expression pathways. J Virol 2008;82:5295-306.
166. Lieu YK, Reddy EP. Conditional c-myb knockout in adult hematopoietic stem cells leads to loss of self-renewal due to impaired proliferation and accelerated differentiation. Proceedings of the National Academy of Sciences of the United States of America 2009;106:21689-94.

167. Feng J, Yang Y, Zhang P, et al. miR-150 functions as a tumour suppressor in human colorectal cancer by targeting c-Myb. Journal of cellular and molecular medicine 2014;18:2125-34.
168. Lennox KA, Behlke MA. Chemical modification and design of anti-miRNA oligonucleotides. Gene therapy 2011;18:1111-20.
169. White JR, Weston K. Myb is required for self-renewal in a model system of early hematopoiesis. Oncogene 2000;19:1196-205.
170. Skinner AM, Grompe M, Kurre P. Intra-hematopoietic cell fusion as a source of somatic variation in the hematopoietic system. Journal of cell science 2012;125:2837-43.
171. El-Badri NS, Wang BY, Cherry, Good RA. Osteoblasts promote engraftment of allogeneic hematopoietic stem cells. Exp Hematol 1998;26:110-6.
172. Colmone A, Amorim M, Pontier AL, Wang S, Jablonski E, Sipkins DA. Leukemic cells create bone marrow niches that disrupt the behavior of normal hematopoietic progenitor cells. Science 2008;322:1861-5.
173. Kumar B, Garcia M, Weng L, et al. Acute myeloid leukemia transforms the bone marrow niche into a leukemia-permissive microenvironment through exosome secretion. Leukemia 2017.
174. Chandran P, Le Y, Li Y, et al. Mesenchymal stromal cells from patients with acute myeloid leukemia have altered capacity to expand differentiated hematopoietic progenitors. Leuk Res 2015;39:486-93.
175. Reikvam H, Brenner AK, Hagen KM, et al. The cytokine-mediated crosstalk between primary human acute myeloid cells and mesenchymal stem cells alters the local cytokine network and the global gene expression profile of the mesenchymal cells. Stem Cell Res 2015;15:530-41.
176. Huang JC, Basu SK, Zhao X, et al. Mesenchymal stromal cells derived from acute myeloid leukemia bone marrow exhibit aberrant cytogenetics and cytokine elaboration. Blood Cancer J 2015;5:e302.
177. Passaro D, Di Tullio A, Abarrategi A, et al. Increased Vascular Permeability in the Bone Marrow Microenvironment Contributes to Disease Progression and Drug Response in Acute Myeloid Leukemia. Cancer Cell 2017.
178. Duarte D, Hawkins ED, Akinduro O, et al. Inhibition of Endosteal Vascular Niche Remodeling Rescues Hematopoietic Stem Cell Loss in AML. Cell Stem Cell 2018;22:64-77 e6.
179. Woll PS, Kjallquist U, Chowdhury O, et al. Myelodysplastic syndromes are propagated by rare and distinct human cancer stem cells in vivo. Cancer Cell 2014;25:794-808.
180. Battula VL, Le PM, Sun JC, et al. AML-induced osteogenic differentiation in mesenchymal stromal cells supports leukemia growth. JCI Insight 2017;2.
181. Mirantes C, Passegue E, Pietras EM. Pro-inflammatory cytokines: emerging players regulating HSC function in normal and diseased hematopoiesis. Exp Cell Res 2014;329:248-54.
182. Rodvold JJ, Chiu KT, Hiramatsu N, et al. Intercellular transmission of the unfolded protein response promotes survival and drug resistance in cancer cells. Sci Signal 2017;10.

183. Rodvold JJ, Mahadevan NR, Zanetti M. Immune modulation by ER stress and inflammation in the tumor microenvironment. Cancer Lett 2016;380:227-36.
184. Moore KA, Hollien J. The unfolded protein response in secretory cell function. Annu Rev Genet 2012;46:165-83.
185. Hornick NI, Doron B, Abdelhamed S, et al. AML suppresses hematopoiesis by releasing exosomes that contain microRNAs targeting c-MYB. Sci Signal 2016;9:ra88.
186. Doron B, Handu M, Kurre P. Concise Review: Adaptation of the Bone Marrow Stroma in Hematopoietic Malignancies: Current Concepts and Models. Stem Cells 2017.
187. Su X, Yu M, Qiu G, et al. Evaluation of nestin or osterix promoter-driven cre/loxp system in studying the biological functions of murine osteoblastic cells. Am J Transl Res 2016;8:1447-59.
188. Hawkins ED, Duarte D, Akinduro O, et al. T-cell acute leukaemia exhibits dynamic interactions with bone marrow microenvironments. Nature 2016;538:518-22.
189. Boot-Handford RP, Briggs MD. The unfolded protein response and its relevance to connective tissue diseases. Cell Tissue Res 2010;339:197-211.
190. Hamamura K, Liu Y, Yokota H. Microarray analysis of thapsigargin-induced stress to the endoplasmic reticulum of mouse osteoblasts. J Bone Miner Metab 2008;26:231-40.
191. Heusermann W, Hean J, Trojer D, et al. Exosomes surf on filopodia to enter cells at endocytic hot spots, traffic within endosomes, and are targeted to the ER. J Cell Biol 2016;213:173-84.
192. Riggs AC, Bernal-Mizrachi E, Ohsugi M, et al. Mice conditionally lacking the Wolfram gene in pancreatic islet beta cells exhibit diabetes as a result of enhanced endoplasmic reticulum stress and apoptosis. Diabetologia 2005;48:2313-21.
193. Oslowski CM, Urano F. Measuring ER stress and the unfolded protein response using mammalian tissue culture system. Methods Enzymol 2011;490:71-92.
194. Shim SH, Xia C, Zhong G, et al. Super-resolution fluorescence imaging of organelles in live cells with photoswitchable membrane probes. Proc Natl Acad Sci U S A 2012;109:13978-83.
195. Hoshino A, Costa-Silva B, Shen TL, et al. Tumour exosome integrins determine organotropic metastasis. Nature 2015;527:329-35.
196. Mulcahy LA, Pink RC, Carter DR. Routes and mechanisms of extracellular vesicle uptake. J Extracell Vesicles 2014;3.
197. Zanetti M, Rodvold JJ, Mahadevan NR. The evolving paradigm of cell-nonautonomous UPR-based regulation of immunity by cancer cells. Oncogene 2016;35:269-78.
198. Krause DS, Scadden DT. A hostel for the hostile: the bone marrow niche in hematologic neoplasms. Haematologica 2015;100:1376-87.
199. Schardt JA, Mueller BU, Pabst T. Activation of the unfolded protein response in human acute myeloid leukemia. Methods Enzymol 2011;489:227-43.

200. Sun H, Lin DC, Guo X, et al. Inhibition of IRE1alpha-driven pro-survival pathways is a promising therapeutic application in acute myeloid leukemia. Oncotarget 2016;7:18736-49.
201. Yadav RK, Chae SW, Kim HR, Chae HJ. Endoplasmic reticulum stress and cancer. J Cancer Prev 2014;19:75-88.
202. Murakami T, Saito A, Hino S, et al. Signalling mediated by the endoplasmic reticulum stress transducer OASIS is involved in bone formation. Nat Cell Biol 2009;11:1205-11.
203. Montgomery TA, Ruvkun G. MicroRNAs visit the ER. Cell 2013;153:511-2.
204. Stalder L, Heusermann W, Sokol L, et al. The rough endoplasmatic reticulum is a central nucleation site of siRNA-mediated RNA silencing. EMBO J 2013;32:1115-27.
205. Christodoulides C, Laudes M, Cawthorn WP, et al. The Wnt antagonist Dickkopf-1 and its receptors are coordinately regulated during early human adipogenesis. J Cell Sci 2006;119:2613-20.
206. Geyh S, Rodriguez-Paredes M, Jager P, et al. Functional inhibition of mesenchymal stromal cells in acute myeloid leukemia. Leukemia 2016;30:683-91.
207. Krause DS, Fulzele K, Catic A, et al. Differential regulation of myeloid leukemias by the bone marrow microenvironment. Nat Med 2013;19:1513-7.
208. Viola S, Traer E, Huan J, et al. Alterations in acute myeloid leukaemia bone marrow stromal cell exosome content coincide with gains in tyrosine kinase inhibitor resistance. Br J Haematol 2016;172:983-6.
209. Horton TM, Pati D, Plon SE, et al. A phase 1 study of the proteasome inhibitor bortezomib in pediatric patients with refractory leukemia: a Children's Oncology Group study. Clin Cancer Res 2007;13:1516-22.
210. Battula VL, Chen Y, Cabreira Mda G, et al. Connective tissue growth factor regulates adipocyte differentiation of mesenchymal stromal cells and facilitates leukemia bone marrow engraftment. Blood 2013;122:357-66.
211. Jacamo R, Chen Y, Wang Z, et al. Reciprocal leukemia-stroma VCAM-1/VLA-4-dependent activation of NF-κB mediates chemoresistance. Blood 2014;123:2691-702.
212. Schoofs T, Berdel WE, Muller-Tidow C. Origins of aberrant DNA methylation in acute myeloid leukemia. Leukemia 2014;28:1-14.
213. Zambetti NA, Ping Z, Chen S, et al. Mesenchymal Inflammation Drives Genotoxic Stress in Hematopoietic Stem Cells and Predicts Disease Evolution in Human Pre-leukemia. Cell Stem Cell 2016;19:613-27.
214. Xia J, Hu Z, Yoshihara S, et al. Modeling Human Leukemia Immunotherapy in Humanized Mice. EBioMedicine 2016;10:101-8.
215. Reinisch A, Thomas D, Corces MR, et al. A humanized bone marrow ossicle xenotransplantation model enables improved engraftment of healthy and leukemic human hematopoietic cells. Nat Med 2016;22:812-21.
216. Chen Y, Jacamo R, Shi YX, et al. Human extramedullary bone marrow in mice: a novel in vivo model of genetically controlled hematopoietic microenvironment. Blood 2012;119:4971-80.

217. Reinisch A, Hernandez DC, Schallmoser K, Majeti R. Generation and use of a humanized bone-marrow-ossicle niche for hematopoietic xenotransplantation into mice. Nat Protoc 2017;12:2169-88.
218. Vaiselbuh SR, Edelman M, Lipton JM, Liu JM. Ectopic human mesenchymal stem cell-coated scaffolds in NOD/SCID mice: an in vivo model of the leukemia niche. Tissue Eng Part C Methods 2010;16:1523-31.
219. Antonelli A, Noort WA, Jaques J, et al. Establishing human leukemia xenograft mouse models by implanting human bone marrow-like scaffold-based niches. Blood 2016;128:2949-59.
220. Travlos GS. Normal structure, function, and histology of the bone marrow. Toxicol Pathol 2006;34:548-65.
221. Grun D, van Oudenaarden A. Design and Analysis of Single-Cell Sequencing Experiments. Cell 2015;163:799-810.
222. Van Loo P, Voet T. Single cell analysis of cancer genomes. Curr Opin Genet Dev 2014;24:82-91.
223. Hodne K, Weltzien FA. Single-Cell Isolation and Gene Analysis: Pitfalls and Possibilities. Int J Mol Sci 2015;16:26832-49.
224. Takahashi Y, Nishikawa M, Shinotsuka H, et al. Visualization and in vivo tracking of the exosomes of murine melanoma B16-BL6 cells in mice after intravenous injection. J Biotechnol 2013;165:77-84.
225. Risom T. Measuring And Managing Phenotypic Heterogeneity And Plasticity In Breast Cancer To Improve Therapeutic Control. https://digitalcommonsohsuedu/etd/3940 2017;3940.
226. von der Heide EK, Neumann M, Vosberg S, et al. Molecular alterations in bone marrow mesenchymal stromal cells derived from acute myeloid leukemia patients. Leukemia 2016.
227. Patel DM, Shah J, Srivastava AS. Therapeutic potential of mesenchymal stem cells in regenerative medicine. Stem Cells Int 2013;2013:496218.
228. Dominici M, Le Blanc K, Mueller I, et al. Minimal criteria for defining multipotent mesenchymal stromal cells. The International Society for Cellular Therapy position statement. Cytotherapy 2006;8:315-7.
229. da Silva Meirelles L, Caplan AI, Nardi NB. In search of the in vivo identity of mesenchymal stem cells. Stem Cells 2008;26:2287-99.
230. Ramakrishnan A, Torok-Storb B, Pillai MM. Primary marrow-derived stromal cells: isolation and manipulation. Methods Mol Biol 2013;1035:75-101.
231. Ito S, Barrett AJ, Dutra A, et al. Long term maintenance of myeloid leukemic stem cells cultured with unrelated human mesenchymal stromal cells. Stem Cell Res 2015;14:95-104.